

On the Reduction of Oxygen from Dispersed Media

by

Omar H. Roushdy

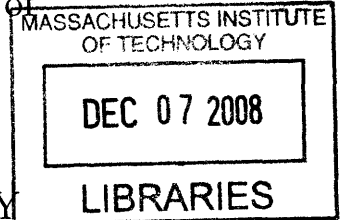
Submitted to the Department of Mechanical Engineering
in partial fulfillment of the requirements for the degree of

Doctor of Philosophy

at the

MASSACHUSETTS INSTITUTE OF TECHNOLOGY


June 2007



© Omar H. Roushdy, MMVII. All rights reserved.


The author hereby grants to MIT permission to reproduce and
distribute publicly paper and electronic copies of this thesis document
in whole or in part.

Author


 Department of Mechanical Engineering

May 31, 2007

Certified by

 Donald R. Sadoway
Professor of Materials Chemistry
Thesis Supervisor

Certified by

 Ain. A. Sonin
Professor of Mechanical Engineering
Thesis Supervisor

Accepted by

Lalit Anand
Chairman, Department Committee on Graduate Students

On the Reduction of Oxygen from a Dispersed Medium

by

Omar H. Roushdy

Submitted to the Department of Mechanical Engineering
on May 31, 2007, in partial fulfillment of the
requirements for the degree of
Doctor of Philosophy

Abstract

The reduction of oxygen from an organic phase dispersed in a concentrated electrolyte is investigated. Dispersed organic phases are used to enhance oxygen transport in fermenters and artificial blood substitutes. This work evaluates the feasibility of using a dispersed organic phase to transport oxygen in a fuel cell. An emulsion of perfluorohexane in a 20 wt% potassium hydroxide solution was formed with a lecithin surfactant. Oxygen was reduced from the emulsion on a rotating disk electrode. The dispersed phase did not contribute to the oxygen transport to the surface of a rotating disk electrode. An explanation is given based on the hydrodynamics of an emulsion under a rotating disk electrode. To eliminate the effect of hydrodynamics, the results of a hydrostatic transient diffusion experiment (Cottrell Experiment) are reported. Again, no significant enhancement of the oxygen transport rate was observed. The dispersed phase is shown to contain oxygen by NMR spectroscopy. It is argued that the expectation of an enhancement from the use of a dispersed phase may be based on inapplicable transport models. The presence of the lecithin surfactant may also impede transport. An oscillating electrode is used to reduce oxygen from a continuous perfluorohexane phase. In this case, the rate of reduction of oxygen is limited by diffusion across an aqueous layer trapped at the surface of the electrode by its relative affinity for aqueous solution over perfluorohexane. The implications for the use of a dispersed organic phase in fuel cells are discussed. The use of a rotating disk electrode in heterogeneous media and the need for a mass transport model in liquid-liquid dispersions are also discussed.

Thesis Supervisor: Donald R. Sadoway
Title: Professor of Materials Chemistry

Thesis Supervisor: Ain. A. Sonin
Title: Professor of Mechanical Engineering

Acknowledgments

I owe many thanks for much help provided by many people over the duration of this project. Some of them are mentioned here. I was very fortunate to have Professor Donald Sadoway as a thesis supervisor. He taught me a great deal, by instruction and example, and gave me a degree, both of which I'm grateful for. I was also fortunate to have Professor Ain Sonin as a thesis supervisor. His insistence on the use of scaling laws was very educational. As well I owe him special thanks for his constant encouragement, especially at critical junctures. Professor Jung-Hoon Chun chaired the thesis committee and provided a sharp, unique, and much appreciated critique of the work. He was also responsible for the allocation of much of the funding for the project.

Professor Samir Nayfeh taught me much of the mechanical design used in the construction of the apparatus, as well as providing wise consult and council.

Professor Joseph L. Smith, Jr. welcomed me in his office for many years, where we discussed many aspects of this project and others. I learned from him much that I would not have learned otherwise.

Professor John Brisson always lent a willing ear and a critical eye. He suggested some modelling approaches which proved very educational, and shared much experience and wisdom.

I had the outstanding fortune of being a teaching assistant for Professor Bora Mikić. It will remain amongst the most enjoyable and educational experiences of my time in graduate school.

Dr. Ted Lee showed me how to formulate emulsions at the very onset of the project. He was kind enough to share his lab equipment and experience.

In Professor Daniel Blankschtein's lectures and office hours I received much knowledge and encouragement which were of considerable help with this project.

I've been fortunate to know and work with many great labmates and colleagues. Amongst them, Professor Shorya Awtar, The Great Iason Chatzakis, Franklin Miller, with whom I've had many formative conversations, Luke Theogarajan, without whom

the NMR data would not have been possible, Professor Kaveh Milaninia, Professor Valeriy Ivanov, and Kripa Varanasi.

The oscillating electrode could not have been made without the aid and patience of Mr. Peter Houk at the MIT glass shop. Mr. Brendon Edwards, also of the glass shop, was of great help particularly in blowing glass tubes on short notice.

Ms. Yin-Lin Xie was kind enough to allow access to lab space and equipment that helped in preparation of the setup.

Ms. Leslie Regan and the staff of the Mechanical Engineering Graduate office kept me registered, and have been far more patient than should be expected.

I owe thanks to Dan Engelhardt of the registrar's office. His knowledge of the administration, and willingness to help, have been great assets.

The work was funded in part by the Korean Institute of Machinery and Materials and others. Special thanks are due to the Korean Institute for their support and the extended loan of equipment without which it would have been much more difficult to complete the work.

Contents

1	Introduction	15
2	A Review of the Literature	25
2.1	Work on the Electrochemical Reduction of Oxygen	27
2.2	Work on Oxygen Transport	28
2.3	Emulsions	30
3	Modelling	35
3.1	The Wire Mesh Electrode	39
4	Experimental Setup and Procedures	45
4.1	The Rotating Disk Electrode	45
4.2	The Oscillating Electrode	50
4.3	Measurements and Data Collection	53
4.4	Experimental Procedures	54
4.4.1	Transport Limited Experiments	58
4.5	Preparation of the Emulsion	58
5	Experimental Results and Discussion	61
5.1	The Emulsion	61
5.2	Rotating Disk Electrode Results	63
5.2.1	Discussion of the Rotating Disk Electrode Results	72
5.3	Transient Diffusion	76
5.4	Oxygen Content of the Emulsion	78

5.5	Oscillating electrode results	82
5.5.1	Discussion of the Oscillating Electrode Results	86
6	Conclusions	91
A	The Relationship Between Potential and Efficiency	101

List of Figures

1-1	Idealized schematic of a fuel cell operating on hydrogen and oxygen. The product, water, is not shown because where it is formed and expelled depends on the type of cell, which has not been specified. . . .	16
1-2	Flow schematic for an alkaline fuel cell	17
1-3	Idealized Schematic of a typical porous gas diffusion electrode. The electrode is typically some fraction of a millimeter wide. Pore diameters vary from tens of microns to less than a micron. The pores are often highly irregular. The thickness of the reaction zone at the electrode-electrolyte-gas interface is estimated to be between 1 μm and 1 nm [7].	19
1-4	Schematic of an Idealized Flooded Electrode	21
2-1	The effect of adding electrolyte on electrostatic repulsion. Taken from J. N. Israelachvilli, Intermolecular and Surface Forces.[59]	32
3-1	Predicted mass transport limited current flux for a rotating disk electrode in an emulsion of 15% by volume perfluorohexane in a 20 wt% solution of KOH (lines a and b) and in a solution of 20 wt% KOH with no dispersed phased (c). In both cases the liquid is saturated with oxygen at 1 atm pressure. Line a) assumes the diffusivity of oxygen in emulsion is that of the continuous phase ($0.92 \times 10^{-9} \text{ m}^2/\text{s}$) and the concentration is the volume average concentration b) assumes the same concentration as a) with diffusivity equal to half that of the continuous phase, as suggest by Ju et al. [62]	38

3-2	The effect of varying volume fractions of perfluorocarbon on the current from oxygen reduction on a wire mesh screen electrode with a flow speed of 0.01 m/s, with $i_o = 10^{-10}$ A/cm ² , and $\alpha = 0.54$ [12].	43
4-1	The rotating disk electrode shape suggested by Blurton and Riddiford [15]. The major diameter of the disk is 26.4 mm. The minor diameter is 12.1 mm.	47
4-2	The rotating disk electrode used in this work. The minimum diameter is 4.5 mm and the maximum diameter is three times that. The disk is immersed in fluid such that the fluid level is just below the shoulder, but far enough from the shoulder not to be affected by in.	48
4-3	The rotating disk electrode supplied by Pine Instrument Company.	49
4-4	A diagram of the reciprocating electrode used to traverse two phases	51
4-5	Schematic of Potentiostat and cell electrode setup, taken from Gamry Instruments (gamry.com)	55
4-6	Measured voltammogram of a clean platinum electrode surface in 20 wt% KOH solution	57
5-1	Lecithin stabilized emulsion of perfluorohexane in 20 wt% KOH, within minutes of formation. No length scale was available on the microscope.	62
5-2	Mass transport limited currents as measured on a rotating disk electrode in KOH compared with theoretical calculations in 20 wt% KOH in water saturated with a) nitrogen, b) reconstituted air and c) oxygen. The solid lines represent the theoretically calculated values for cases b and c.	63
5-3	Mass transport controlled reduction of oxygen on a rotating disk electrode a) 20 wt% KOH saturated with N ₂ , b) 20 wt% KOH saturated with O ₂ , c) an emulsion of 15% by volume perfluorohexane in 20 wt% KOH saturated with O ₂	65

5-4	Measured mass transport controlled reduction of oxygen on a rotating disk electrode from the emulsion saturated with oxygen compared with that in the solution saturated with oxygen, and with the emulsion saturated with nitrogen.	67
5-5	Measured transport controlled reduction of oxygen on a rotating disk electrode from the saturated with oxygen, compared with reduction from the solution saturated with oxygen, the emulsion saturated with nitrogen, and the sum of the currents from the emulsion saturated with nitrogen and the pure solution saturated with oxygen. The data presented are the average of trials over a period of time and indicate that the increase in current observed with the emulsion is not due to increased oxygen transport.	68
5-6	Mass transport controlled reduction of oxygen on a rotating disk electrode from the emulsion saturated with oxygen compared the solution saturated with oxygen and with the emulsion saturated with nitrogen. The observed enhancement is due to the reaction of a species other than oxygen. The data presented are from individual trials, and not averaged over the entire data set.	69
5-7	Mass transport controlled reduction of oxygen on a rotating disk electrode from the emulsion compared with reduction from the solution, and a 20wt% solution of KOH with surfactant dissolved. The results show that the enhancement is due to the dissolved surfactant	71
5-8	A comparison of the momentum and concentration boundary layer thicknesses below a rotating disk surface. The momentum boundary layer, where emulsion droplets are forced away from the center of the disk is much larger than the concentration boundary layer, where drops must enter to affect the transport to the disk.	73
5-9	The ratio of azimuthal to vertical velocity at the edge of the concentration boundary layer beneath a rotating disk at various rotation speeds	74

5-10	Mass transport limited currents from a semi-infinite body diffusion showing little advantage to the emulsion.	77
5-11	^{19}F NMR spectra of 15 %vol perfluorohexane in a 20 wt% solution of potassium hydroxide stabilized by lecithin. Lines are shown in red and blue. If viewed in black and white, the spectrum of the oxygenated emulsion can be identified as one shifted to the right.	80
5-12	^{19}F NMR spectra of 15 solution of potassium hydroxide stabilized by lecithin. If viewed in black and white, the spectrum of the oxygenated emulsion can be identified as one shifted to the right.	81
5-13	Measured currents from an oscillating electrode with 10 mm stroke in single phase 20 wt% KOH solution saturated with oxygen (\diamond), and traversing the interface between a 20 wt% KOH solution and a perfluorohexane phase at the mid-point of its travel (\circ). Both phases were saturated with oxygen.	83
5-14	Measured currents in a 20 wt% KOH solution. The obtainable current appears to be independent of the stroke length of the electrode and linear with oscillation speed, but also appears to begin to plateau between 250 and 300 oscillations per minute.	84
5-15	Data taken at two different temperatures in 20 wt% KOH solution indicate that a slight temperature increase does not seem to have appreciable effect.	85
5-16	Calculated diffusion limited current as a function the thickness of a film of solution trapped beneath the electrode. The trapped aqueous layer is observed under a microscope to be about 10 μm	87
5-17	Model predictions and theoretical data for an oscillating electrode in oxygen saturated 20 wt% KOH solution. If viewed in black and white, the model is the smooth line, while experimental data shows oscillations. The negative currents indicate reduction. The ordinate shows current in milliamperes.	89

6-1 Schematic of a fuel cell. The unit shown above would be repeated to form a stack, typically with the cathode of one cell forming the back of the anode of the adjacent cell. Taken without permission from http://www.fueleconomy.gov/feg/fcv_PEM.shtml. 94

6-2 A schematic cross section of one possible configuration of a flooded fuel cell showing the electrolyte flow orthogonal to the thin dimension of the electrodes. The membrane area available for transport in this configuration is greatly reduced when compared with the typical configuration. 96

Chapter 1

Introduction

The spontaneous, exothermic, reaction of hydrogen and oxygen to form water is a source of energy for most living creatures, both through biological mechanisms and, for many people, through man made mechanisms. If the reaction occurs directly (thermochemically) the result is the release of heat and light. The reaction may be violent if the mixture is ignited by a spark and allowed to spread through a pre-mixed volume. Or it may be controlled if occurring on a catalyst surface.¹ If, instead, oxygen is reduced on an electrically isolated electrode (i.e. gains electrons from the electrode, making it the cathode) and hydrogen is oxidized on another electrically isolated electrode (i.e. loses electrons to the electrode making it the anode) an excess of electrons accumulates on the anode and a deficit of electrons accumulates on the cathode. If the two electrodes are connected through an external electrical circuit, current will flow that can be used to do work. If the electrodes are then re-supplied with reactants, the reaction continues to transfer electrons, and the flow of current in the external electrical circuit can continue. In effect, this is a battery with a continuous supply of reactants and removal of products. Devices that provide a continuous supply of reactants to produce a continuous flow of current are often

¹This is the basis for the lamp invented by Johann Döbereiner. In 1823 Döbereiner found that if hydrogen mixed with air and was directed over a platinum catalyst the gas mixture would ignite. He used the mixing of zinc with dilute sulphuric acid to generate a hydrogen stream which he then directed over the platinum catalyst. The Döbereiner lamp replaced the tinder box as a source of flame until it was replaced by the phosphorus match [81].

referred to as fuel cells. Figure 1-1 shows a schematic of a fuel cell operated on hydrogen and oxygen (the only kind discussed in this work). Figure 1-2 shows a flow schematic for an alkaline fuel cell. The reasons for selecting an alkaline fuel cell are mentioned later in this chapter. Analogous reactions exist in other media, and are listed in most general fuel cell books. See the Fuel Cell Handbook [110] for example, which was freely available on the internet as of this writing.

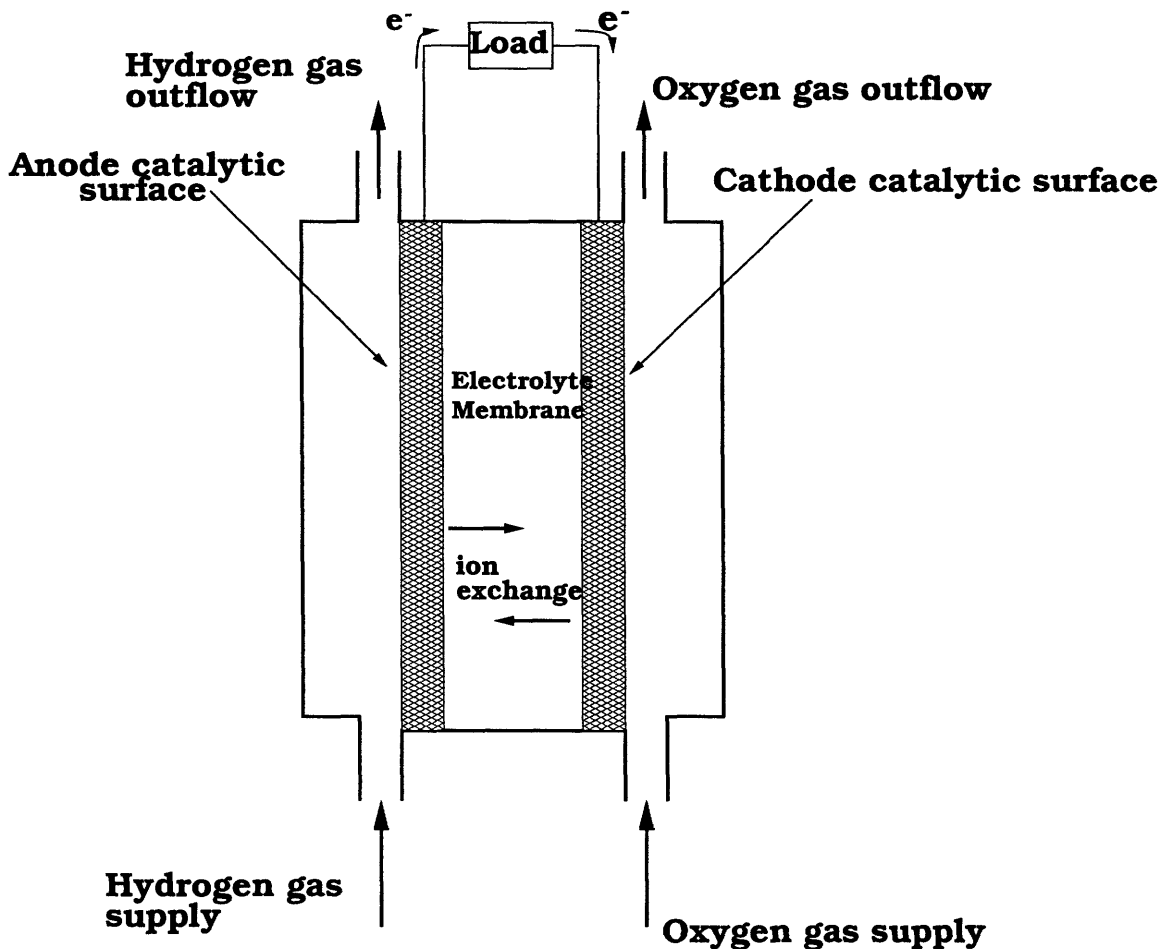


Figure 1-1: Idealized schematic of a fuel cell operating on hydrogen and oxygen. The product, water, is not shown because where it is formed and expelled depends on the type of cell, which has not been specified.

As can be seen from Figure 1-2, in order for the fuel cell to operate continuously, the electrodes must be separated by an electrolyte which allows the flow of ions, but prevents the flow of electrons and gaseous reactants (the latter usually referred to as

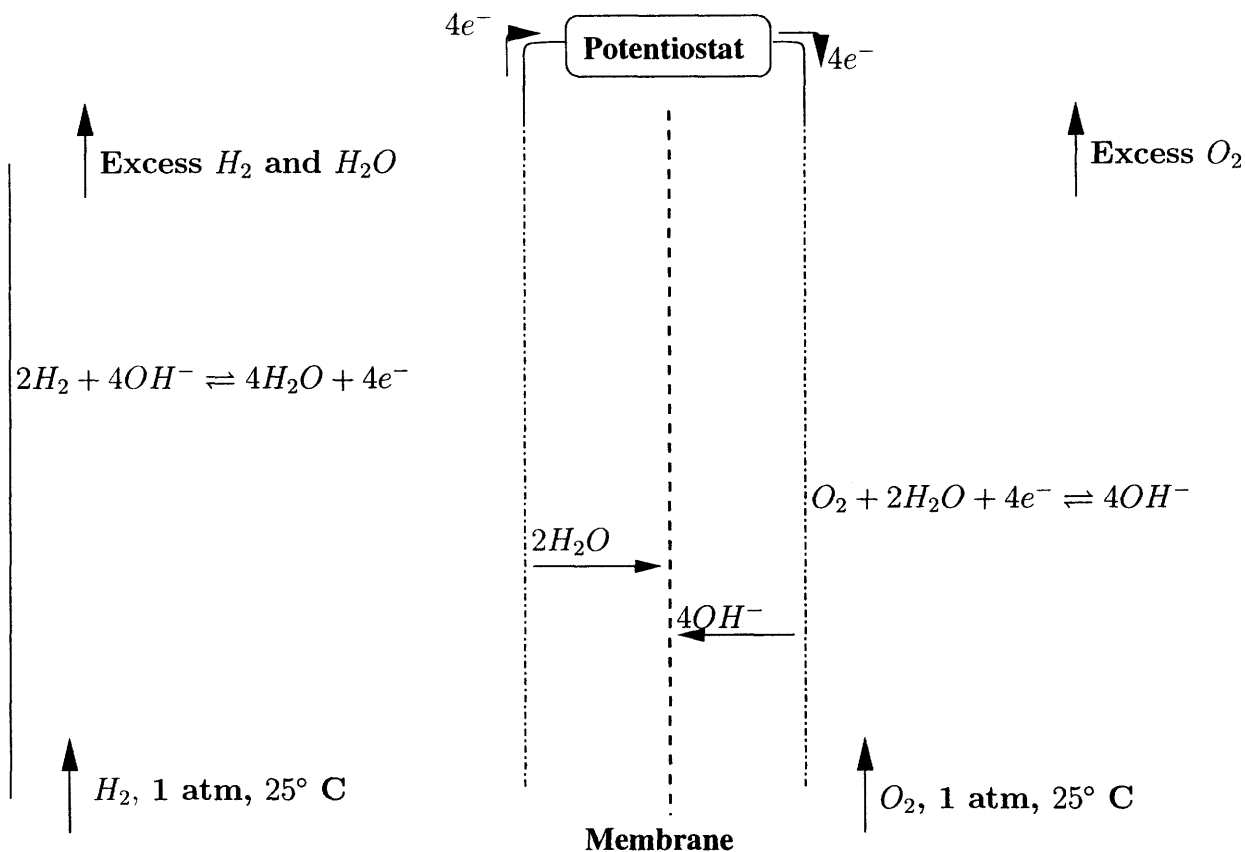


Figure 1-2: Flow schematic for an alkaline fuel cell

crossover in the fuel cell literature).

When the electrodes of an electrochemical cell are isolated from an external circuit (i.e., the cell sees an open circuit through its terminals), they adopt their equilibrium potentials. The difference between them is then equilibrium potential of the cell, often called the open circuit voltage. The equilibrium potential of each electrode, with respect to some reference in the solution, is such that the Gibbs free energy required to add an electron to the anode, or remove it from the cathode, is equal to the Gibbs free energy of the respective reaction (see Vetter [123] for a more detailed discussion of reference potential and inner and outer electrode potentials). The equilibrium potential is then a thermodynamic quantity determined by the chemical reaction, and the temperature and pressure (or concentration of species) at which it occurs.

A practical device must produce a net flow of current, and so must be operated

at some deviation from the equilibrium potential. The potential of each electrode is determined by the relative rates of charge addition and removal at the electrode. For each mole of reaction, a known number of electrons are transferred to or from the electrode. The result is that the current through the electrode is directly proportional to the chemical reaction rate. The chemical reaction rate at an electrode is dependent on the activation energy of the reaction, which in turn depends on the potential of the electrode (for a discussion see a text on electrochemistry, such as Bard and Faulkner [13]). As the electrode deviates further from its equilibrium potential, the activation energy decreases, therefore increasing the chemical reaction rate and the current through the electrode. Steady state is reached when the potential of the electrode is such that the rate of charge flow from the reaction matches that from the external circuit. Thus, to achieve the maximum current obtainable from a cell, the cell must be operated with the electrodes as far as possible from their equilibrium potential. However, operating far from the equilibrium potential reduces the efficiency of the cell, as discussed in the next paragraph. The preceding arguments apply to exothermic reactions, such as the formation of water, and endothermic ones, such as hydrolysis.

The thermodynamic efficiency of a fuel cell, defined as the ratio of work produced to the enthalpy of reaction can be written as

$$\eta_{actual} = \frac{\eta_{ideal} E_{actual}}{E_{ideal}} \quad (1.1)$$

where η is the efficiency, and E the cell voltage. The subscripts *actual* and *ideal* refer to an actual cell and a thermodynamically ideal cell, respectively. The ideal open circuit voltage for a cell reacting hydrogen and oxygen to form water at 25 °C and one atmosphere of pressure is 1.23 V. Its ideal efficiency is 0.83. The actual efficiency is then $\eta_{actual} = 0.67 E_{actual}$ (where the constant 0.67 has units of 1/V such that the efficiency is dimensionless). See Appendix A for a more detailed derivation.

Because electrochemical reactions must occur at the surface of an electrode, the reactive surface area directly multiplies the reaction rate and therefore the current

through the electrode. The preceding is true provided that reactants can be supplied to the reactive surface and products removed fast enough to match the reaction rate. A typical porous gas diffusion electrode is a structure with fine pores and a catalyst (typically platinum) deposited on the surface of the pores. Figure 1-3 shows an idealized schematic of a porous gas diffusion electrode. Note that the reaction occurs only in a thin region at the electrode-electrolyte-gas interface where aqueous and gaseous species mix over a catalytic surface [7].

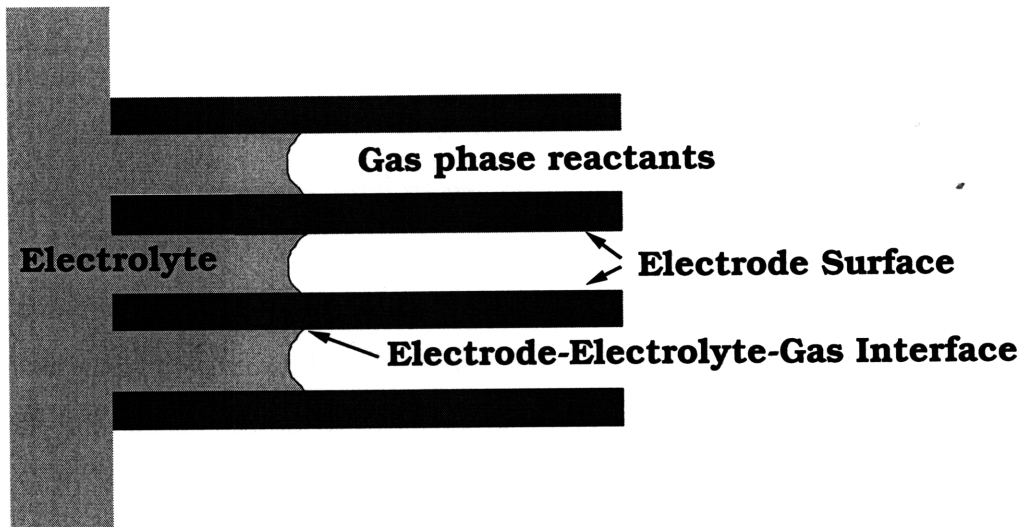


Figure 1-3: Idealized Schematic of a typical porous gas diffusion electrode. The electrode is typically some fraction of a millimeter wide. Pore diameters vary from tens of microns to less than a micron. The pores are often highly irregular. The thickness of the reaction zone at the electrode-electrolyte-gas interface is estimated to be between $1 \mu m$ and $1 nm$ [7].

At a given cell potential, temperature, and pressure, the current produced by a fuel cell is dependent upon: the rate of mass transport to and from the reaction zone, the chemical reaction rate, and the area available for reaction. In certain operating regimes, one of these may be limiting.

The reaction rate can be increased by increasing the temperature, but it brings other problems such as reduced material life. Because the reaction is exothermic, it is thermodynamically less favorable at high temperature (i.e., the Gibbs free energy of the reaction is reduced, and consequently, the cell open circuit voltage). The best

catalysts are platinum based compounds. But even on these catalysts, the reduction of oxygen is very slow (exchange current densities² vary from 10^{-10} to 10^{-13} A/m², depending on the medium) [12]. The reaction rate can be increased through better catalysis, but to date, platinum and platinum based catalysts are the best available.

While porous gas diffusion electrodes have very large internal areas, the diffusive transport of reactants and products along the internal pores is slow. The area over which the reaction can occur is limited to a region estimated to be between one micron and one nanometer at the electrode-electrolyte-gas interface [7].

The focus of this work is on investigating the possibility of enhancing the mass transport of oxygen in a fuel cell by adding to the electrolyte a substance with high oxygen solubility. With such an enhanced electrolyte, the line of the electrode-electrolyte-gas interface can be replaced with an electrode-electrolyte interface, as depicted in Figure 1-4. Circulating the electrolyte through the electrode would transport reactants and products by convection, rather than by diffusion alone as in a porous gas diffusion electrode. The pores would have to be of considerably larger dimension than those in a porous gas diffusion electrode, to allow the flow of liquid. If the width of the triple-phase interface in a porous gas diffusion electrode is taken as being one micron, then covering the entire pore area with oxygen saturated electrolyte would provide several hundred or more times the reactive area per pore, which compensates for the reduced number of pores.

An electrode such as the one shown in Figure 1-4 was called flooded by its originator, Herman Meissner [56]. At present, the term flooded, in the context of fuel cells, usually refers to a pore which has become filled with electrolyte. The result is that there is no interface between the gaseous reactants and the electrolyte in the pore, and no reaction takes place in it. The loss of reactive area due to the flooding of pores is one of the reasons given for degradation of the performance of a cell over time. Given the present use of the term flooded, a more appropriate name might be

²The exchange current is magnitude of the current at the electrode surface associated with the forward and backwards reactions when the overall reaction is at equilibrium and no net current flows from the electrode. It is a measure of the kinetics of the reaction, see Bard and Faulkner [13], first ed., p.100, for a further explanation.

given to the electrode shown in Figure 1-4, such as *single fluid convection electrode* in contrast to the porous gas diffusion electrode. When used in this document, a flooded electrode means one as in Figure 1-4. *The working fluid* refers to the oxygen rich electrolyte fluid shown circulated through the electrode, as shown in Figure 1-4.

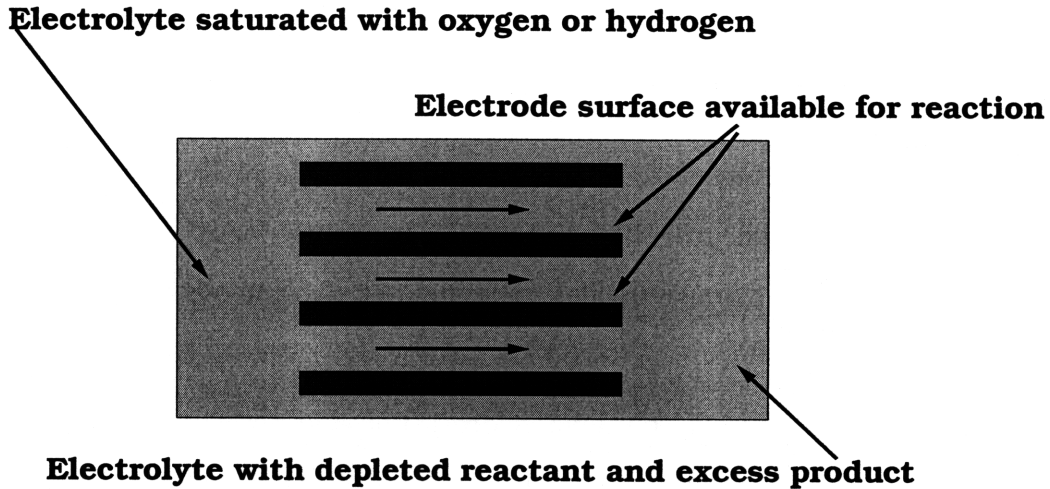


Figure 1-4: Schematic of an Idealized Flooded Electrode

Because the working fluid is the only supply of reactants in a flooded electrode it must deliver both gaseous and ionic reactants and remove water as the product. Herein lies the fundamental problem: covalent fluids, such as the gaseous reactants, are practically immiscible with strongly ionic fluids, such as the aqueous electrolyte.

The solubility of gases is often expressed in terms of the dimensionless Ostwald coefficient L , which is the ratio of the gas volume dissolved, V_{gas} , to the volume of the solvent, V_{liquid} , at a given temperature and pressure.

$$L = \frac{V_{gas}}{V_{liquid}}$$

If a gas obeys the ideal gas law and its solution in an incompressible solvent obeys Henry's law, then it follows that for this solution the Ostwald coefficient depends only on temperature. For hydrogen and oxygen in pure water at 25° C, the Ostwald coefficients are 0.019 and 0.03 respectively, or their solubilities are 1.9% and 3% by volume [87, 39, 56]. The effect of adding an electrolyte, such as KOH, on the solubility

of gases is described by the salting coefficient, k_{sc} , which is defined as

$$k_{sc} \equiv \frac{\log(L^{\circ}/L)}{c} \quad (1.2)$$

where c is the concentration of electrolyte, L° is the Ostwald coefficient for the pure solvent and L is the Ostwald coefficient for the solution of solvent and electrolyte. At 25° C the salting coefficients for hydrogen and oxygen in pure water are 0.132 L/mol and 0.176 L/mol respectively [39, 56]. In a 20 wt% solution of KOH, the Ostwald coefficient for oxygen is 0.003, the solubility is 0.3% by volume, or 10% of that in pure water. The solubility of hydrogen is also approximately 0.3% by volume, or 20% of that for pure water [39, 56].

In contrast to ionic aqueous solutions, hydrocarbon and perfluorocarbon oils are highly covalent and have a very large capacity for dissolving diatomic gases, but are very poor electrolytes. Perfluorocarbons are carbon chain molecules where the hydrogens of a hydrocarbon have been replaced by fluorine atoms. The Ostwald coefficients for oxygen in n-hexane, $n - C_6H_{14}$, are 0.395 at 288.89 K, and 0.296 at 312.44 K, while those in perfluorohexane, $n - C_6F_{14}$, are 0.592 at 288.89 K and 0.366 at 312.44 K [32].

The solubility of one substance in another is fixed, at a given temperature and pressure, by the thermodynamics of their interaction. Increasing the pressure can increase the solubility. However, given the very low solubility of covalent gases in strongly ionic liquids, such as used for fuel cell electrolytes, increasing the pressure only results in a modest increase in the amount of dissolved gas. In addition, it requires additional components, with the associated additional power requirements, weight, cost, etc...

In order to achieve higher gas solubility, it is proposed that the electrolyte be mixed with a fluid that can dissolve large amounts of gas. Such fluids are typically non-polar oils, and hence immiscible with aqueous electrolyte solutions. Since the electrolyte and the oil are immiscible, they can only be mixed for an appreciable period of time by the aid of an emulsifying agent. If the resulting emulsion is of oil

droplets in a continuous aqueous phase, then it can be expected to have the high ionic conductivity of the aqueous phase in addition to having the capacity to dissolve large amounts of gas in the emulsified oil droplets. Emulsified oil droplets are used to increase oxygen transport in biological fermenters [61, 63, 64] and, in research, for artificial blood substitutes [104].

In effect, operating a fuel cell flooded such that there is an increased catalyst area available for reaction is akin to adding electrodes in parallel with the existing electrodes. It is not, however, identical to adding fuel cells in parallel because the area available for ion transfer between the electrodes is not increased. Impedances to the reaction at the electrode surface add in parallel, other impedances in the cell are not directly affected. The changes in the design of a fuel cell and fuel cell stack required to make use of flooded electrodes are discussed in Chapter 6.

This work follows primarily the works of Reti [102]; Holeschovsky [56]; Holeschovsky, Tester and Deen [57]; and Kronberger, Bruckner, and Fabjan [69]. It furthers the work of Reti, and Holeschovsky et al. by studying an electrolyte emulsion that can dissolve significantly larger amounts of reactant gases than a simple electrolyte solution can. It furthers the work of Kronberger by using a concentrate electrolyte solution, closer to the concentrations used in practical fuel cells. Practical considerations for the use of a dispersed phase in fuel cells are discussed (see Chapter 6).

This work was performed in an alkaline medium for three reasons: 1- the formation of emulsions in alkaline media is slightly easier than in acidic media because the acidic media are likely to attack many surfactants, 2- the use of such emulsions would be enhanced by a circulating electrolyte medium and present alkaline cells already have circulating electrolytes [41], and 3- this work follows on work of others who used alkaline aqueous solutions [56, 69, 102].

Chapter 2

A Review of the Literature

In 1962 Reti, under the supervision of Meissner, studied the rate limiting steps in low temperature aqueous fuel cell electrodes [102]. He concluded that at current densities of 10^{-7} to 10^{-4} A/cm² the kinetics of oxygen electroreduction limit the reaction rate. At current densities of 10^{-4} to 10^{-2} A/cm² the chemisorption (chemical adsorption) of oxygen limits the reaction rate, resulting in high overpotentials and what Reti termed “premature deviation from the Tafel line”. The reduction of peroxide, as a secondary step was found to be very fast when compared with the chemisorption of oxygen. See Reti [102] or Kinoshita [65] for a discussion.

Reti operated a six millimeter thick porous carbon electrode (Kordesch type electrode), as a gas diffusion electrode, both with a stagnant gas-liquid interface, and by pumping electrolyte saturated with oxygen through the electrode. As a gas diffusion electrode, he measured a maximum current density of 50 mA/cm². The area used is the projected area of the electrode. With oxygen saturated electrolyte flowing through the electrode he reported a mass transport limited current density of approximately 125 mA/cm². Bubbling oxygen through the electrode to disturb the interface produced transport limited currents of 90-100 mA/cm².

Holeschovsky et al. [56, 57] constructed a fuel cell with platinum wire mesh electrodes through which they pumped an aqueous potassium hydroxide electrolyte. The current densities they observed were low, of order 1 mA/cm², due in part to the low surface area offered by the wire mesh electrodes. When testing porous electrodes

of higher internal surface area they measured currents of 30 mA/cm^2 and concluded that at the flow velocities necessary to generate substantial currents the pressure drop across the electrode would be impractically large. They concluded that the solubility of oxygen in the electrolyte was the main controlling parameter and that increasing it would increase the performance. Holeschovsky [56] suggested the use of fluorocarbons as a means of increasing the solubility.

Kronberger, Bruckner, and Fabjan [69] reported on the reduction of oxygen from perfluorocarbon emulsions in dilute solutions of sodium hydroxide (apparently 0.1 M) with both perfluorocarbon and hydrocarbon surfactants. They found a maximum enhancement of 77% in the mass transport limited currents despite having a four fold enhancement in the oxygen concentration. Enhancements were only observed with perfluorocarbon surfactants. Emulsions stabilized by non-fluorinated surfactants showed mass transport limited currents similar to the single-phase electrolyte. They concluded that the oxygen seemed trapped by the non-fluorinated surfactants. This is somewhat surprising given how thin the surfactant layer is, but is corroborated by the observations in this work. Ju et al. [62] report that the surfactant presents no impedance to the transport of oxygen, but they don't report the surfactants they used except to say that they were non-ionic and non-toxic.

In a flooded fuel cell, the aqueous working fluid must transport the oxygen needed for reaction. The need to transport oxygen in an aqueous environment arises in at least two other fields: biological fermenters, and artificial blood substitutes. Work in the literature relevant to this work falls into three broad categories: 1- the electrochemical reduction of oxygen in fuel cells, 2- the transport of oxygen by organic phases, and 3- the fluid mechanics of dispersed systems and rotating disk electrodes.

2.1 Work on the Electrochemical Reduction of Oxygen

Several authors have studied the electrochemical reduction of oxygen under various conditions. In 1906 Haber [49, 50, 102] measured open circuit potentials for oxygen reduction at temperatures of $300^{\circ}C$ to $1000^{\circ}C$ and found his measurements to be in agreement with the calculated theoretical values. At such temperatures the reaction rates are high, and so equilibrium is quickly established and it is possible to measure the equilibrium potential and reaction rate.

At room temperature, an open circuit potential corresponding to the theoretical value was not measured until 1956 when Bockris and Shamsul-Huq [16] observed that because platinum catalyzed oxygen reaction is very slow at the reversible potential, any impurities are likely to have a dominating effect. Using solutions purified by cathodic and anodic pre-electrolysis to impurity concentrations of less than 10^{-11} mol/liter, they observed a potential of 1.24 ± 0.03 V, in agreement with theoretical reversible potential of 1.23 V. Until then measurements of the open circuit potential at room temperature were approximately 1 Volt [16].

The mechanism of oxygen reduction seems to be poorly understood. For the purposes of this study we are concerned with the case where the reaction is mass transport limited. Consequently, the reaction mechanism is not of great concern, so long as the chemical kinetics can be made fast enough such that the reaction is transport limited. Kinoshita [65] provides a review of oxygen reduction mechanisms.

Several authors have studied the effect of various additives to a fuel cell electrolyte on the reduction of oxygen. Trifluoromethane sulfonic acid in particular has received attention as a candidate electrolyte in fuel cells [2, 3, 8]. Appleby and Baker report an exchange current density for the reduction of oxygen on platinum in 1.1 M trifluoromethane sulfonic acid at $20^{\circ}C$ of 6×10^{-11} A/cm², two orders of magnitude greater than the 4×10^{-13} A/cm² reported in 85 wt% orthophosphoric acid [8]. They attribute this to a reduced activation energy which they state is “probably due to the effect of the heat of adsorption of anions and differences in the heat of solution of

oxygen.” Additionally, they note an effect due to the Arrhenius preexponential term [8, 25].

Adams, Foley, and Barger [2] have demonstrated a ten-fold enhancement in the electroreduction of air in trifluoromethane sulfonic acid monohydrate ($\text{CF}_3\text{SO}_3\text{H} \cdot \text{H}_2\text{O}$). They report open circuit voltages approximately 150 mV higher than the potential observed in phosphoric acid, which they attributed to a reduction in the activation energy of the reaction. However, they observed as well that the monohydrate acid wets teflon which makes it unsuitable for use in teflon bonded electrodes.

Gang et al. [38] found improvements in the performance of a phosphoric acid fuel cell by adding to the electrolyte: potassium perfluorohexanesulfonate ($\text{C}_6\text{F}_{13}\text{SO}_3\text{K}$), potassium nonafluorobutanesulfonate ($\text{C}_4\text{F}_9\text{SO}_3\text{K}$), perfluorotributylamine [$(\text{C}_4\text{F}_9)_3\text{N}$], and polymethylsiloxanes [$(-\text{Si}(\text{CH}_3)_2\text{O} - n)$]. They attributed the enhancements observed to the enhanced oxygen transport rate due to higher oxygen solubility and diffusivity in electrolytes modified with these additives as compared with conventional phosphoric acid electrolyte. This explanation is somewhat surprising given the small (0.5 to 3 percent by weight) amounts of additives they used.

While such enhancements are reported none have made it to practical use. In some cases the authors have not reported why. In other cases the additive interacts with the electrode or electrolyte in ways that make it impractical for long term use (for example, the wetting of the electrode as reported by Adams et al. [2]).

2.2 Work on Oxygen Transport

The simultaneous transport of oxygen and ionic species dissolved in an aqueous solvent has received considerable attention because of its importance in biological fermenters and blood substitutes.

Riess [104] provides a review of blood substitutes and points out that the term is a misnomer “since the products under development only transport the respiratory gases, O_2 and CO_2 , and only for a limited period of time at that. These products provide none of the complex and interrelated metabolic, regulatory, hemostatic, and

host defense functions of blood.”

Perfluorocarbon oils, in particular, have been used as a dispersed phase for enhancing oxygen transport because of their high stability and high oxygen solubility, approximately 52% by volume at 26 °C for perfluorohexane [32]. They have been under development for use in blood substitutes for many years [111, 51, 104], and for Nuclear Magnetic Resonance imaging [31, 78, 112].¹

Because of the low solubility and small diffusivity of oxygen in aqueous media, oxygen transport rates are often the limiting factor in aerobic fermenters [83]. Consequently, the transfer of oxygen in fermenters has received considerable attention, particularly by the use of a dispersed organic phase [61, 63, 64, 83, 105].

Junker, Hatton, and Wang [63, 64] have reported enhancement ratios of five to ten using a dispersion of 75% perfluorocarbon. Ju, Lee, and Armiger [61] show similar results. Mehra has reported on the enhancement of multiphase reactions with the introduction of a gas dissolving microphase [84, 85] and on the modeling of oxygen transport from blood substitutes [84, 85, 86].

In fermenters there is often sparging by gas, and stirring vigorous enough to produce turbulence in some cases. In fuel cells, as a consequence of the desire for larger reaction areas, the length scales are very small. Consequently, the transport of species within the electrode pores is purely diffusive.

Lowe [75] provides a review of the use of perfluorocarbons in cell culture media. Pratt et al. [99] report a quantitative study of perfluorocarbons in biological tissues using magnetic resonance spectroscopy.

It should be noted that as of this writing there are no commercially available blood substitutes, perfluorocarbon based or otherwise. Perfluorocarbons are relatively inert, but they have been connected with adverse effects on the environment and on human health [74].

Although many have reported on the modelling of mass transport in dispersed

¹NMR spin-lattice relaxation rates of perfluorocarbon emulsions are highly sensitive to oxygen tension (partial pressure of oxygen), which is a measure of tissue health. The NMR spectra of perfluorocarbons is also sensitive to temperature, which facilitates NMR thermometry. See Mason [78] for more detail.

media [62, 86], Dumont and Delmas [33] lament the lack of a “unique theory explaining the influence of the presence of an immiscible oil on mass transport enhancement.” This can be attributed, at least in part, to the differing hydrodynamic behavior of dispersed particles in a continuous medium under different hydrodynamic conditions.

Many authors have demonstrated that the flow of dispersed particles in a continuous fluid is quite complex. It cannot be assumed that the particles are evenly distributed, particularly near the walls. Depending on the nature of the flow and the nature of the particles they may be, in effect, repelled by or attracted to the walls, and may collect at some location in the flow. Ho and Leal discuss the migration of spheres suspended in a flow [54, 55]. They report effects due to the nature of the flow, variations in the density of the spheres, and their deformability. de Ficquelmont-Loizos et al. [28] and Caprani et al. [21] provide a data for and a discussion of particulates in a flow induced by a rotating disk electrode. They report effects due to the properties of the particles, the fluid, and disk, including the material the disk is made of. See Ungarish, p.56 [122] for a discussion of particles in rotating fluids.

2.3 Emulsions

The terms emulsion and dispersion are used to refer to a liquid that consists of two immiscible phases, one of which is dispersed as small droplets or particulates in the other. The terms are often used interchangeably in the literature and they are in this work. Typically, the two phases are an aqueous phase and an organic phase, referred to as the *water* and *oil*, respectively.²

Because oil and water are immiscible, a mixture of the two can only be formed by dispersing one liquid in the other and stabilizing the interface with an emulsifier, or surface acting agent (surfactant). Such a dispersion, if not stabilized by a surfactant, will separate into a continuous oil phase and a continuous aqueous phase to minimize the energetically unfavorable oil-water interface. If stabilized by a surfactant the

²Common examples of an oil in water emulsion are milk, or salad dressing. Examples of water in oil emulsions are margarine, butter, and various hydrated petroleum products.

separation can be delayed for long enough that the emulsion appears stable over the time scale of interest. While a surfactant may slow the kinetics of separation, emulsions in general are thermodynamically unstable and ultimately they must separate. Microemulsions are a notable exception (see Hiemenz and Rajagopalan [52] p. 389). Microemulsions were not considered in this work.

In order for the working fluid in a flooded fuel cell to have the desired high ionic conductivity, the aqueous phase must be continuous. The stabilization of an emulsion relies on a repulsive force between the dispersed oil droplets to oppose the attractive van der Waals forces and prevent the droplets from coalescing. This repulsive force can be due to an electrostatic or a steric repulsion, or by the presence of particulates at the surface of the emulsified droplet. Tadros considers these cases in some detail [117].

Electrostatic repulsion acts when the dispersed phase droplets acquire a surface charge, either by the formation of an electrical double layer, or by the adsorption of molecules with ionic moieties³ exposed to the continuous phase. The classic theory describing the balance between attractive and repulsive forces in a dispersion is the Derjaguin Landau Verway and Obverbeek theory, most often referred to as the DLVO theory. See Hiemenz and Rajagopalan [52] p. 585 for an introduction to the DLVO theory. See *ibid* p.604 for a discussion of non-electrostatic stabilization, and p. 575 for a discussion of electrostatic and polymer induced stability.

Albers and Overbeek [5] point out that the DLVO theory cannot be applied to most oil in water emulsions because of the very low dielectric constant of most oils. Because of the low dielectric constant of the oils, the electrostatic forces act over a distance considerably larger than the size of the oil droplets.

The presence of relatively small concentrations of electrolyte (of order 10^{-3} M) dramatically reduces the length over which electrostatic repulsion acts between droplets. The very high concentrations of electrolyte necessary to give a fuel cell electrolyte its ionic conductivity result in a dramatic screening (shortening) of the distance over which the electrostatic effects are felt from one drop to the next. Over such small dis-

³the functional part or group of a molecule

tances, the van der Waals forces dominate electrostatic forces with the result that one cannot hope for electrostatic stabilization in any practical fuel cell electrolyte. Figure 2-1 depicts the effect of added electrolyte on the electrostatic double layer interaction. See Hiemenz and Rajagolapan [52] or Israelachvili [59] for further discussion.

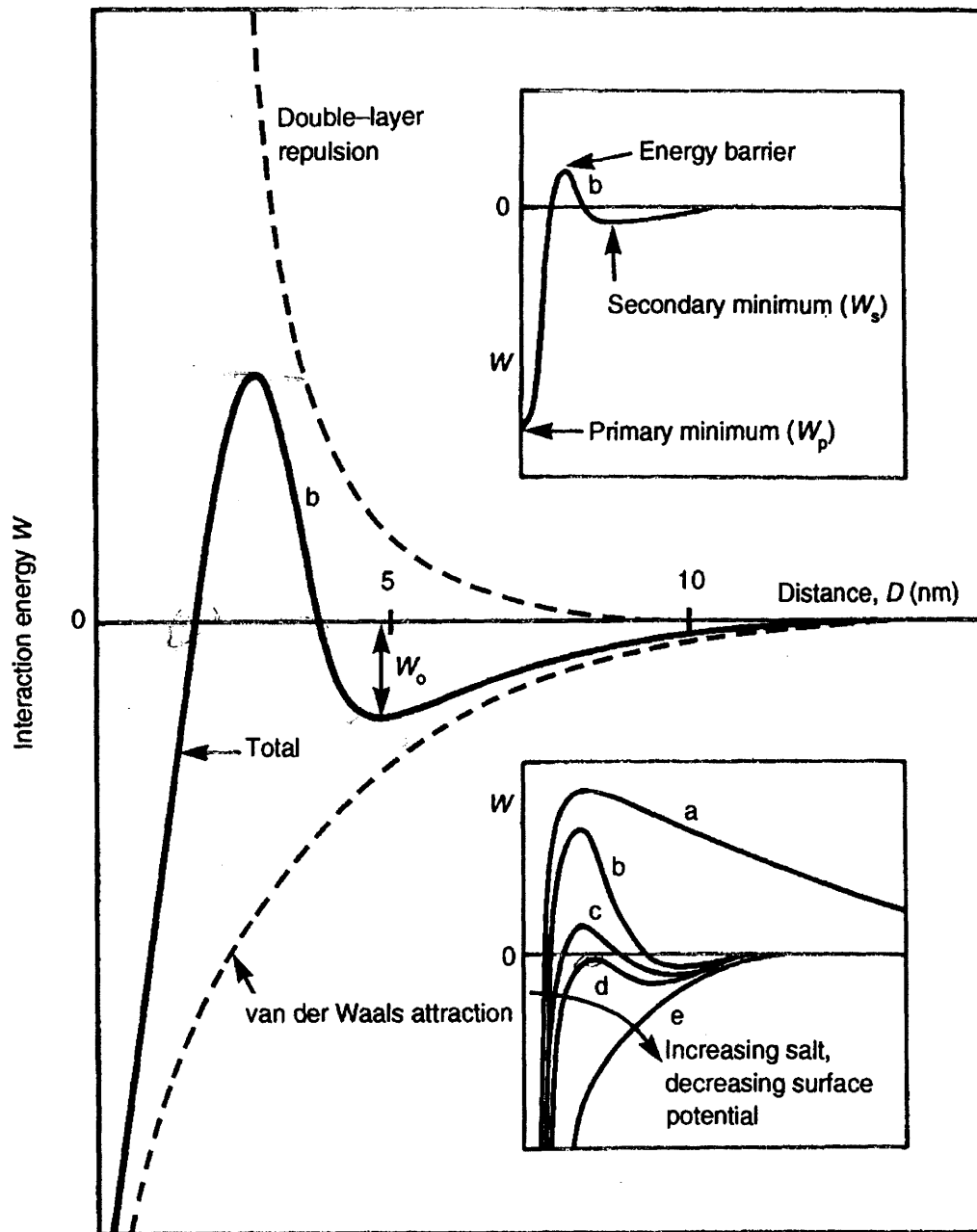


Figure 2-1: The effect of adding electrolyte on electrostatic repulsion. Taken from J. N. Israelachvili, Intermolecular and Surface Forces.[59]

Pashley [95] reports that the degassing of an oil and water mixture results in the spontaneous emulsification of oil drops in the water, approximately 5% by volume. The volume fractions of oil in the emulsions reported by Pashley, and in the emulsions formulated in this work using his techniques, are in rough agreement and are too small to be of practical importance to this work. We found that these emulsions destabilized with the addition of small amounts of potassium hydroxide, rendering them impractical for our use. Consequently, no attempt was made to quantify the amount of potassium hydroxide required to destabilize the emulsion. Francis and Pashley [35] report that the degassed dispersion of oil in water is stabilized in the pH range of 7-10. Maeda et al. [76] report that the addition of salts has no effect on the stability of degassed emulsions, neither does increasing the pH to 11. They do not report data beyond a pH of 11.

Because of the complexity of colloidal systems, theoretical predictions of their behavior are often very difficult. There are, however, various empirical rules. One of the more common of these rules is due to W.D. Bancroft, which he provided without explanation [10, 11].

Bancroft stated that the liquid in which the emulsifying agent is more soluble will form the continuous phase of the emulsion. The rule holds generally true, except when the volume of the dispersed phase exceeds about 70% of the total volume of the dispersion. Bancroft's rule can be explained heuristically based on the geometric arrangement of the surfactant molecules. If a surfactant is hydrophilic, it can be expected to have a hydrophilic component larger than its hydrophobic component. The surfactant molecules can then be expected to arrange such that the larger end is on the outside of a droplet where more volume is available. The result is an oil in water emulsion, as predicted by Bancroft for a hydrophilic surfactant. The opposite case is also true. See Morrison and Ross [88] for a further discussion.

In an attempt to provide a quantitative means for surfactant selection, W.C. Griffin developed the Hydrophilic-Lipophilic Balance (HLB) [45]. A value of one on the scale was assigned to oleic acid, and a value of 20 to sodium oleate. The HLB number is based on the mass fraction of oleic acid and sodium oleate. Other

surfactants are then tested and assigned a number that corresponds to the mix of oleic acid and sodium oleate that most closely approximates the behavior of the surfactant. See Morrison and Ross [88] pg. 429, or Hiemenz and Rajagopalan [52] p.352.

Chapter 3

Modelling

The purpose of this chapter is to estimate the enhancement of oxygen transport¹ possible from the use of an emulsified perfluorocarbon phase. Dumont and Delmas [33] point out there is not a unique theory that can be applied to mass transport in a dispersion. It is most convenient to treat the dispersion as a homogeneous medium with appropriate representative values. Mehra [85] suggests that the average concentration can be used, but also presents a heterogeneous model [86]. The approach here is to use mass transport models for homogeneous media, with effective values used for the emulsion.

Gregory and Riddiford [44, 103] have shown the transport limited current density from a horizontal rotating disk to be given by

$$i_{lim} = \pm \frac{0.554}{I(\infty)} zFD^{2/3}\nu^{-1/6}\omega^{1/2}C(\infty) \quad (3.1)$$

where z is the number of electrons per mole of reactants, F is Faraday's constant, D the diffusivity of the reactant in the bulk medium, ν the kinematic viscosity, and $I(\infty)$ is given by

¹While *transfer* typically refers to a short range transfer, such as the transfer at the surface of an electrode, *transport* typically refers to transport over longer distances, such as transport to the surface of an electrode. The two are often used interchangeably in the literature. Transport is usually used in this document, except where necessitated by convention, such as when referring to mass transfer coefficients.

$$I(\infty) = 0.8934 + 0.316 \left(\frac{D}{\nu} \right)^{0.36} \quad (3.2)$$

They report that Equation 3.1 offers a 3% improvement in accuracy over Levich's famous result

$$i_{lim} = 0.62nFD^{2/3}\nu^{-1/6}C_{\infty} \quad (3.3)$$

Thus, if D , ν , and C_{∞} can be determined for an emulsion, it can be treated as a homogeneous fluid. Equation 3.1 can be used to find the transport limited current from the rotating disk.

Ju, Lee and Armiger [62], present a method for calculating transport from an emulsion based on effective diffusivity. The approach is modeled after that used by Maxwell [80] for the effective electrical conductance of dilute two phase dispersions of spherical particles. They present Maxwell's famous result as

$$K_{eff} = \frac{K_d + 2 - 2f_d(1 - K_d)}{K_d + 2 + f_d(1 - K_d)} \quad (3.4)$$

where $K_{eff} = k'_{eff}/k'_c$ and $K_d = k'_d/k'_c$; k'_{eff} is the effective conductivity of the dispersion; k'_d is the conductivity of the dispersed particle; k'_c is the conductivity of the continuous liquid phase; f_d is the volume fraction of the dispersed phase. They then derive the result

$$\frac{D_L k_L}{D_w k_w} = \frac{\frac{1}{R_{w2}} - \frac{1}{R_{w1}}}{\frac{1}{R_{L2}} - \frac{1}{R_{L1}}} \quad (3.5)$$

where D is the diffusivity, k the concentration, and R the reading of their oxygen electrode, which provides a measure of the oxygen partial pressure. The subscripts w and L refer to pure water and a test liquid, respectively. By comparing the oxygen saturation at an electrode separated from a pure oxygen atmosphere by a thin layer of the test liquid they were able to determine the permeability of the test liquid relative to pure water. The concentration of oxygen in the test liquid is

$$k_L = f_{PFC}k_{PFC} + (1 - f_{PFC})k_w \quad (3.6)$$

where f_{PFC} is the volume fraction of the perfluorocarbon in the test liquid, k_{PFC} is the solubility of oxygen in the pure perfluorocarbon, and k_w is the solubility of oxygen in pure water. Then, an effective diffusivity can be calculated based on the measured permeability and the average concentration of oxygen in the test fluid. The minimum value reported by Ju et al. for the diffusivity of oxygen in the test dispersion is one half of that in the continuous phase. They reported this value for a test dispersion with a PFC volume fraction, f_{PFC} , of 0.1379. The volume fraction used in this work is 0.15. The emulsion in this work is treated as having an oxygen concentration equal to k_L , the volume average oxygen concentration of the emulsion, and a diffusivity equal to half that of oxygen in the continuous phase. Mehra's suggestion that the average concentration can be used with no adjustment to the diffusivity is also presented, and considered an upper bound.

Figure 3-1 shows the calculated transport limited current for a disk rotating in an emulsion of 15 % perfluorohexane in water, by volume.

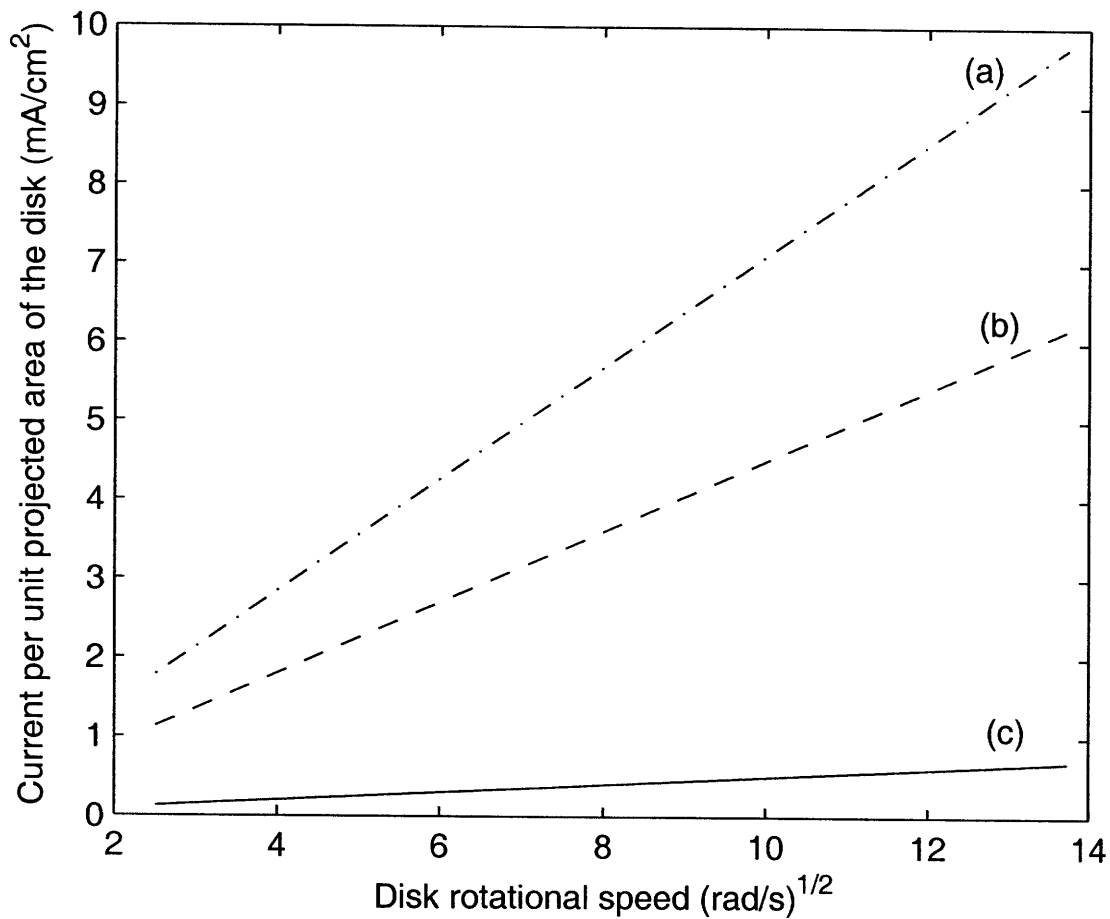


Figure 3-1: Predicted mass transport limited current flux for a rotating disk electrode in an emulsion of 15% by volume perfluorohexane in a 20 wt% solution of KOH (lines a and b) and in a solution of 20 wt% KOH with no dispersed phase (c). In both cases the liquid is saturated with oxygen at 1 atm pressure. Line a) assumes the diffusivity of oxygen in emulsion is that of the continuous phase ($0.92 \times 10^{-9} \text{ m}^2/\text{s}$) and the concentration is the volume average concentration b) assumes the same concentration as a) with diffusivity equal to half that of the continuous phase, as suggest by Ju et al. [62]

3.1 The Wire Mesh Electrode

Wire mesh electrodes were used by both Reti and Holeschovsky. The previous section was concerned with transport limited currents and so no mention was necessary of the chemical kinetics. This section calculates, using conventional models, the currents expected from wire mesh electrodes with an oxygen saturated emulsion pumped through them. To estimate the benefit of using a perfluorocarbon emulsion in fuel cell electrode, one must combine a model of the chemical kinetics with that for mass transport. The model for the fluid is as used in the previous section, but Mehra's suggestion of using the diffusivity of the continuous phase unmodified is used, with the consequence that the predictions in this section should be viewed as an upper bound. The electrochemical model has long since been developed. A version of Equation 3.7, with some rearrangement, appears in most electrochemistry texts (see, for example, Bard and Faulkner [13], First ed., Equation 3.5.32 p.109). Equation 3.7 gives the Faradaic current² per unit electrode area, i , as a function of the deviation of the electrode potential, E , from the equilibrium electrode potential, E_{eq} and a number of electrochemical and transport parameters. The deviation of the electrode potential from the equilibrium is captured by the term $\eta = E - E_{eq}$, often referred to as *the electrode overpotential*.

$$i = i_o \left[\frac{e^{-\alpha f \eta} - e^{(1-\alpha) f \eta}}{1 + \frac{i_o e^{-\alpha f \eta}}{i_{i,O}} + \frac{i_o e^{(1-\alpha) f \eta}}{i_{i,R}}} \right] \quad (3.7)$$

where i_o is the exchange current density; α is the transfer coefficient³; $f = nF/RT$, where n is the number of moles of electrons per mole of reaction; F is Faraday's constant, the charge per mole of electrons, R the universal gas constant, and T the absolute temperature; $i_{i,O}$ and $i_{i,R}$ are the transport limited oxidation and reduction currents, respectively.

²The Faradaic current is the current due to net reaction at the electrode, to be distinguished from, for example, a capacitive charging current.

³The transfer coefficient is a measure of the symmetry of the activation energy barrier to the forward and backwards reactions, i.e. for a given change in the electrode potential, α captures the relative changes in the forward and backward reaction rates

If the parameters in Equation 3.7 can be evaluated, then the current from the electrode can be predicted over the entire range of electrode potentials, from equilibrium where the reaction is dominated by the chemical kinetics, to where the reaction is dominated by the transport kinetics.

The transport limited currents $i_{l,O}$ and $i_{l,R}$ can be written in terms of the mass transfer coefficients as

$$i_l = zFm_jC_j^* \quad (3.8)$$

where m_j is the mass transfer coefficient of species j , and C_j^* , the bulk concentration species j . Species j can represent either the oxidized species, O , or the reduced species, R . Because the reaction is transport limited, reactants are consumed as they arrive at the electrode surface and the concentration at the electrode surface is taken to be zero. If Equation 3.8 is substituted into Equation 3.7, the result,

$$i = i_o \left[\frac{e^{-\alpha f\eta} - e^{(1-\alpha)f\eta}}{1 + \frac{i_o e^{-\alpha f\eta}}{nFm_O C_O^*} + \frac{i_o e^{(1-\alpha)f\eta}}{nFm_R C_R^*}} \right] \quad (3.9)$$

can then be used to evaluate the current from the electrode as a function of electrode potential, given the values of the remaining parameters. Values for i_o , and α , are measured and reported in the literature under various conditions, though reports vary widely [12].

The mass transfer coefficients, m_O and m_R , for the oxidized and reduced species, respectively, can be calculated for some simple laminar flow cases. Otherwise they are measured or deduced by analogy to measured heat transfer coefficients.

Much work has been done on determining mass transfer coefficients to wire screens and packed beds of wire screens using homogeneous media. Cano and Böhm [20] measured the mass transfer coefficients to wire mesh screens by measuring the mass transfer limited current of an electrochemical reaction and using relation 3.8.

Coppola and Böhm [26] modeled mass transfer to wire mesh screens as flow around cylinders and flow to a collection of screens as flow through a duct. They have also compiled data from others and fitted it to the correlation due to Hilpert [53, 26]

$$Sh = ASc^{0.33}Re^b \quad (3.10)$$

where Sh is the Sherwood number, Sc the Schmidt number, and Re the Reynolds number, defined as

$$\begin{aligned} Sh &= \frac{md}{D} \\ Sc &= \frac{\nu}{D} \\ Re &= \frac{Ud}{\nu} \end{aligned}$$

respectively. As before, m is the mass transfer coefficient, d the wire screen diameter, D the diffusivity of the transferred species, ν the kinematic viscosity of the bulk fluid, and U the flow speed. The average values of the published data collected by Coppola and Böhm for the coefficients A and b in Equation 3.10 are 0.82 and 0.359 respectively, which is in reasonable agreement with the results of Hilpert [53], and Knudsen and Katz [66] who report for $Re = 0.4$ to 4 , 0.989 for A and 0.330 for b . For $Re = 4$ - 40 the reported values of A and b are 0.911 and 0.33 respectively [58].

Given the large range of Reynolds number to which Coppola and Böhm's correlations apply ($Re = 2 \times 10^{-3}$ to 45), they should be considered in good agreement with those of Hilpert, and Knudsen and Katz. In light of the range of Reynolds numbers to which each correlation applies, the deviation of Holeschovsky's results from Coppola and Böhm's correlation can be explained by the low Reynolds numbers in a flooded fuel cell. Typical Reynolds numbers vary from 0.3 to 3 ($U = 0.01$ to 0.1 m/s, $d = 43 \times 10^{-6}$ m, $\nu = 1.36 \times 10^{-6}$ m²/sec).

The mass transfer coefficients used in calculating the figures in this work are obtained from Equation 3.10 with $A = 0.82$ and $b = 0.33$ where a lower value for b is used because of the low Reynolds numbers calculated for the flooded fuel cell design.⁴

⁴The slight discrepancy between measured and calculated results in Holeschovsky's work may be due to his choice of a value for b that is averaged over the entire range of Reynolds numbers where the relations are valid, whereas the fuel cell experiments are at relatively low Reynolds numbers.

With these mass transfer coefficients, it is possible to plot Equation 3.9 for various concentrations of the perfluorocarbon phase in the emulsion.

Given the lack of a proper mass transport model from a dispersed medium, one cannot place much confidence in these models. However, they serve as a guideline to encourage further investigation. The diffusivity used is that of the continuous phase, and the concentration is the average concentration in the emulsion. These values were used, as suggested by Mehra, in the expectation that flow through wire mesh electrodes more closely resembles the flow in Mehra's work than it does the flow to a rotating disk, reported by Ju et al. It was expected that some of the emulsion droplets may interact with the electrode surface, therefore exposing it directly to the average concentration of the bulk fluid. The results below should be viewed as an upper limit.

The same type of calculation was carried out for various flow speeds, for the oxidation of hydrogen as well as the reduction of oxygen, and for a porous electrode such as those used by Reti. Ultimately, the experimental results show that these predictions are wrong, and so they will not be discussed further. They are here simply as a means of outlining the procedure and to demonstrate a sample of the results. As discussed in the Conclusions, a more thorough transport model is needed.

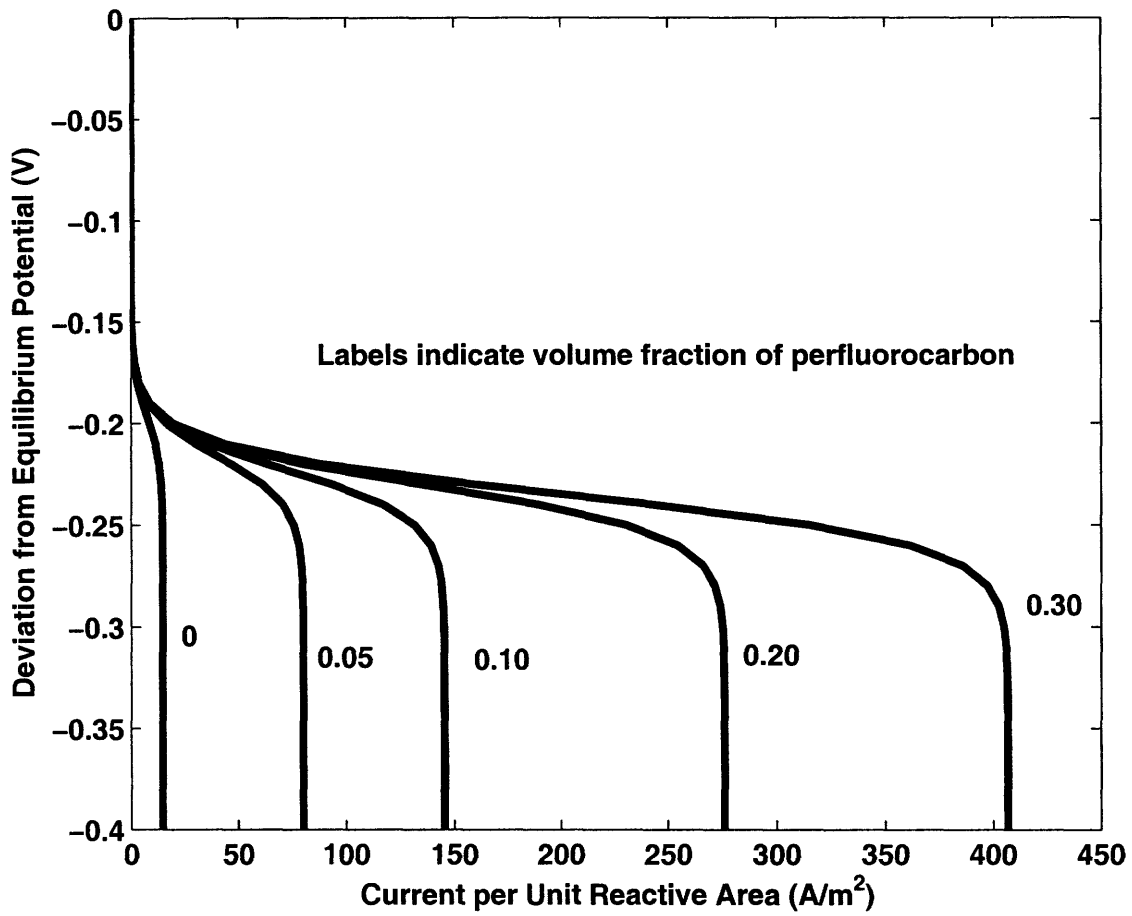


Figure 3-2: The effect of varying volume fractions of perfluorocarbon on the current from oxygen reduction on a wire mesh screen electrode with a flow speed of 0.01 m/s, with $i_0 = 10^{-10}$ A/cm², and $\alpha = 0.54$ [12].

Chapter 4

Experimental Setup and Procedures

The purpose of the experiments is to evaluate the effect of an emulsified perfluoro-carbon phase on the oxygen transport properties of a highly ionic aqueous fluid. The effect is determined by measuring the transport limited rate of oxygen reduction from an emulsion of perfluorohexane in 20 wt% KOH, and comparing it with the transport limited rate of oxygen reduction from the 20 wt% KOH solution with no emulsified perfluorohexane.

4.1 The Rotating Disk Electrode

A rotating disk electrode of the shape shown in Figure 4-2 was used, following the suggestion of Blurton and Riddiford [15]. The electrode shape used by Blurton and Riddiford is shown in Figure 4-1. They reported on this shape to a maximum rotational speed of 240 rpm. The active region of the disk they used was of diameter 3.32 mm. Blurton and Riddiford tested electrode housings with three different ratios of maximum radius to minimum radius. Not surprisingly, the electrode with the largest ratio of maximum to minimum radius gave the results closest to the theoretical prediction, with 1% error. The maximum diameter of the electrode housing used by Blurton and Riddiford was 26.4 mm and the minimum housing diameter was

12.1 mm.

In this work, the diameter of the active platinum electrode was 4.39 mm. In an attempt to increase the range of rotational speeds over which the results conform to theory, the ratio of the major diameter of the disk to the minor diameter was approximately 3, with the minor diameter being limited by the structural integrity of the teflon housing, to about 4.5 mm. The result was a disk as shown in Figure 4-2. The major diameter was limited by the size of the inlet to the reaction vessel, and the robustness of the fine edge. The dimensions used here seem to have produced satisfactory results, and so weren't adjusted further. The electrode is suspended such that the fluid level is as close as possible to the minor diameter without the shoulder interfering with the free surface.

After the platinum disk was mounted into the teflon body, the platinum-teflon surface was polished while mounted on the rotating disk shaft and the shaft mounted in a holder to ensure that the polished surface was flat and orthogonal to the axis of disk rotation. They were polished with progressively finer alumina grits to 0.3 μm , then with a clean felt polishing wheel. The disk was then cleaned with acetone and distilled running water, and soaked in a mix of sulfuric and nitric acids overnight, then rinsed with distilled water again. Sonication is often prescribed to remove particles from polishing. It was not used in this case.

The rotating disk was a solid teflon housing into which a platinum disk is pressed. This eliminated the leakage problems encountered with the housing supplied by Pine Instruments corporation which was assembled of several pieces (Figure 4-3). The Pine Instruments electrode was not used because, based on their results Blurton and Riddiford [44, 103] suggest that disks of the Pine Electrode shape are not suited for quantitative work.

To ensure minimal eccentricity, the teflon housing was machined while mounted on the shaft to be used in the setup. Two identical housings were made. The first of these housings was concentric such that no eccentricity could be detected. Because teflon is white and offers no color contrast, it was impossible to determine visually whether the shaft was spinning or not, even at several thousand revolutions per minute. A

later version of the electrode did have some slight eccentricity (approximately $25\ \mu\text{m}$), but the eccentricity does not seem to have adversely affected the results.

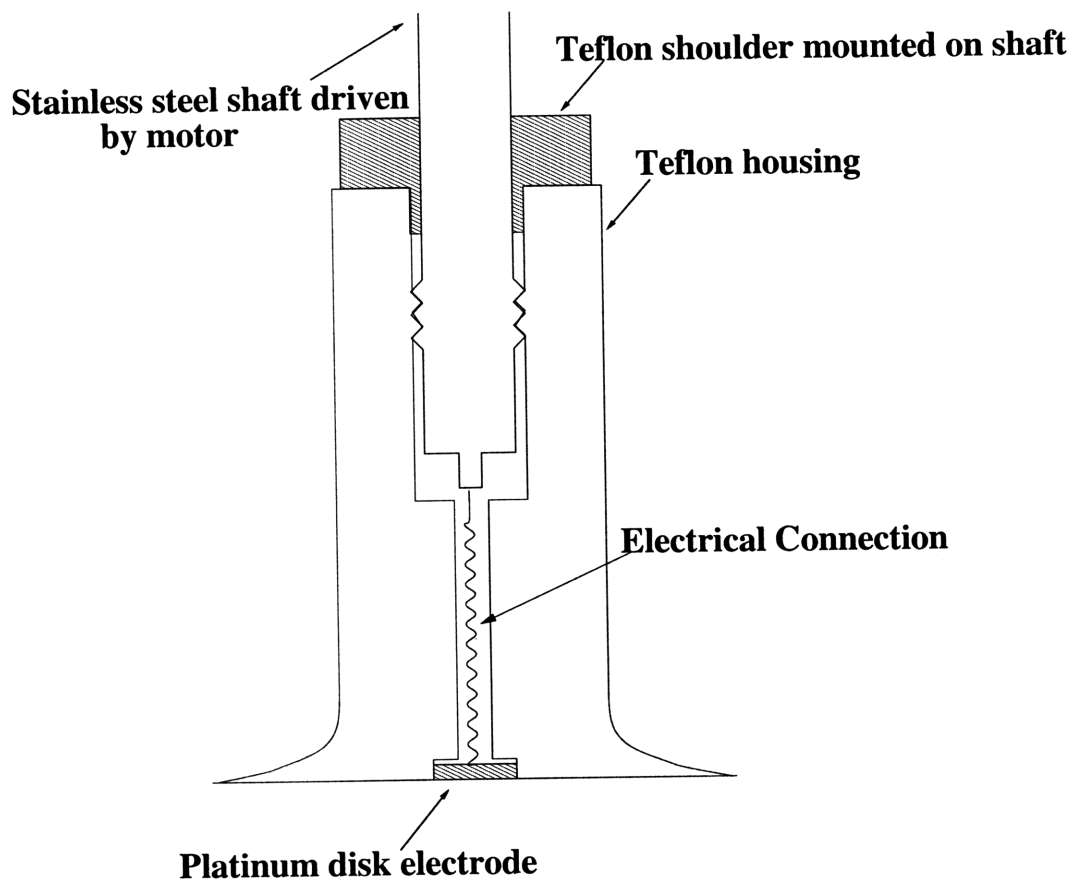


Figure 4-1: The rotating disk electrode shape suggested by Blurton and Riddiford [15]. The major diameter of the disk is 26.4 mm. The minor diameter is 12.1 mm.

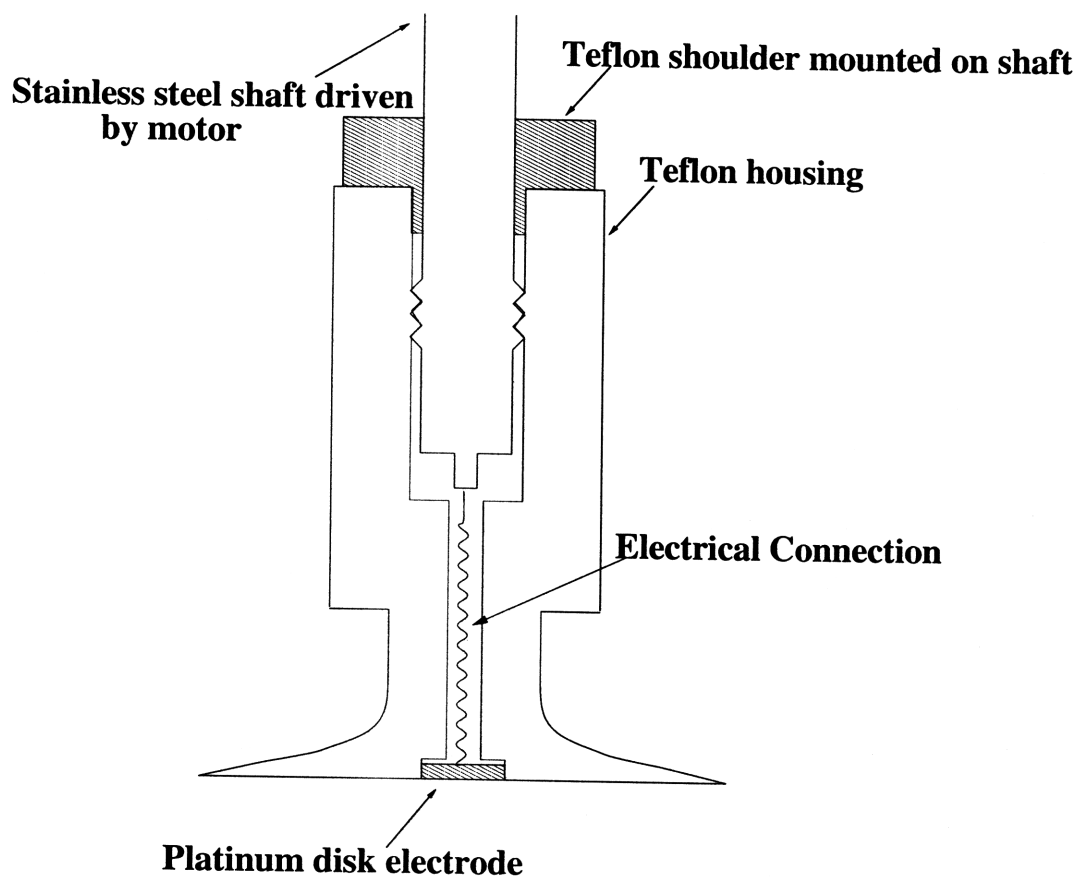


Figure 4-2: The rotating disk electrode used in this work. The minimum diameter is 4.5 mm and the maximum diameter is three times that. The disk is immersed in fluid such that the fluid level is just below the shoulder, but far enough from the shoulder not to be affected by it.

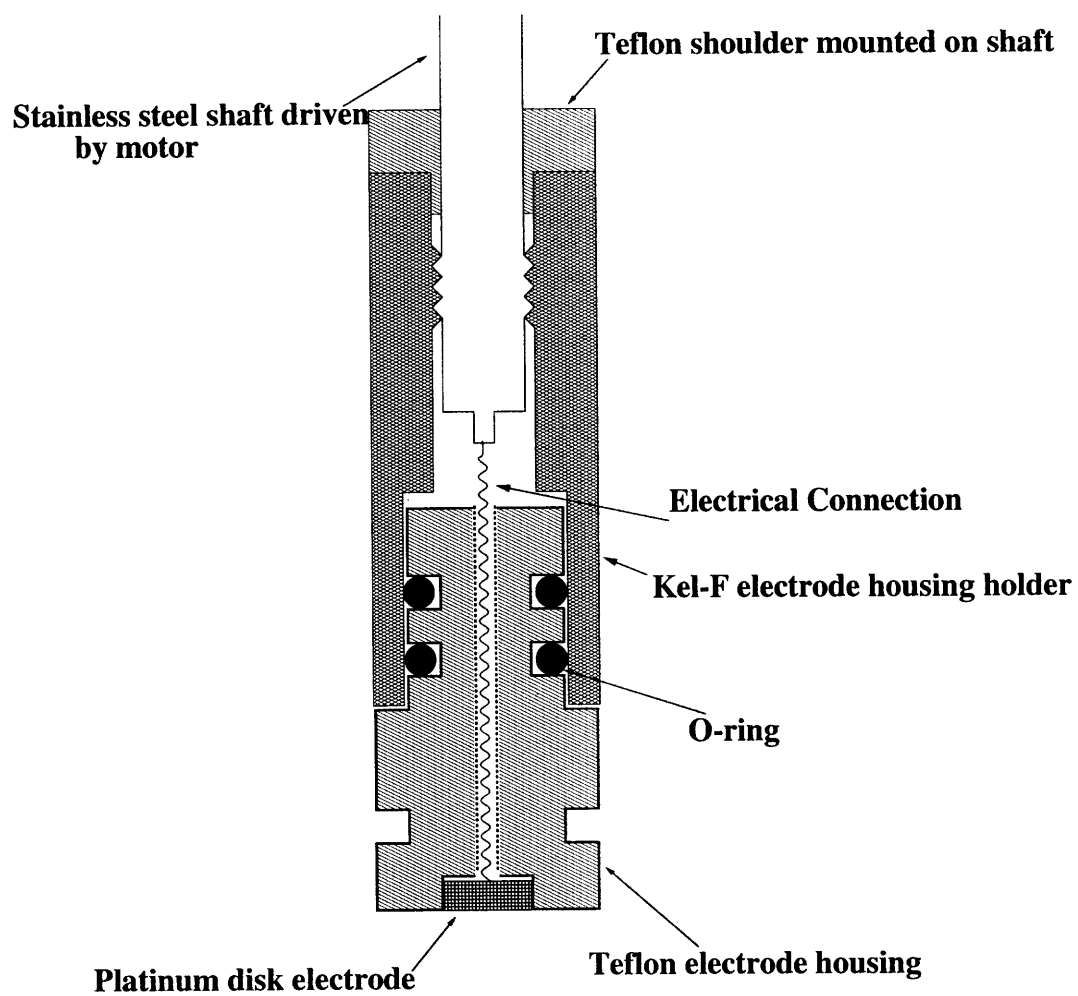


Figure 4-3: The rotating disk electrode supplied by Pine Instrument Company.

4.2 The Oscillating Electrode

The results of the rotating disk electrode experiments indicated that the surfactant used to stabilize the emulsion was participating in the reaction. To eliminate the effect of the surfactant, Professor Donald Sadoway suggested the use of a vertically oscillating electrode [1] to traverse the interface between a continuous aqueous phase and a continuous perfluorocarbon phase in the absence of a surfactant, as shown in Figure 4-4. The oscillating electrode was used by Pint and Flengas [96] in high temperature liquids where reactants are transferred by convection currents induced by heating elements as well as the fluid flow induced by the electrode under study.

For the reaction of interest in this work, the reciprocating apparatus alternately exposes the electrode to an aqueous phase and a non-aqueous phase. The aqueous phase provides the ionic components of the reaction and acts as a sink for the aqueous products, while the non-aqueous phase provides a higher concentration of oxygen. In this manner, the reduction of the oxygen directly from the perfluorocarbon can be studied without effects from the surfactant. Implicit is the assumption that reactants adsorb onto the surface and so can be carried by the electrode from one phase into the other.

A rotating disk electrode which rotates about a horizontal axis with the aqueous-perfluorocarbon interface at the level of the axis was considered as a means of studying the system in the absence of a surfactant. The oscillating electrode was chosen because the hydrodynamics of the horizontal rotating disk would distort the interface making it difficult to draw conclusions.

The electrode was a 0.5 mm diameter platinum wire coated in 3 mm diameter soda-lime glass sleeve. The ratio of platinum to glass area was 0.0278, within in the range reported by Pint and Flengas where surface area ratios do not affect results. Soda-lime glass was used because the thermal expansion coefficient matches almost exactly that of platinum (8.8×10^{-6} for platinum, and 9×10^{-6} for soda-lime glass).¹

¹It is apparently because of this match in thermal expansion coefficients that platinum is used with soda-lime glass for the sealing of vacuum apparatuses. It is possible, if the part is carefully cooled, to coat the wire in a glass of somewhat mismatched thermal expansion coefficient. However, the resulting piece will have residual stresses which make it more likely to fracture. Whether it

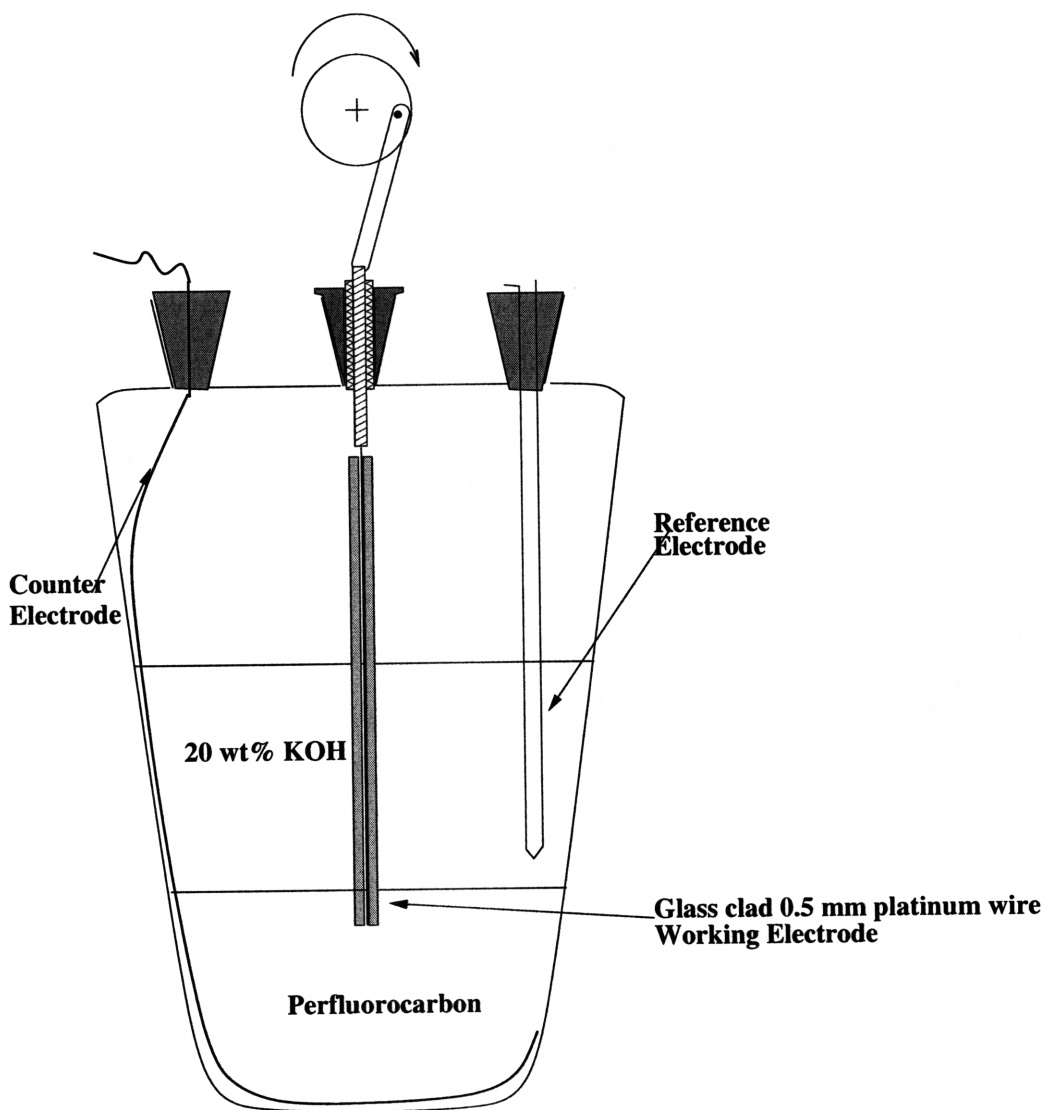


Figure 4-4: A diagram of the reciprocating electrode used to traverse two phases

The electrode was coated by drawing glass tubes a few meters long with an outer diameter of approximately 3 mm, and an inner diameter just large enough to insert the 0.5 mm platinum wire. From a glass tube drawn to a few meters, the majority of the length was of uniform wall thickness and inner hole size over the 150 mm length of the platinum wire to be coated. By selecting a 150 mm piece closer to the ends or closer to the center of the long tube it was possible to select slightly different wall thicknesses. The wire was then inserted into the glass and the glass melted onto the wire at one end with a MAPP gas torch. The wire was then mounted in a vertical drill press. Three MAPP gas torches were placed evenly spaced on a circle so as to provide radially even heating of the glass. The drill press was then used to rapidly push the wire with glass coating down through the flames and slowly draw it upward, softening the glass and causing it to collapse onto the wire. With some practice it was possible to produce uniform cylindrical coatings of the wire. The drill press was not used to rotate the wire because the minimum rotation speed of the press (approximately 150 rpm) was too high. Rotating the wire at some tens of rotations per minute could make it easier to produce a uniform coating. The diameter of the outer coating cannot be controlled very precisely by this method, but it was possible by trial and error to obtain a diameter within a few tenths of a millimeter of the desired, which was more than sufficiently accurate for our purposes. Pint and Flengas report that the results are not influenced by total electrode area when the area of the active area of the electrode is between 2.5% and 5% of the total area of the electrode. They do not report data above 5%. The glass was then scored and broken, and the glass-platinum interface sanded flat, then polished. The sanding and polishing were done with the electrode in a holder that kept it vertical such that the result was a right cylinder. The edges were very lightly rounded to avoid the hydrodynamics of flow around a sharp corner.

The electrode was oscillated by a crank arm mounted on the shaft of a speed

fractures or not depends on how carefully the electrode is handled and the environment it is exposed to. For example, spraying acetone on the glass surface cooled it enough rapidly enough to crack Pyrex on a steel test wire. It also happens that soda-lime glass is what was available in the MIT glass blowing shop.

controlled motor (the same one as used for the rotating disk electrode, mounted as in Figure 4-4). The electrode wire was mounted by passing it through a tight fitting hole in a teflon cylinder. The teflon cylinder fit into a teflon stopper with a hole, providing a close clearance fit for the cylinder. The combination of teflon cylinder in teflon stopper made a bearing that also provided adequate sealing for the reaction vessel.

If the electrode attachment is not rigid enough the vertical oscillation of the electrode can produce small lateral vibrations, particularly at higher speeds. In this case the problem was minimized by abutting the glass cladding almost to the teflon plunger, thereby relying on the lateral stiffness of a very short and reasonably stiff piece of the platinum wire for rigidity. The verticalness of the electrode was checked by hanging a plumb line by the electrode, rotating the electrode and making any adjustments necessary. At higher oscillation speeds a slight out of plane vibration could be observed. It could be remedied by affixing the teflon plunger to the glass sleeve (either by glue or heat, or by forming the electrode in a different manner). The effect of any vibration was assumed negligible for first experiments, to be improved upon if necessary in later experiments. No effect was observed. Given the nature of the results in our trials this further work was not justified.

The electrode was positioned such that the oil-water interface was at the mid-point of the stroke. The electrode was set to the mid-point of its travel by rotating the crank mechanism 90 degrees from the top electrode position (almost the position depicted in Figure 4-4). The reaction flask was then moved vertically until the electrode was at the interface. Because of the different affinities of the oil and water for the glass, and the difference refractive indices, it was easy to see when the electrode started to interact with the oil-water interface.

4.3 Measurements and Data Collection

The data were collected using a Solartron 1287 potentiostat operated by Corrware software. A circuit diagram for the cell and potentiostat is shown in Figure 4-5.

A typical three electrode setup was used. The counter-electrode was a 90% platinum 10% iridium wire mesh of $43\ \mu\text{m}$ (0.0017 in) diameter wires, with 5.9 wires/mm ($150\ \text{wires/in}$)² of area per centimeter length approximately 30 times the area of the rotating disk electrode and 200 times the area of the oscillating electrode.

The reference electrode was Hg/HgO in 20 wt% KOH, purchased from Koslow Scientific. The potential of the reference electrode is +0.098 V versus the Normal Hydrogen Electrode at 25 °C.

Because of the small area of the working electrodes, particularly the reciprocating electrode, the measured currents are in the range of microamps, and therefore easily affected by any electronic noise. For example, it was observed that switching then temperature controller on had a significant effect on the measured currents. The effect was not through altering the temperature of the system because it was noticeable immediately when the controller was turned on, before the system could have responded thermally. It was also observed when the controller was turned on while not connected to the heating element. The observed effect abated immediately after the controller was turned off. Similar effects, though less pronounced, were caused by other sources for example, the operation of a laptop computer near the potentiostat.

4.4 Experimental Procedures

To ensure that variables not being studied did not affect the results, the system was perturbed in many different ways. The position of the working electrode was changed with respect to the counter electrode and vessel walls to ensure that neither the cell walls nor the other electrodes affected the results and to exclude the effect of migration current.³

²Obtained from Unique Wire Weaving, Hillside, NJ, USA, www.uniquewire.com

³Migration current is the current due to the motion of ions in the electric field induced by the working electrode and counter electrode. By changing the separation between them the electric field is changed. If the migration current driven by the electric field is significant, some change in the overall current should be observed. Conventionally, the effects of migration current are excluded by adding a strong electrolyte of ions that do not participate in the reaction such that the number of non-reacting charge carriers is much larger than the number of reacting charge carriers. Given the high concentrations of ions participating in the reaction in this work, it is impractical to use this method.

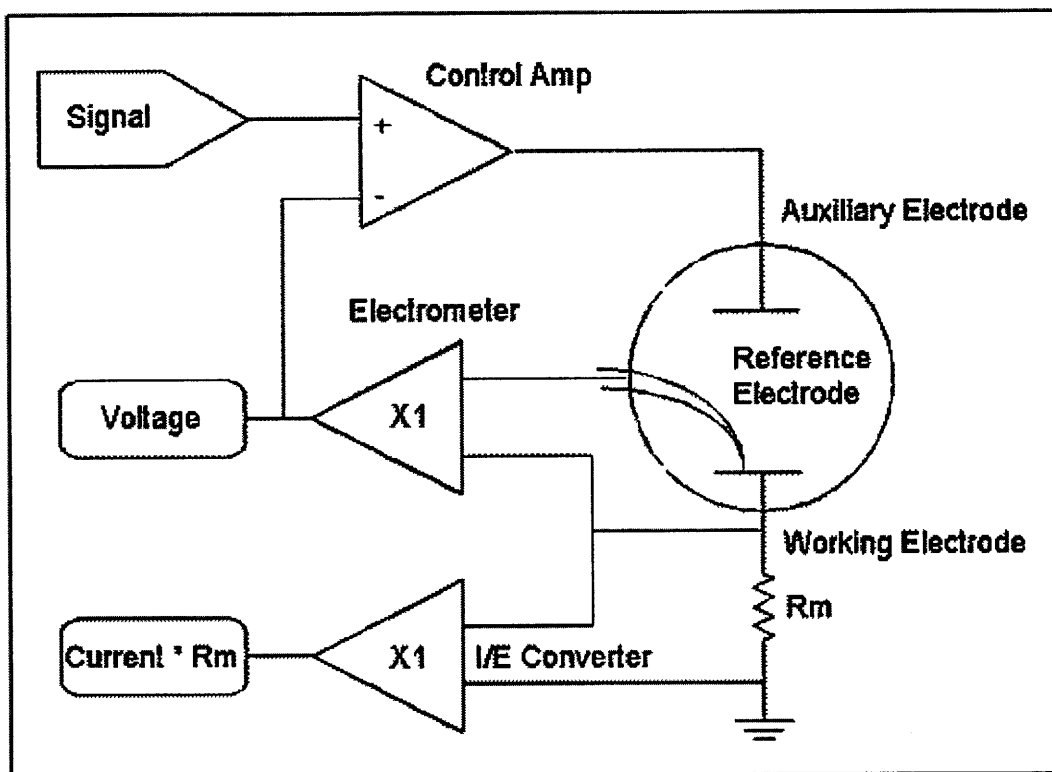


Figure 4-5: Schematic of Potentiostat and cell electrode setup, taken from Gamry Instruments (gamry.com)

The effective area of the counter electrode was altered (by submerging more or less of it) to ensure that the results were not influenced by the counter electrode area. Typically five to eight centimeters of the counter electrode were immersed. Similarly, the relative positions of all three electrodes were varied to ensure that there were no effects due to the electric field or migration current. The reference electrode was connected to the experiment via Luggin capillary, the position of which had no effect on the results, presumably because of the high conductivity of the potassium hydroxide solution. The flask was filled with liquid to different levels. The output of the system was unaffected by any of the preceding alterations.

The oxygen used was grade 5.0 (99.999% pure), the nitrogen was standard purity (99.7%), and the air was reconstituted air (a mixture of 99.7% pure oxygen and nitrogen, with $21.5\% \pm 2\%$ oxygen and the remainder nitrogen). All gases were supplied by Airgas. Given that the experiments were run in a fume hood with a normal atmosphere, and only the standard cleanliness procedures, the use of ultra pure gases is not justified. The results are not of accuracy to justify concern over 10 parts per million of impurity in the supply gas. Carbon monoxide, because it poisons platinum, may be of concern for precision surface area limited measurements. No special effort was made to address this concern, and no effect attributable to it was observed. In this case high purity oxygen was used only because it was available and space constraints prevented the presence of additional gas tanks.

Saturation of the test liquids with gas was ensured by bubbling the gas through the liquid for approximately ten minutes, recording data, then bubbling gas for an additional time period and repeating the experiments to verify that there was no change in the result. In general the system was saturated for 10-15 minutes prior to running the experiments. This was apparently well in excess of what was needed. Bubbling for a few minutes is likely sufficient. In between experiments the system was routinely saturated for 1-2 minutes, the experiment repeated, and the results checked with the previous experiment to ensure that no depletion had occurred. Less than 0.01% of the oxygen dissolved in the fluid (for experiments under 100% oxygen) is consumed in each thirty second experiment. The reaction flask was in a water bath

maintained at $25\text{ }^{\circ}\text{C} \pm 2^{\circ}\text{C}$. The bath was perturbed to higher and lower temperatures and again no effect on the results was observed.

Before experimentation several cyclic voltammograms were run under nitrogen until the typical adsorption-desorption cyclic voltammogram was obtained. Cyclic voltammetry was performed on the electrode prior to taking data until the typical shape was observed, indicating the expected adsorption and desorption on the surface of the electrode and a clear surface (Figure 4-6. Again, this was successful only in the aqueous solution. In the presence of surfactant or emulsion the results were erratic. It was only possible to obtain voltammograms under aqueous solution. We could not obtain any meaningful or repeatable charge transfer data with the emulsion or surfactant in the KOH solution.

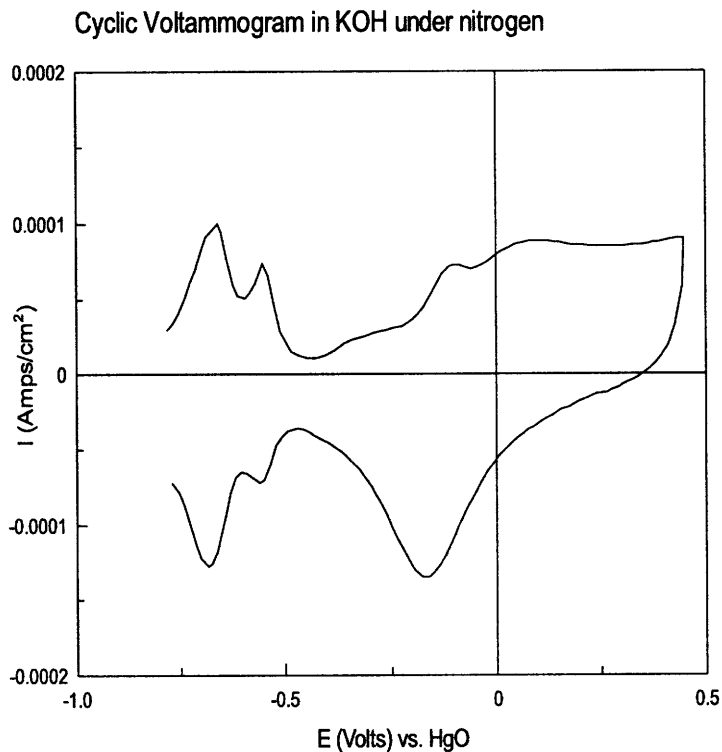


Figure 4-6: Measured voltammogram of a clean platinum electrode surface in 20 wt% KOH solution

4.4.1 Transport Limited Experiments

For transport experiments, the electrode is polarized to a potential extreme enough that the chemical kinetics become very facile in comparison with the reactant transport kinetics. The current measured is then limited by the rate of mass transport and provides a direct measure of the rate of reactant transport to the electrode surface. The potential was stepped to its final value (-0.5 V vs. Hg/HgO in KOH reference electrode). The typical time scale for decay of any current that charges the double layer capacitance at the electrode-electrolyte interface is on the order of 100 μ s, much smaller than the time scale for our experiments.

To ensure that the reaction is transport limited the potential of the electrode was perturbed to more cathodic and more anodic potentials relative to the potential used for experiments. No effect on the reduction rate was observed. By contrast, any agitation of the solution showed an increased reduction rate. The currents measured at various disk rotation speeds are linear with the square root of rotation speed, corresponding to Levich's theoretical prediction for transport limited current at the rotating disk electrode [72, 70, 71], and confirming that the experiment is transport limited.

Some charge transfer limited experiments were performed. In alkaline solution, the results were generally in agreement with published data. Data for the emulsion were erratic such that it was not possible to estimate the exchange current or transfer coefficient with any certainty.

4.5 Preparation of the Emulsion

The aqueous medium was prepared of distilled water and potassium hydroxide pellets obtained from VWR. The potassium hydroxide was weighed on a balance and mixed to achieve a 20 wt% solution. Although this was done fairly rapidly and in a relatively dry environment, it cannot be considered exact because potassium hydroxide is hygroscopic, and so will absorb some water from the air. The organic phase used in experiments was 99% pure n-perfluorohexane obtained from Sigma-Aldrich.

Attempts were made to prepare emulsions with various surfactants and two different perfluorocarbon oils. A commercial perfluorocarbon oil, Galden, supplied by Solvay Solexis and perfluorohexane. Galden was used because it was available as a sample. The solubility of air in Galden was quoted as 26.5% by volume. The Galden emulsion was not used in our experiments. Perfluorohexane was used instead because of its oxygen solubility of 52% by volume [32], which is high even amongst perfluorocarbons, and because data on its properties are readily available in the published literature [32, 113].

The surfactants used in this study were lecithin, sodium dodecyl sulfate, Fluorolink C (a commercial fluorocarbon surfactant with carboxylic acid moiety supplied by Solvay Solexis corporation), nonaioic acid, perfluoro-nonaioic acid. Only Fluorolink and lecithin formed emulsions. Fluorolink emulsions quickly became gelatinous. Lecithin emulsions were stable, but required volume fractions of approximately 4% by volume lecithin. The best emulsions were formed by first mixing lecithin and the KOH solution, then adding the perfluorohexane and sonicating with a sonic wand for 2 minutes. If sonicated sufficiently, the order of addition of components did not seem to matter. We were not able to obtain the surfactants used by Kronberger et al. On conversations with the technical department at Dow Chemical Corporation, they said that an emulsion could not be formed in an electrolyte as strong as 20 wt% KOH in water, used in our experiments. The use of weaker electrolytes is not practical in fuel cells because they are not conductive enough.

Degassed emulsions were formed, according to the suggestions by Pashley [95] was repeated, (see Chapter 2). However, they were not used because of small volume fraction of emulsified oil, and the instability with added potassium hydroxide. Further experiments to quantify the amount of electrolyte required to separate the emulsion were not carried out because the emulsion was not of practical relevance to this work.

Chapter 5

Experimental Results and Discussion

The error bars on plots in this chapter represent one standard deviation above and below the mean. Where enough data points were available, the highest and lowest data points were excluded, or those beyond three standard deviations from the mean. The emulsion used was 15% by volume perfluorohexane in a 20 wt% KOH solution with 4 wt% lecithin surfactant. Since it is the only emulsion used, it is simply referred to as *the emulsion*. The solution used was 20 wt% KOH solution in distilled water, and is referred to as *the solution*.

5.1 The Emulsion

Figure 5-1 shows a photograph of the lecithin emulsion under a microscope. The emulsion is held between a glass cover slip and microscope slide. No means of establishing a length scale were available. It can be seen from the photo that the droplets are not monodisperse.

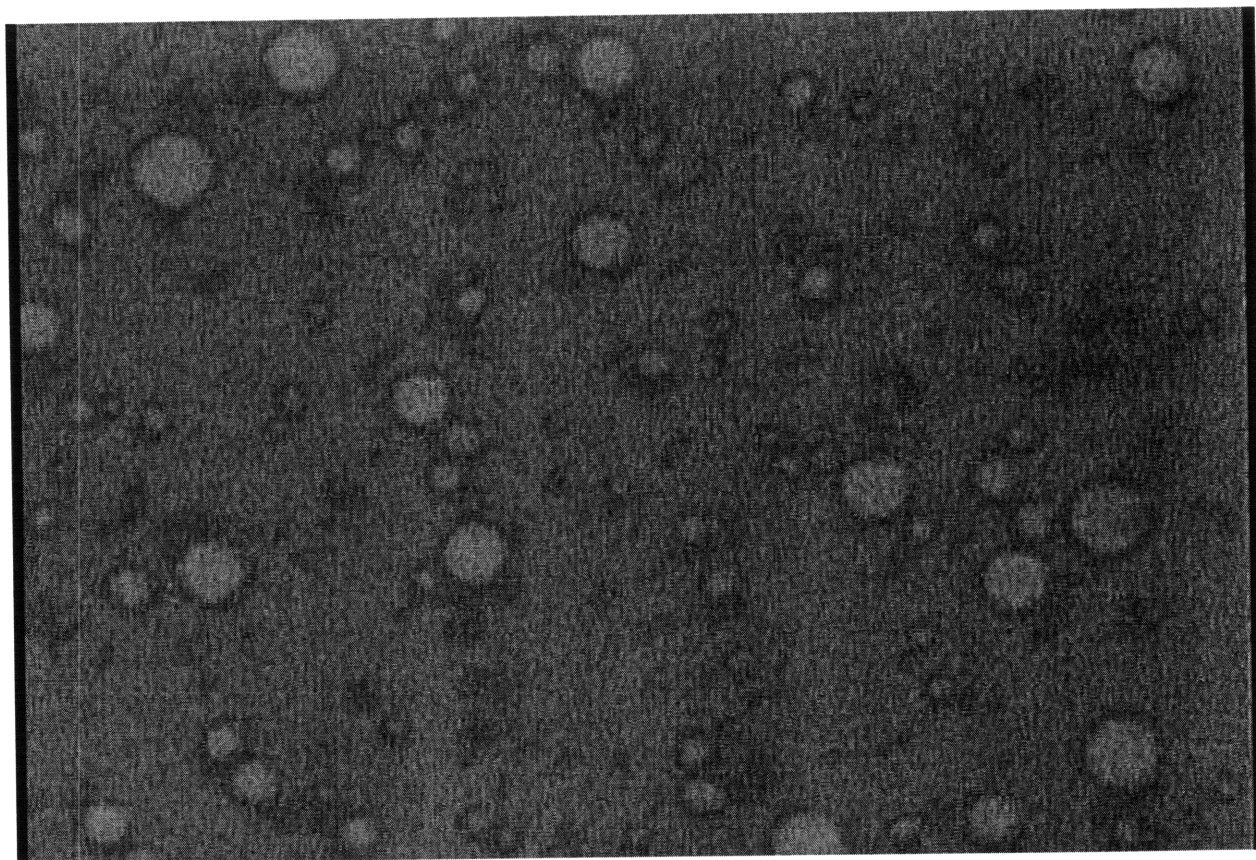


Figure 5-1: Lecithin stabilized emulsion of perfluorohexane in 20 wt% KOH, within minutes of formation. No length scale was available on the microscope.

5.2 Rotating Disk Electrode Results

Figure 5-2 shows the results for a rotating disk operated in the solution of potassium hydroxide.

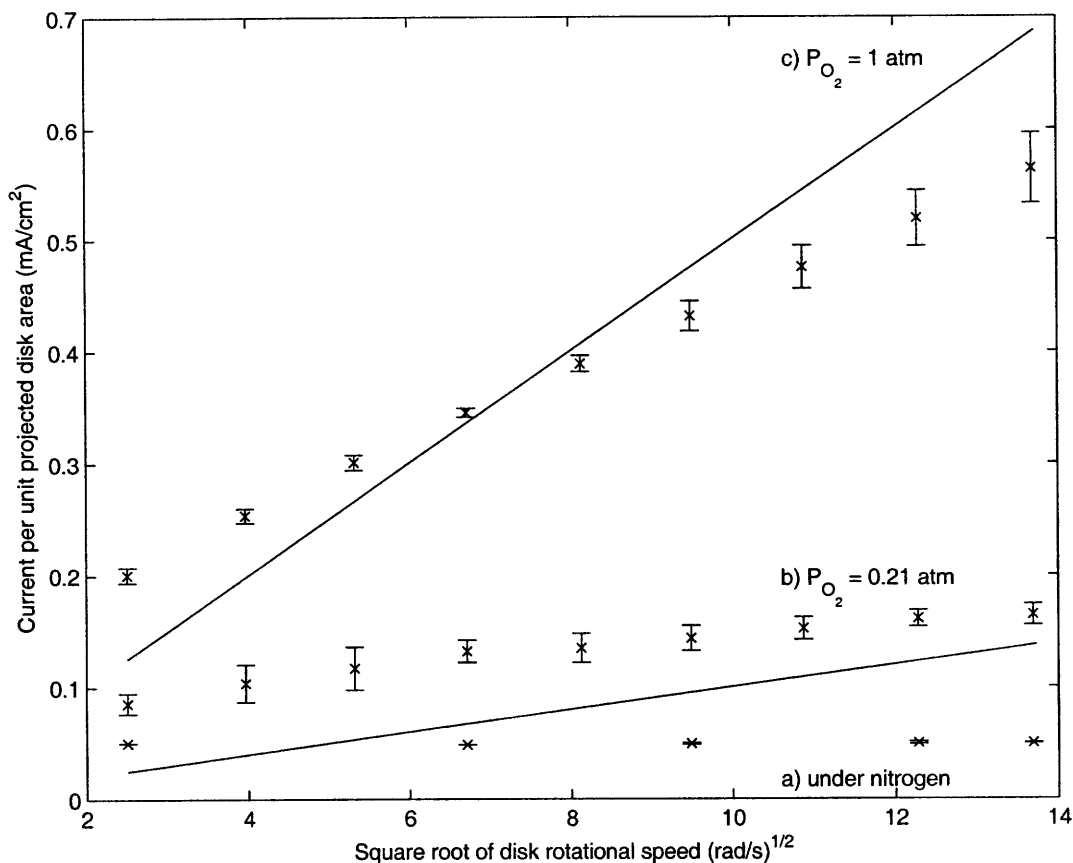


Figure 5-2: Mass transport limited currents as measured on a rotating disk electrode in KOH compared with theoretical calculations in 20 wt% KOH in water saturated with a) nitrogen, b) reconstituted air and c) oxygen. The solid lines represent the theoretically calculated values for cases b and c.

As can be seen from Figure 5-2, under nitrogen the current is negligible and independent of rotational speed. Some small current is measured and is attributed to background noise. The data points for the operation of the rotating disk electrode in the solution saturated with reconstituted air and the solution saturated with oxygen fall on a straight line to very good tolerance, particularly those for oxygen. They

are in reasonable, though not excellent, agreement with the theoretical predictions. The deviation of the experimental measurements from the theoretical line can be at least partly attributed to the property values used for the solution. The diffusion coefficients reported for oxygen in 20 wt% KOH solution vary from $0.7 \times 10^{-9} \text{ m}^2/\text{s}$ to $1.1 \times 10^{-9} \text{ m}^2/\text{s}$ [56]. The values used in the calculation of the theoretical lines are $D = 0.92 \times 10^{-9} \text{ m}^2/\text{s}$, $\nu = 1.4 \times 10^{-6} \text{ m}^2/\text{s}$, and $C_\infty = C_{sat} = 0.25 \text{ mol}/\text{m}^3$ [46]. It should also be noted that because the results are scaled by the area of the rotating disk electrode (0.15 cm^2), errors are magnified. The deviations of some fraction of a millivolt shown, translate to measurement errors on the order of a few microvolts. The theoretical lines are calculated according to Equation 3.1.

The fact that the points lie so close to a straight line is in satisfying agreement with Riddiford's predictions for the electrode shape used, although his studies were limited to rotational speeds of 25 radians/s (240 RPM). The speeds reported in this work are up to 187 radians/s (1790 RPM), which are now common in the literature. We are reassured that the measured currents are transport limited because the data points are linear with the square root of the disk rotational speed, as predicted by Levich [72].

Figure 5-3 shows the predicted results for the emulsion. The calculations are made, again, using Equation (3.1), the previously cited values for kinematic viscosity, and an oxygen concentration that is a volume weighted average of the oxygen solubility in the solution and in the perfluorohexane (PFH); $C_{average} = 0.85C_{sat}(KOH) + 0.15C_{sat}(PFH)$. The value of the diffusivity used is half of that used for the pure solution in accordance with Ju et al.'s [62] empirically based suggestion.

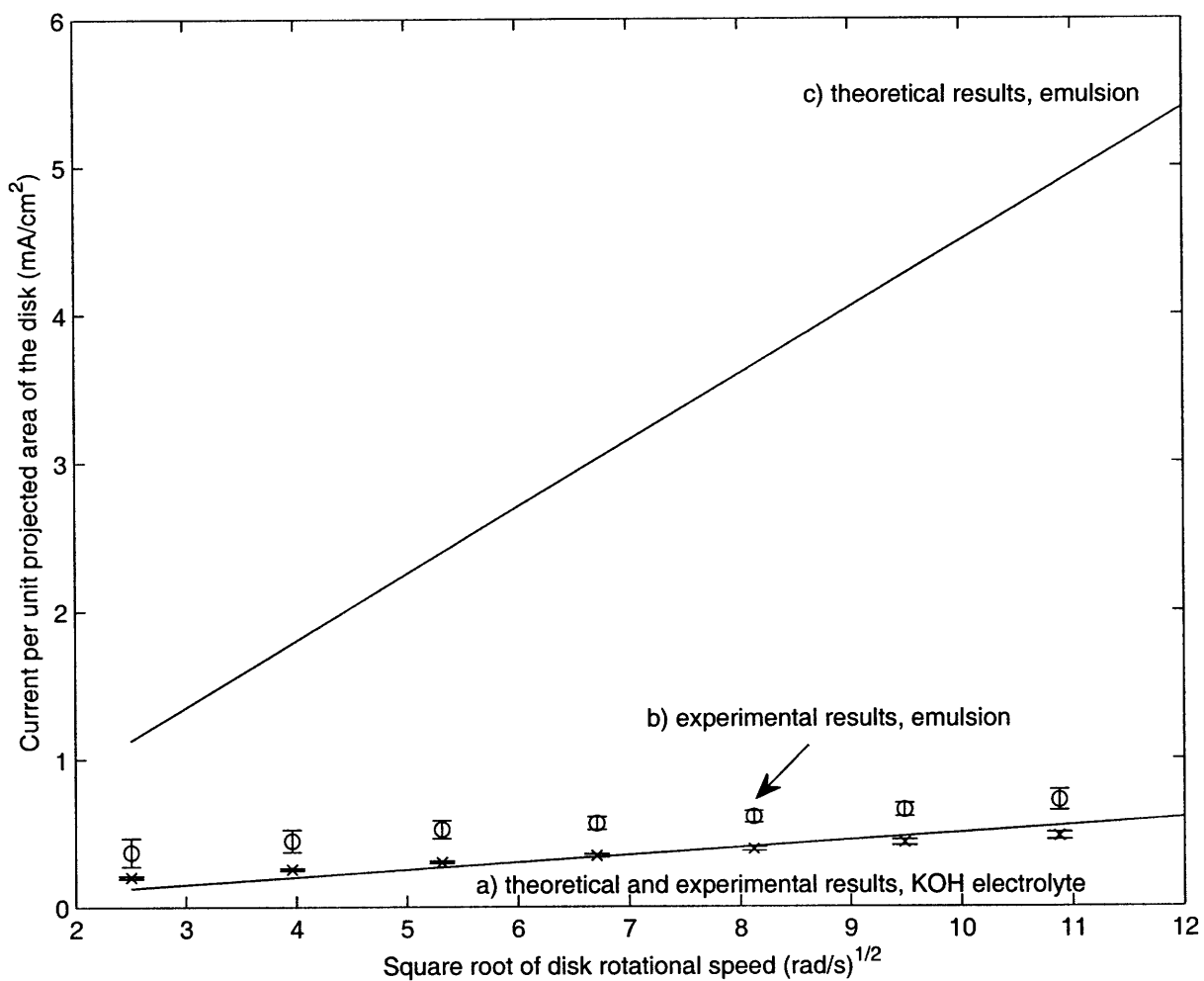


Figure 5-3: Mass transport controlled reduction of oxygen on a rotating disk electrode
 a) 20 wt% KOH saturated with N₂, b) 20 wt% KOH saturated with O₂, c) an emulsion of 15% by volume perfluorohexane in 20 wt% KOH saturated with O₂.

As can be seen, the predicted values for the emulsion are much higher than the measured ones. Figure 5-4 shows the same data as Figure 5-3 but without the theoretical prediction such that the scale can be expanded. It shows that the slope of the line representing oxygen reduction from the emulsions is, to within the accuracy of the experiment, the same as that for oxygen reduction from the KOH solution. According to Levich's equation (3.3), the slope should be proportional to the oxygen concentration in the bulk when the reaction is mass transport limited. Since the data for reduction of oxygen from an emulsion and from the KOH solution are of the same slope we conclude that there is no enhancement in the rate of oxygen transfer. The enhancement seen is independent of the flow rate induced by the rotating disk and must be attributable to a reactant which is not transport limited or which does not depend on the flow for transport.

Figure 5-5 shows that the sum of the current produced from the emulsion under nitrogen and the current from the 20 wt% KOH solution under oxygen matches reasonably closely the current produced from the emulsion under oxygen. Note that the data presented in Figure 5-5 are the average of all trials. Figure 5-6 compares the current from the emulsion saturated with oxygen, 20 wt% KOH solution saturated with oxygen, and the emulsion saturated with nitrogen from selected sets of trials, rather than averages for the overall data. The match in data is quite good, and relevant because the the average current level produced from the emulsion or surfactant alone seemed to slowly increase with time, perhaps suggesting some accumulation of surfactant on the surface of the disk. The result is that averages over the entire data set, as shown in Figure 5-3, show more variation than the individual data sets taken at times close to each other. The current from the reduction of oxygen does not seem to be diminished by the presence of the lecithin, indicating that the lecithin does not block access of oxygen to the disk surface.

Figure 5-7 shows the measured currents from the emulsion saturated with oxygen compared with those from a solution of surfactant (with no perfluorohexane) in 20 wt% KOH saturated with nitrogen, and those from a 20 wt% solution of KOH saturated with oxygen. From these data we conclude that the increase in current is

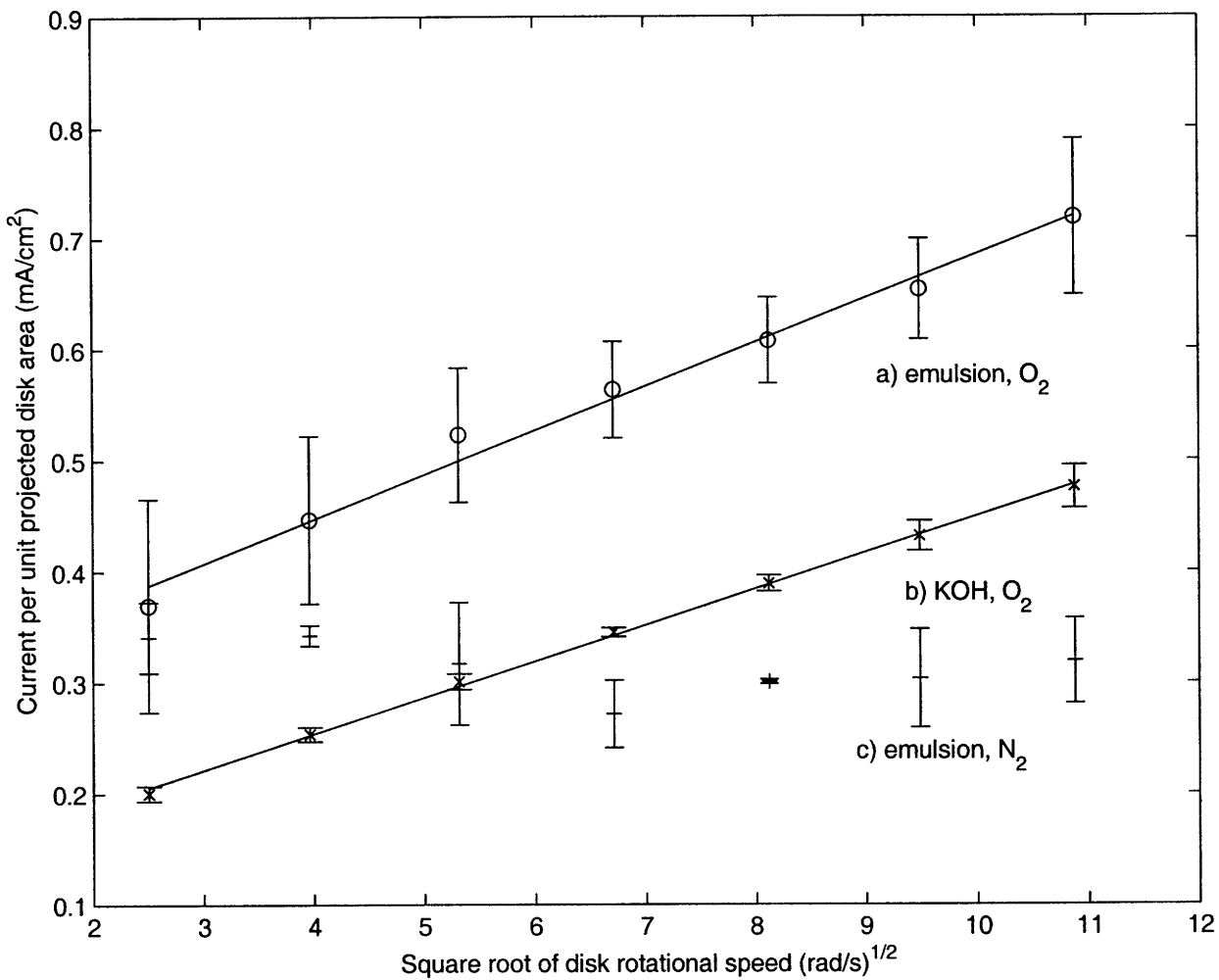


Figure 5-4: Measured mass transport controlled reduction of oxygen on a rotating disk electrode from the emulsion saturated with oxygen compared with that in the solution saturated with oxygen, and with the emulsion saturated with nitrogen.

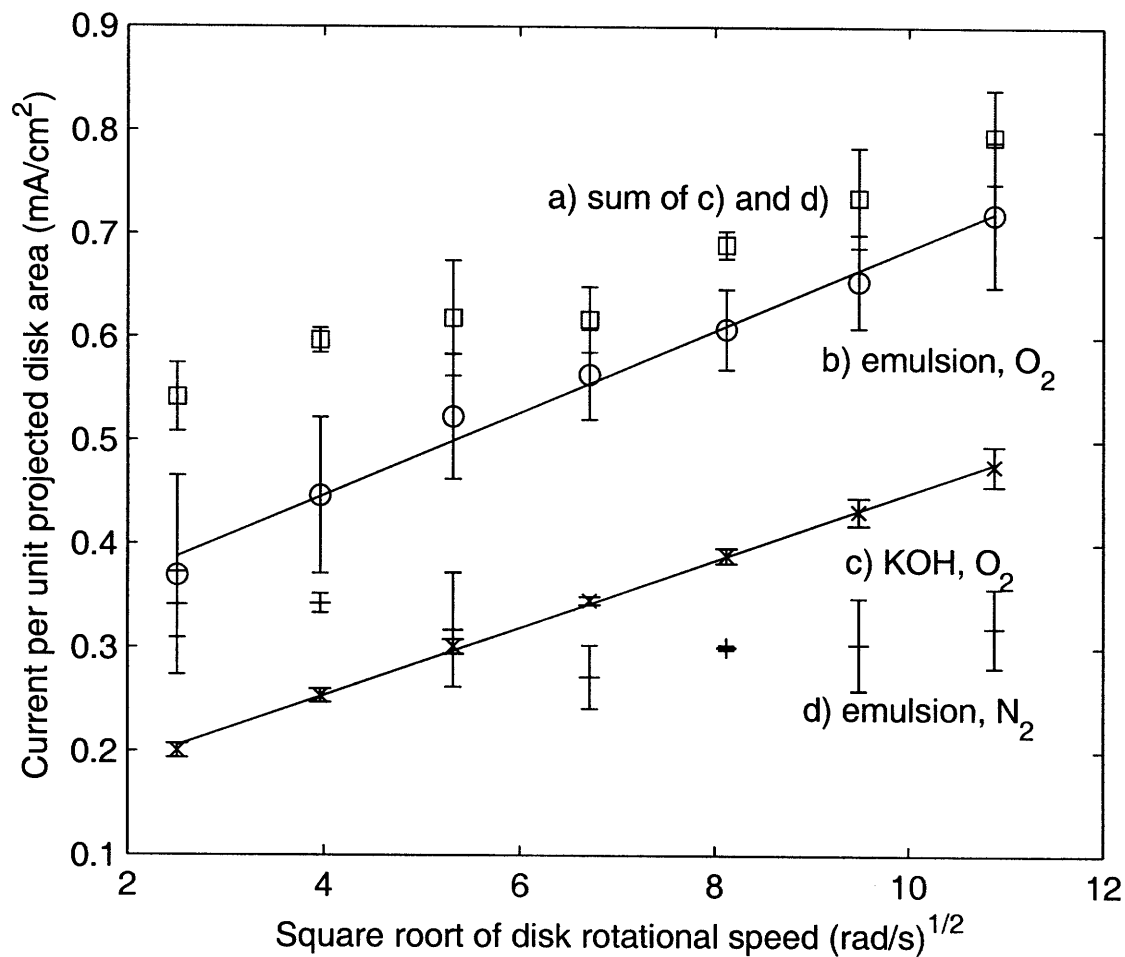


Figure 5-5: Measured transport controlled reduction of oxygen on a rotating disk electrode from the saturated with oxygen, compared with reduction from the solution saturated with oxygen, the emulsion saturated with nitrogen, and the sum of the currents from the emulsion saturated with nitrogen and the pure solution saturated with oxygen. The data presented are the average of trials over a period of time and indicate that the increase in current observed with the emulsion is not due to increased oxygen transport.

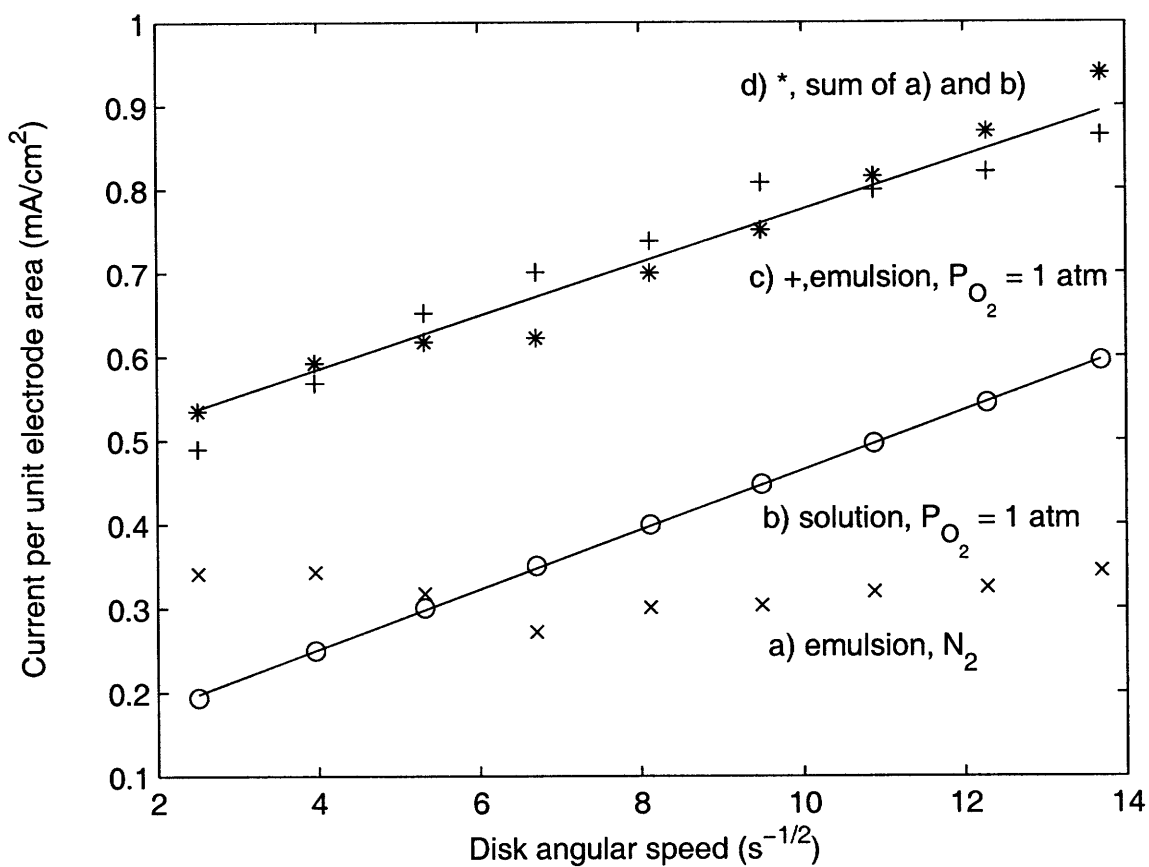


Figure 5-6: Mass transport controlled reduction of oxygen on a rotating disk electrode from the emulsion saturated with oxygen compared the solution saturated with oxygen and with the emulsion saturated with nitrogen. The observed enhancement is due to the reaction of a species other than oxygen. The data presented are from individual trials, and not averaged over the entire data set.

caused by the presence of the lecithin surfactant, and not the perfluorohexane. Because of the correspondence between the current from the oxygen saturated emulsion and the sum of currents from the surfactant solution under nitrogen and the pure 20 wt% KOH solution under oxygen, we conclude that the all the of enhancement is due to the surfactant. That the current increase attributed to lecithin does not depend on rotational speed implies that the reaction of lecithin is limited by its chemical reaction rate, and not the transport of lecithin. This maybe because of the relatively high concentration of lecithin, because of some collection of lecithin (adsorbed or otherwise deposited) at the surface, or because of a relatively slow reaction rate. Over time, the current from the lecithin reaction is observed to increase slightly, which may suggest some adsorption at the surface. It may also be the case that what reacts is not the lecithin, but some byproduct of the reaction of lecithin with the potassium hydroxide solution. The reaction produces a pungent gas (likely ammonia). See Ukita et al. [121], or Brockerhoff [19] for a further explanation of the reactions of lecithin.

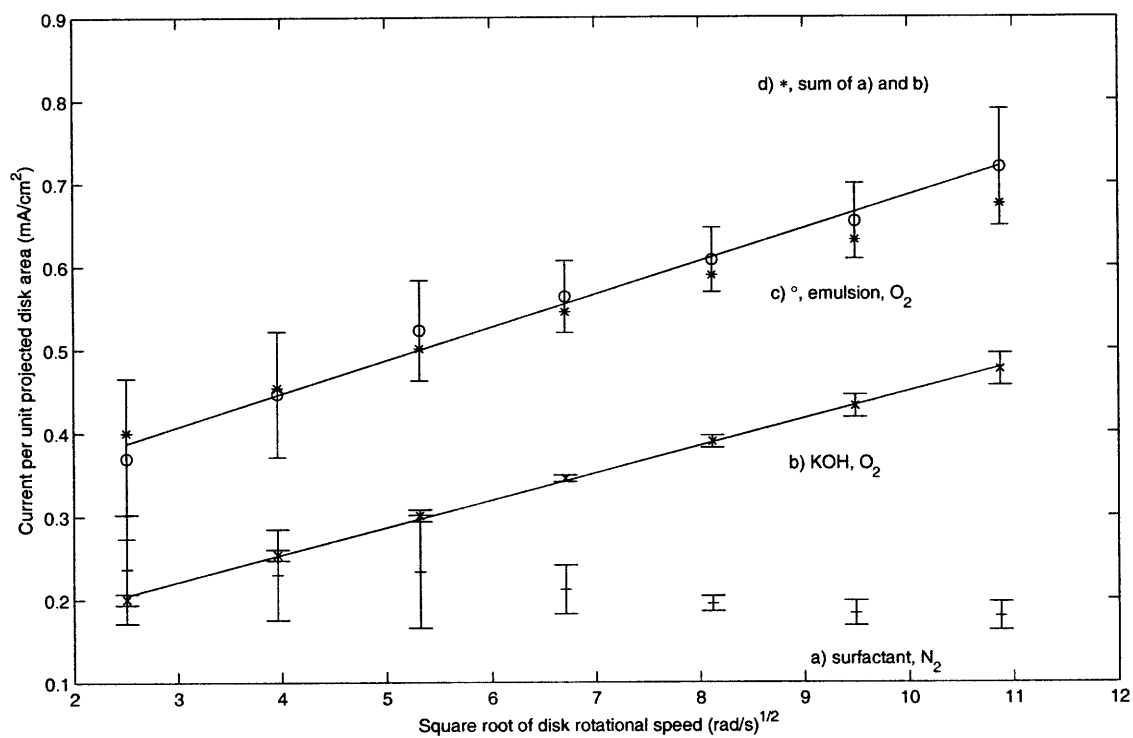


Figure 5-7: Mass transport controlled reduction of oxygen on a rotating disk electrode from the emulsion compared with reduction from the solution, and a 20wt% solution of KOH with surfactant dissolved. The results show that the enhancement is due to the dissolved surfactant

5.2.1 Discussion of the Rotating Disk Electrode Results

No enhancement in the rate of oxygen transport due to the presence of the emulsion was observed. The lecithin surfactant, or a byproduct of its reaction with the KOH solution, was reduced on the electrode. The increase in current attributed to the lecithin was independent of the disk rotation rate, which suggests that the reaction of lecithin was not mass transport limited.

Figure 5-8 shows the concentration and momentum boundary layers at the surface of a horizontal rotating disk electrode.

The momentum boundary layer, δ_M , is taken to be

$$\delta_M = 2.8 \left(\frac{\nu}{\omega} \right)^{1/2} \quad (5.1)$$

and the concentration boundary layer, δ_C , is taken to be

$$\delta_C = 1.805 \left(\frac{D}{\nu} \right)^{1/3} \left(\frac{\nu}{\omega} \right)^{1/2} \quad (5.2)$$

as described by Gregory and Riddiford [44] and Riddiford [103]. The concentration boundary layer used here is the so called *Nernst layer*.¹

Since the diffusivity of oxygen (of order 1×10^{-9} m²/s) is three orders of magnitude smaller than the momentum diffusivity, the momentum boundary layer is much larger than the concentration boundary layer. This suggests that the droplets, once entrained in the momentum boundary layer, are pushed to exit the reactive region of the disk well before they can enter into the concentration boundary layer.

In order for the emulsified phase to contribute oxygen to the reaction, the emulsified droplets must enter into the concentration boundary layer, where there is a reduced concentration of oxygen, and must reside there - under the active region of the disk - long enough for oxygen to diffuse from the droplets into the surrounding medium and to the surface of the rotating disk. Because of the small size of the droplets (microns to a few tens of microns), the time scale for diffusion out of the

¹The Nernst layer is the boundary layer found by assuming a linear concentration gradient throughout the boundary layer thickness. See Gregory and Riddiford [43], or Riddiford [103] for a detailed discussion.

droplet is small compared with the time scale for other processes.

The concentration boundary layer is only a few tens of microns thick, and depends on the rotation speed of the disk. Given that the emulsion droplets are of approximately the same dimension as the concentration boundary layer, they cannot be expected to penetrate very far into it without colliding with the disk surface.

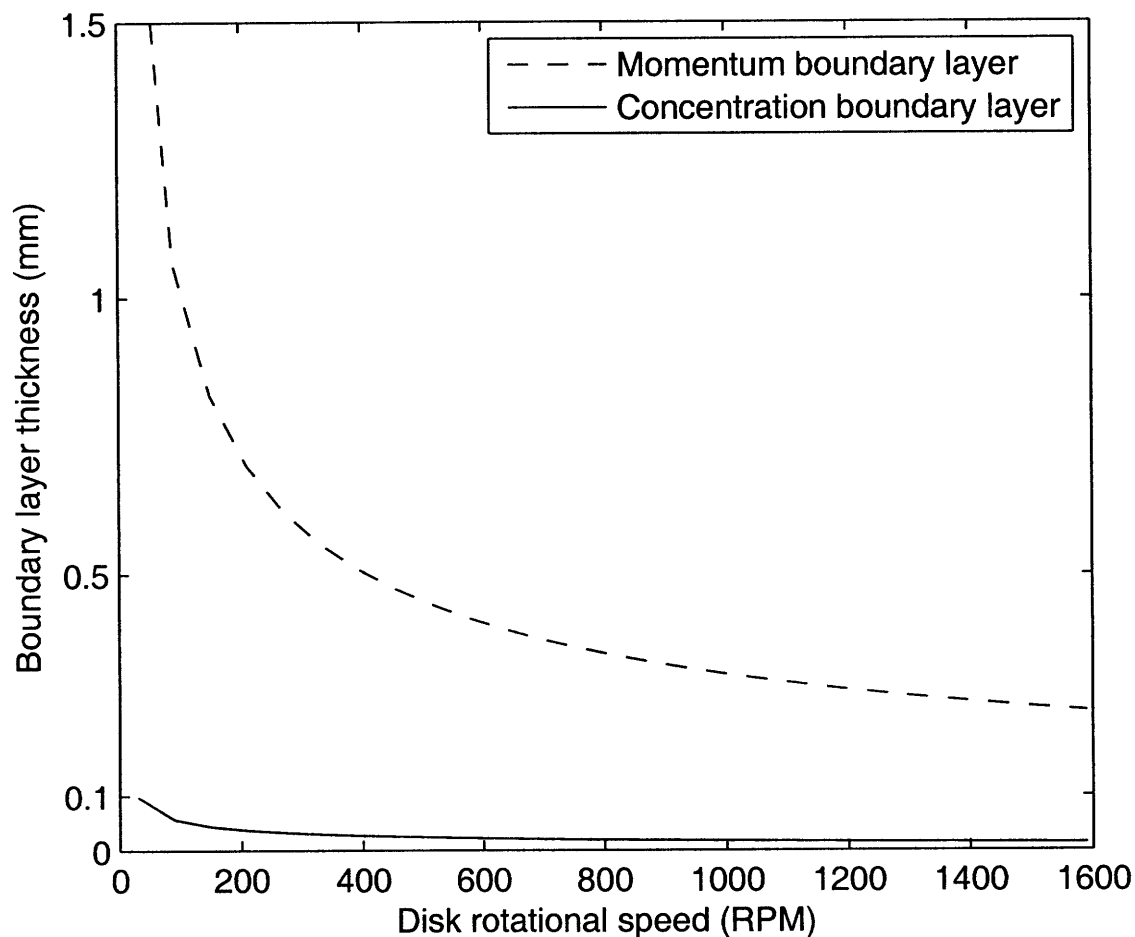


Figure 5-8: A comparison of the momentum and concentration boundary layer thicknesses below a rotating disk surface. The momentum boundary layer, where emulsion droplets are forced away from the center of the disk is much larger than the concentration boundary layer, where drops must enter to affect the transport to the disk.

Povarov, Nazarov, Ignat'evskaya, and Nikol'skii [97] have shown that drops approaching a disk where the azimuthal velocity is much greater than the approach

velocity are reflected by the boundary layer without interacting with the disk. Their study was based on water droplets falling onto a disk rotating in air, where the Reynolds numbers (based on the density of the droplet and viscosity of the air) are expected to be orders of magnitude larger than those involved in the motion of emulsified droplets in a liquid medium. Consequently, one would expect to observe what they observed at even smaller ratios of azimuthal to axial velocity. When an emulsion droplet reaches the concentration boundary layer, the ratio of the azimuthal velocity to the vertical velocity is very large for anything beyond minimal radii (Figure 5-9). Consequently, one would expect that emulsion droplets are expelled by centrifugal force before reaching the concentration boundary layer because of the density difference between the perfluorohexane ($\rho_{PFH} = 1.6 \text{ g/mL}$) and the surrounding solution ($\rho_{sol} = 1.2 \text{ g/mL}$).

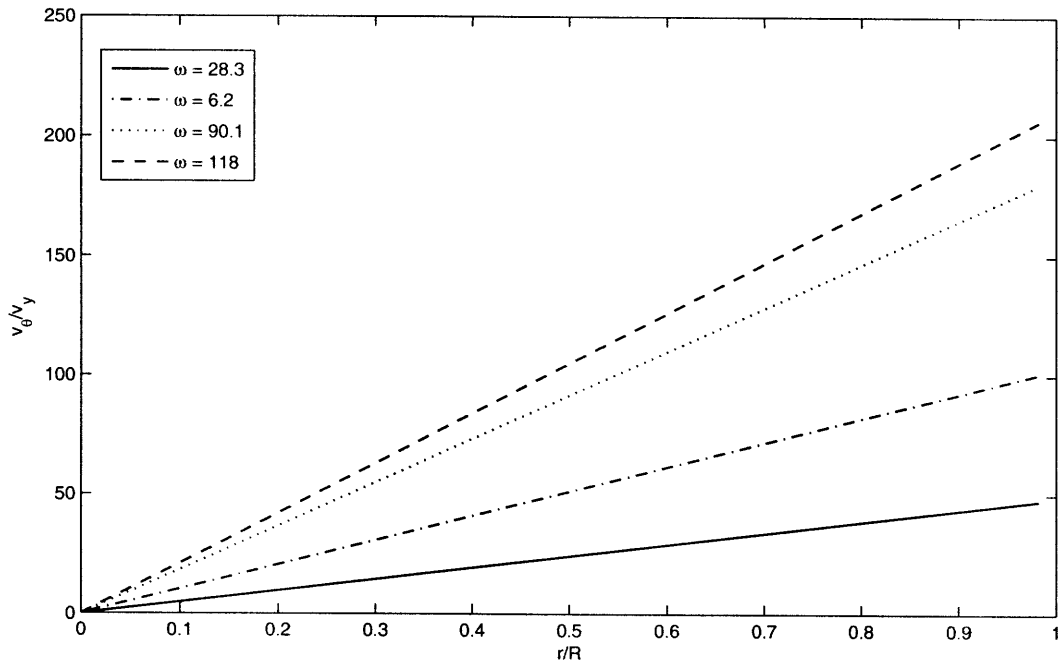


Figure 5-9: The ratio of azimuthal to vertical velocity at the edge of the concentration boundary layer beneath a rotating disk at various rotation speeds

Although we have not succeeded in writing the equations for the behavior of a

droplet below a rotating disk, it is clear that the hydrodynamics of the rotating disk affect the apparent properties of the emulsion so as to inhibit the approach of the dispersed phase into the concentration boundary layer. This does not exclude the possibility that the surfactant acts to inhibit the transfer of oxygen from an emulsion droplet to the surrounding fluid.

If it is true that emulsion does not enhance oxygen transport rates because the fluid dynamics of a rotating disk prevent the entrance of drops into the concentration layer, or their residence in the concentration layer for sufficiently long, then it should be possible to observe an enhancement when the concentration boundary layer is large and the fluid stationary. Such an experiment is discussed in the following section.

5.3 Transient Diffusion

A transient diffusion experiment (so called Cottrell Experiment) provides conditions of a concentration boundary layer growing in a stationary fluid. The potential of the electrode is stepped at time $t = 0$ so as to effectively consume all the oxygen at the surface and make the reaction rate much faster than the oxygen transport rate. The concentration boundary layer grows in time as shown in Figure 5-10. The theoretical lines in the figure are calculated using the previously cited values and the diffusivity suggested by Ju et al. The edge of the boundary layer was defined as the location where the concentration is 99% of the concentration in the bulk fluid, and therefore given by

$$\delta = 3.65\sqrt{Dt} \quad (5.3)$$

as can be found in most heat and mass transfer textbooks (see, for example, Lienhard, [73] p.224).

If oxygen can be supplied by the droplets, then as the concentration boundary layer engulfs emulsion droplets they should transfer oxygen into the surrounding medium which should retard the growth of the boundary layer, and therefore maintain the mass transport rate to the electrode surface for a longer time than in their absence. This in turn should be observable as an increase in current.

Figure 5-10 shows the results of this experiment and demonstrates insignificant enhancement due to the presence of the emulsion, again far less than predicted.

There is little difference between the data for the KOH solution with surfactant under nitrogen and the emulsion under oxygen. This suggests that the majority of the enhancement observed is contributed by the reaction of the surfactant and the emulsion does little to enhance the availability of oxygen. Again, the measured rates are below those predicted from theory. The current limited by diffusion in a semi-infinite medium is given by (the so called Cottrell) Equation 5.4

$$i = \frac{nFD^{1/2}C}{\sqrt{\pi t}} \quad (5.4)$$

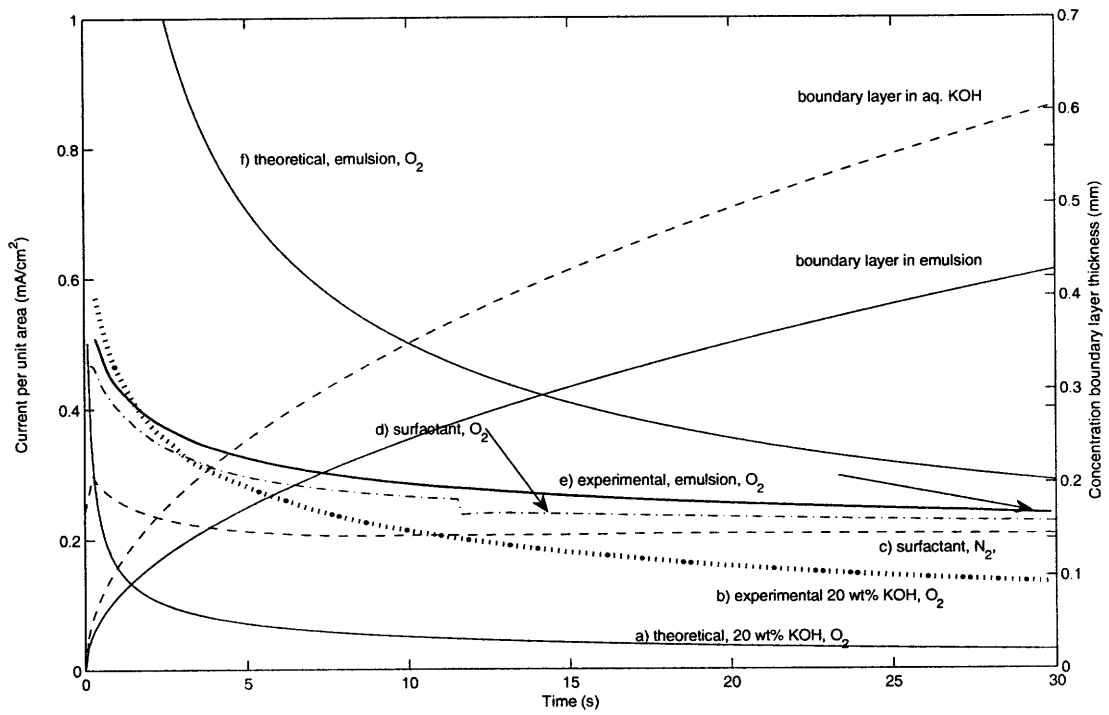


Figure 5-10: Mass transport limited currents from a semi-infinite body diffusion showing little advantage to the emulsion.

where t is time and the remaining variables are as used before. The property values used are as used in the section on results from the rotating disk.

The measured rates of oxygen reduction from the solution without surfactant are considerably higher than the theoretical prediction. The experiment was repeated on several occasions, with the electrode and apparatus thoroughly cleaned in between. The results remain the same. We have no good explanation.

5.4 Oxygen Content of the Emulsion

Having observed only minimal enhancement to the rate of oxygen diffusion from a quiescent emulsion we conclude either that the emulsion does not absorb the oxygen during saturation, or that the oxygen in the bulk does not aid in transport. It may be that it is erroneous to assume that an increase in average oxygen concentration, with no increase in the chemical potential, should increase the oxygen transport rate. Or it may be that presence of the lecithin surfactant significantly impedes the release of oxygen from the emulsion droplets in contrast to what is reported by Ju et al. [61], and by Mehra [86], although they used other surfactants. Kronberger suggests that hydrocarbon surfactants seemed to impede the transport of oxygen in his experiments. Lecithin is used, however, as a surfactant in perfluorocarbon based blood substitutes, so it was expected that it would not impede oxygen transport. The fact that lecithin reacts in strong base [19] suggests that it may form a chemical structure around the emulsion droplet.

Two often used methods for determining oxygen concentration in a liquid are the oxygen electrode (so called Clark Electrode) and the Winkler method. The oxygen electrode is used to measure the chemical potential by measuring the electrical potential of an oxygen reduction electrode in equilibrium with the test medium and separated from the test medium by a membrane. The diffusion of oxygen across the medium is proportional to the chemical potential of oxygen in the test medium. In a homogeneous medium, for relatively low concentrations of oxygen, the concentration can be used as a surrogate for chemical potential. For a heterogeneous system, as

we're concerned with here, differing concentrations of oxygen exist in the different phases at the same chemical potential (both are in equilibrium with each other and with oxygen at one atmosphere pressure). Thus, the oxygen electrode cannot be used for the measurement in this case because the chemical potential of the oxygen has not changed by the addition of an organic phase with large gas solubility.

The Winkler method, proposed in 1888 by Lajos Winkler [125], is based on thermochemically fixing the oxygen, then titrating with a known titer to measure the amount of oxygen present. The dissolved oxygen is first bound by reaction with manganese (II) hydroxide. The manganese(II) is then oxidized to manganese(III) hydroxide. The solution is then acidified in the presence of iodide ions. The manganese(III) oxidizes the iodide ions to iodine. The iodine-iodide complex is then titrated with thiosulphate in the presence of a starch indicator. See Grasshoff [42] for a detailed discussion of the method.

Determining the oxygen concentration by the Winkler method was attempted, but no result could be determined because either the surfactant or, a product of the surfactant's reaction with the potassium hydroxide, was reduced by the manganese(II), as in the electrochemical experiments. The concentration of surfactant overwhelmed the concentration of oxygen, making it impossible to determine directly the oxygen concentration. In principle it would have been possible to repeat the experiment with several different oxygen and surfactant concentrations, and attempt to elucidate the oxygen concentration from the results. In practice, it would have been difficult if not impossible to determine the oxygen concentration with any useful degree of certainty.

Among the properties of perfluorocarbons is that their nuclear magnetic resonance spectra are very sensitive to the amount of dissolved oxygen in the perfluorocarbon [31, 78]. It is this property which makes them useful in NMR studies. To determine the presence of oxygen in the emulsion the ^{19}F NMR spectra of two samples of the same emulsion were taken. One sample was saturated with oxygen and the other with nitrogen. Since the spectra are fluorine spectra, only the fluorine containing compounds appear. The only fluorinated compound in these emulsions is the perfluorohexane. The shift in the NMR spectrum observed, as shown in Figures 5-

11 and 5-12, indicates that the perfluorohexane is oxygenated. While these results show the presence of oxygen in the perfluorohexane, they do not allow a quantitative measurement of the concentration.

It is possible to measure the concentration of oxygen dissolved in a perfluorocarbon by measuring the spin relaxation times [78], but the expertise required is beyond that of the author or anyone whose aid he could enlist. The spectra presented here were taken by Dr. Luke Theogarajan.

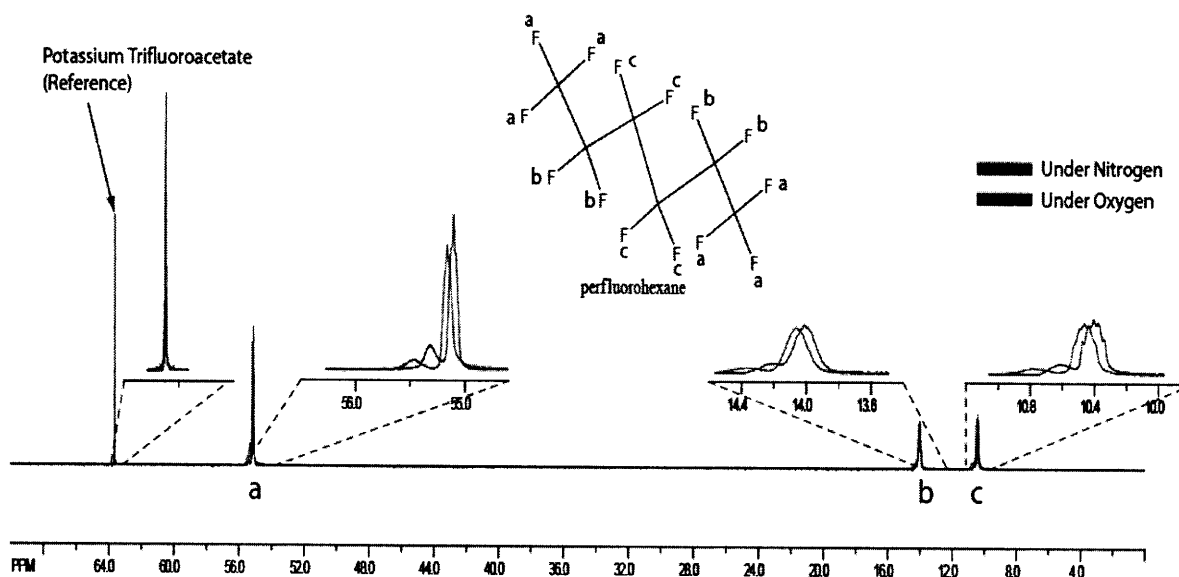


Figure 5-11: ^{19}F NMR spectra of 15 %vol perfluorohexane in a 20 wt% solution of potassium hydroxide stabilized by lecithin. Lines are shown in red and blue. If viewed in black and white, the spectrum of the oxygenated emulsion can be identified as one shifted to the right.

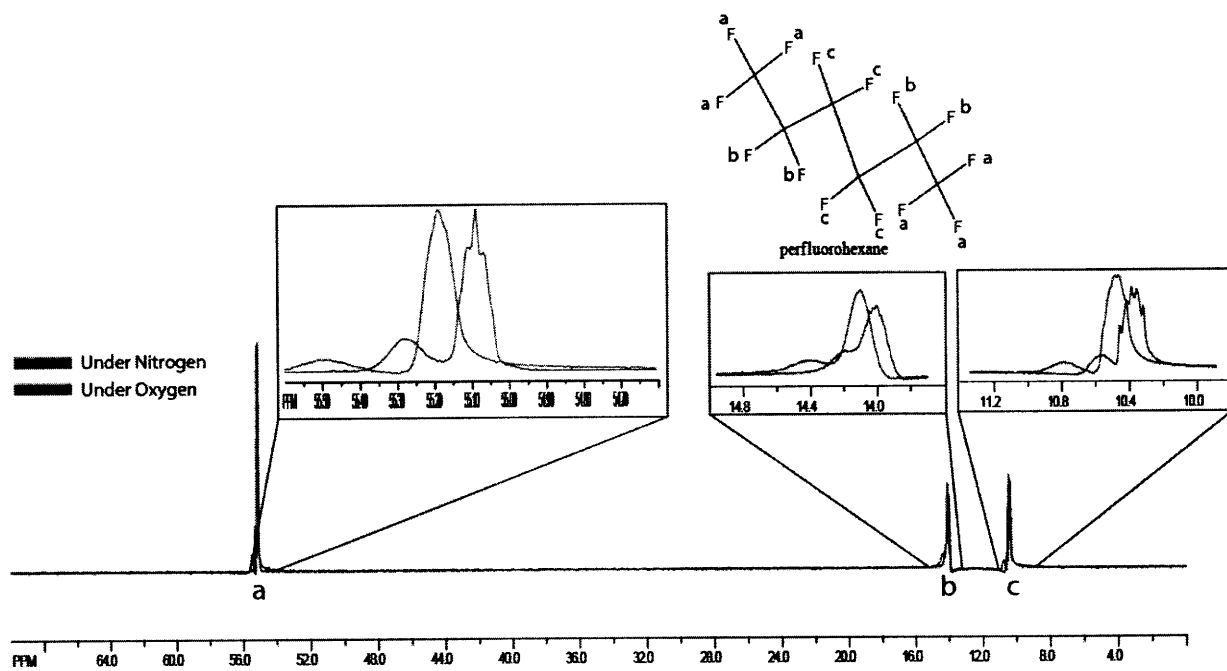


Figure 5-12: ^{19}F NMR spectra of 15 solution of potassium hydroxide stabilized by lecithin. If viewed in black and white, the spectrum of the oxygenated emulsion can be identified as one shifted to the right.

Having concluded that oxygen is present in the emulsified perfluorohexane phase, the lack of enhancement in oxygen transport rate suggests that the surfactant presents some impedance to the transport of oxygen. This is somewhat surprising given the small thickness of the surfactant layer of approximately $1\ \mu\text{m}$. The surfactant layer thickness was calculated by distributing the total surfactant volume over the area of the interface between the perfluorohexane and aqueous solution. The interfacial area was calculated by assuming $10\ \mu\text{m}$ droplets and a number of droplets to make up the total volume of the perfluorohexane. That calculated thickness is considerably larger than typical surfactant layer thicknesses, owing perhaps to the large amount of lecithin required to emulsify the drops. Still, it is not of thickness sufficient to cause a significant impedance to mass transport if the the diffusion of oxygen is similar to that in other liquids. Kronberger *et al.* also observe an apparent impedance of to the transport of oxygen with emulsions using hydrocarbon based surfactants. They attribute the impedance to the surfactant.

5.5 Oscillating electrode results

It is desirable eliminate the effects due to the surfactant. However, without the surfactant present, an emulsion cannot form. The water and oil form two stratified continuous layers. Thus, an electrode that can traverse both phases is needed.

The use of an oscillating electrode to traverse to stratified layers was suggested by Professor Donald Sadoway [1]. The experimental apparatus is modelled after that used by Pint and Flengas [96]. After repeating the work by Pint and Flengas to ensure that our apparatus was not substantially different from theirs, several experiments were performed during which the following were observed: the limiting current is linear with oscillation frequency, as observed by Pint and Flengas, but was observed to plateau above speeds of approximately 250 oscillations per minute. The mass transport limited current does not seem to depend on the stroke length, a variable not investigated by Pint and Flengas. Data were taken at $25\ ^\circ\text{C}$ and $35\ ^\circ\text{C}$ to exclude the possible effects of temperature fluctuations.

The main result for this study is shown in Figure 5-13. It is that in the presence of the perfluorohexane the current output is only slightly enhanced, but is independent of oscillation speed. Data in the following graphs are from solutions saturated with oxygen unless otherwise noted.

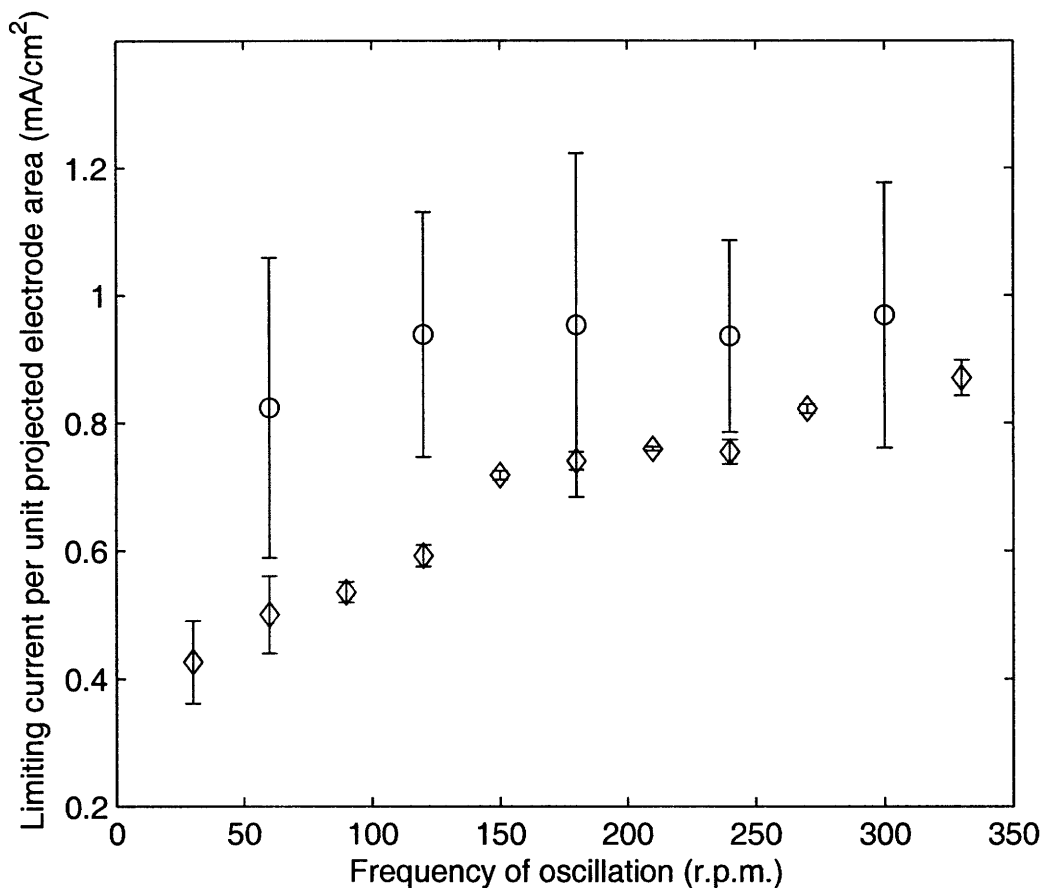


Figure 5-13: Measured currents from an oscillating electrode with 10 mm stroke in single phase 20 wt% KOH solution saturated with oxygen (◇), and traversing the interface between a 20 wt% KOH solution and a perfluorohexane phase at the midpoint of its travel (○). Both phases were saturated with oxygen.

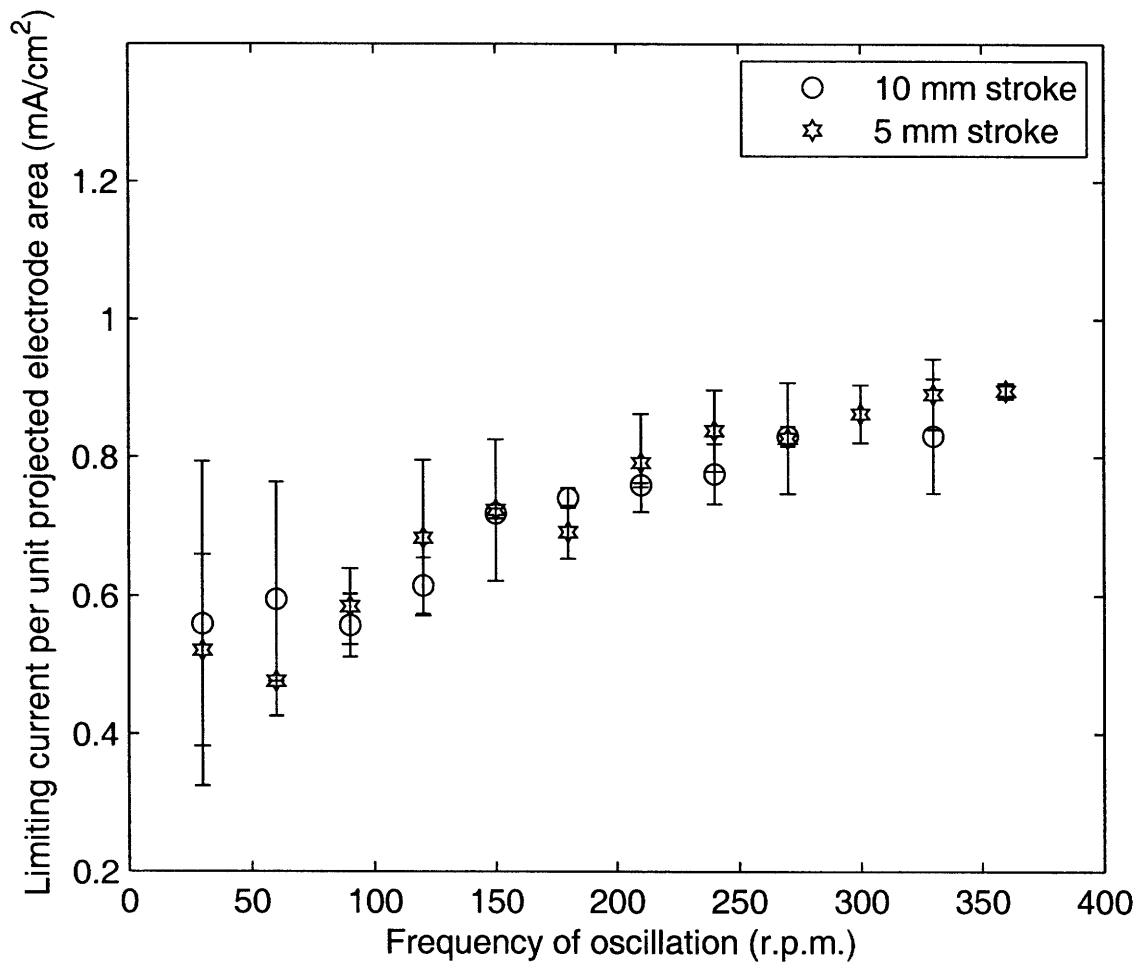


Figure 5-14: Measured currents in a 20 wt% KOH solution. The obtainable current appears to be independent of the stroke length of the electrode and linear with oscillation speed, but also appears to begin to plateau between 250 and 300 oscillations per minute.

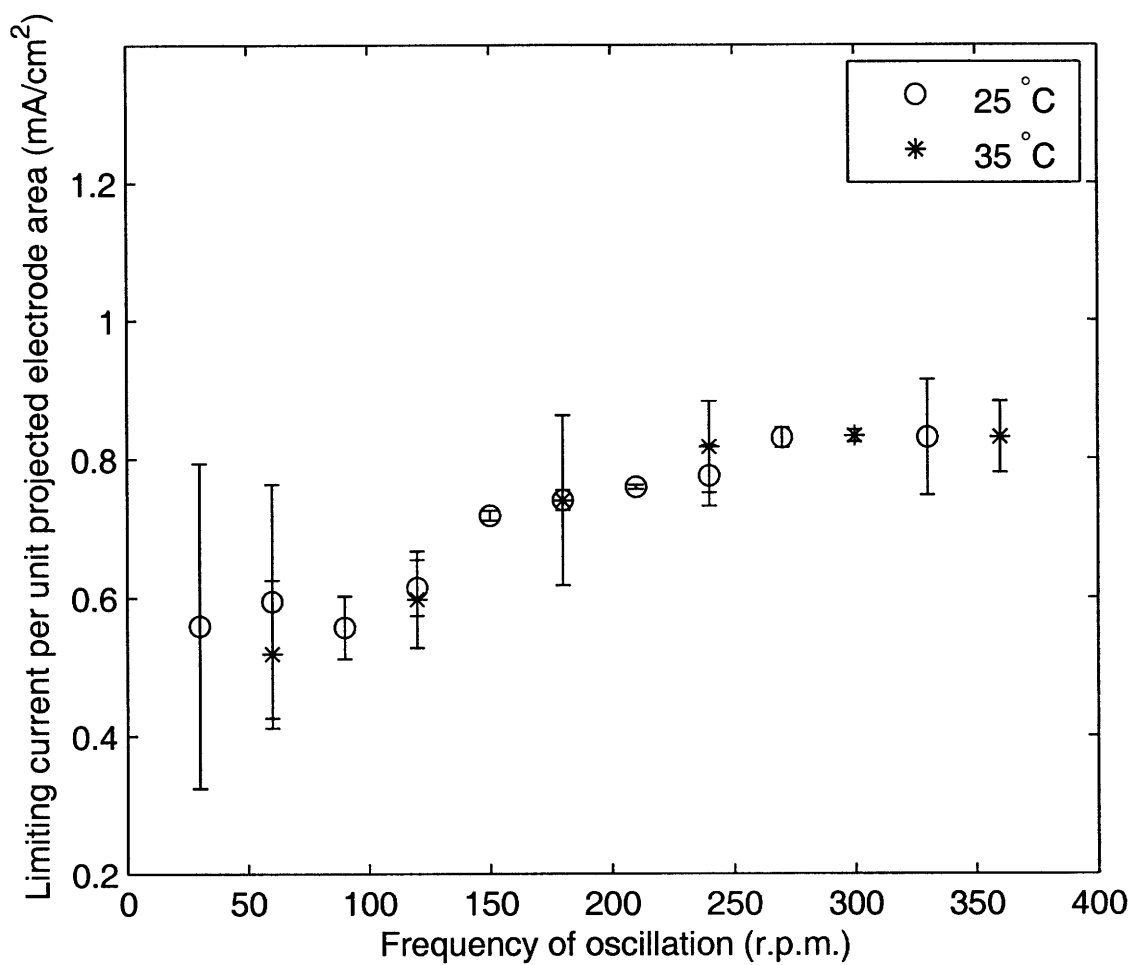


Figure 5-15: Data taken at two different temperatures in 20 wt% KOH solution indicate that a slight temperature increase does not seem to have appreciable effect.

5.5.1 Discussion of the Oscillating Electrode Results

A small enhancement in the oxygen transport rate is observed for an electrode oscillating between the solution and the perfluorohexane, as compared with the electrode oscillating only in solution. The most interesting feature of Figure 5-13 is that the oxygen transport rate becomes independent of the oscillation frequency of the electrode when the electrode traverses the perfluorohexane-solution interface.

Viewed under a horizontal microscope, the electrode is observed to trap a layer of aqueous solution at its surface as it traverses into the perfluorohexane phase. The diffusion of oxygen across the trapped layer is then the rate limiting step, and the current measured is independent of the oscillation frequency of the electrode. The layer was estimated to be about 10 μm thick, based on the observation under a microscope. Figure 5-16 shows the calculated diffusion limited current as a function of the thickness of trapped layer. The observed currents in Figure 5-13 are roughly in correspondence with those calculated for a 10 μm thick film.

A comparison of the relative Hamaker constants of the electrode, aqueous solution, and perfluorohexane shows that indeed it would be expected that the electrode trap a layer of aqueous solution at its surface. If the Hamaker constant, A , of platinum is taken as 40×10^{-20} J, that of the solution taken to be the Hamaker constant of water, 4×10^{-20} J, and the Hamaker constant of perfluorohexane taken to be 2.35×10^{-20} J, then, according to the combining rule discussed by Israelachvili [59], a negative Hamaker constant is found for the interaction of platinum with the perfluorohexane through the aqueous solution, showing that it is favorable for an aqueous layer to be trapped against the electrode. The combining rule discussed by Israelachvili is $A_{132} \approx (\sqrt{A_{11}} - \sqrt{A_{33}})(\sqrt{A_{22}} - \sqrt{A_{33}})$, where A_{132} is the (non-retarded) Hamaker constant for media 1 and 2 interacting through 3. The combining rules are not applicable to media of strong dielectric constants. Israelachvili recommends the calculation of A_{132} using a formula based on dielectric constants and refractive indices of the materials. These properties were not readily available for the media in question. The combining rules, though strictly invalid, were used to show that a trapped aqueous layer would

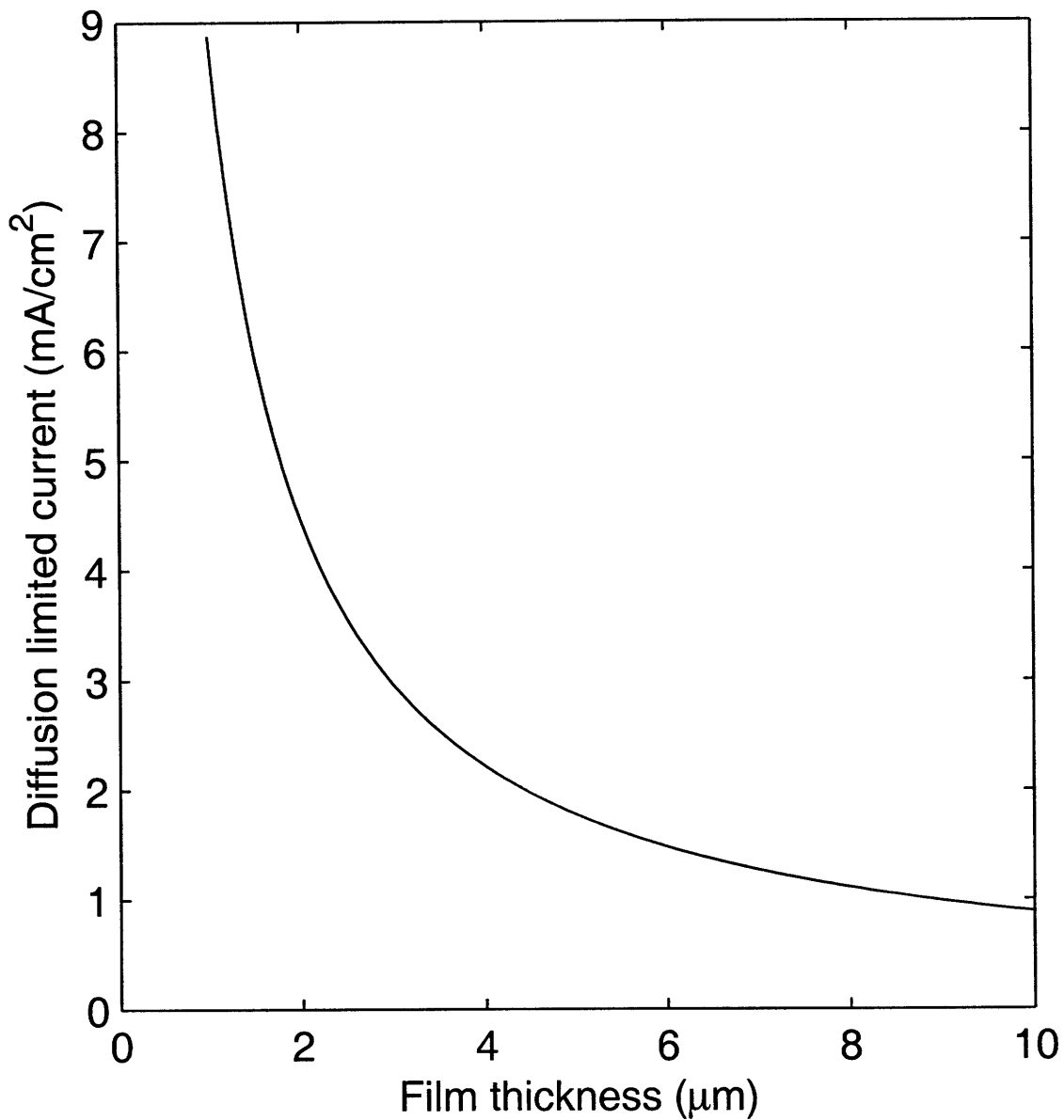


Figure 5-16: Calculated diffusion limited current as a function the thickness of a film of solution trapped beneath the electrode. The trapped aqueous layer is observed under a microscope to be about 10 μm .

be expected, but they give no quantitative insight. The magnitude of the combined Hamaker constant is incorrect, but its sign should be correct. See Israelachvili [59] p.200 for a further discussion.

If the platinum electrode is medium 1, and the perfluorohexane medium 2, then, using the combining rule, $A_{132} \approx -2 \times 10^{-20}$, which indicates that the platinum electrode will repel the perfluorohexane through the aqueous solution. Given that the majority of the area of the electrode is glass and not platinum, it may be more appropriate to use the Hamaker constant of glass (estimated from the Hamaker constant of mica or quartz to be of order 10×10^{-20} J). The combined Hamaker constant remains negative.

If the aqueous potassium hydroxide solution and the perfluorohexane are placed in a glass cylinder, the aqueous solution floats and the aqueous solution-perfluorohexane interface forms a convex meniscus (a meniscus like that of mercury in glass), confirming that the glass will preferentially wet the aqueous solution. The measured angle of the contact line is approximately 25° with the vertical.

The predictions of a model for the oscillating electrode based on the depletion of oxygen in a cylindrical region swept out by the electrode are shown in Figure 5-17. Transport to the surface of the electrode is not taken into account in this model. While the results are not close enough to be of quantitative value they suggest that, for the conditions of this experiment, depletion of the region the electrode sweeps plays a significant role.

Pratt provides a review of the use of oscillating electrodes [98].

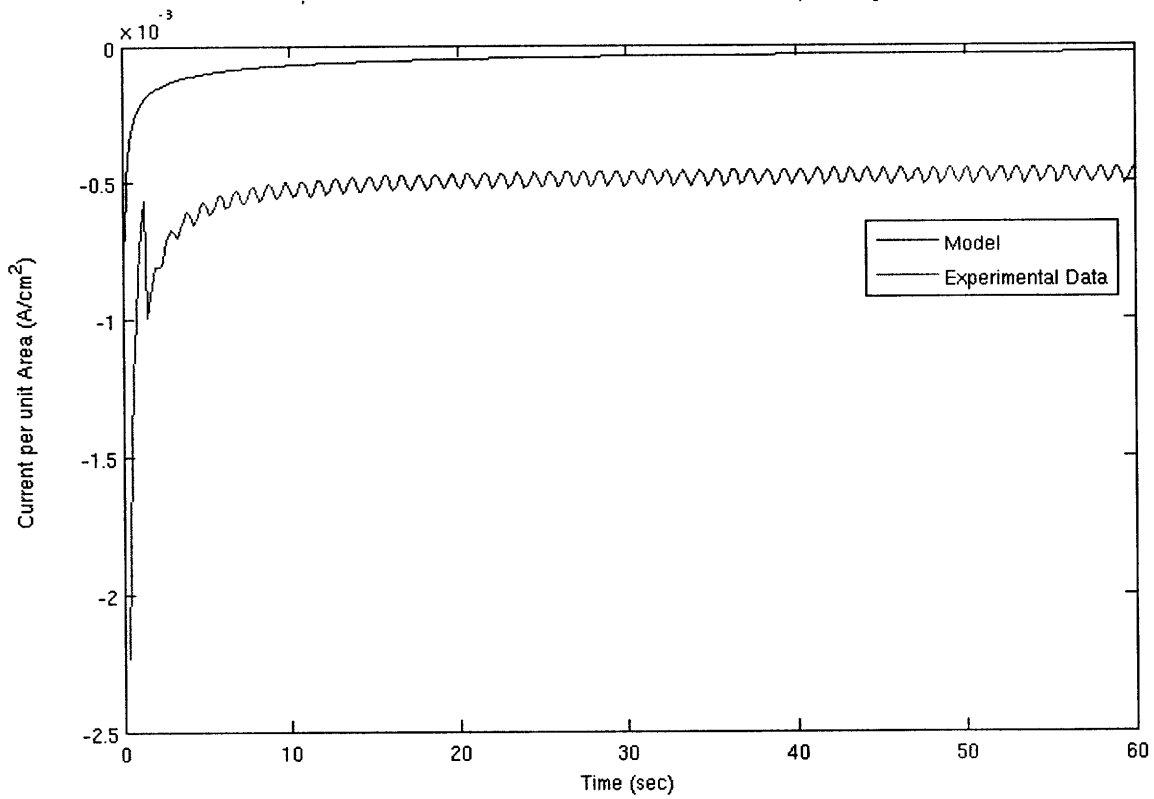


Figure 5-17: Model predictions and theoretical data for an oscillating electrode in oxygen saturated 20 wt% KOH solution. If viewed in black and white, the model is the smooth line, while experimental data shows oscillations. The negative currents indicate reduction. The ordinate shows current in milliamperes.

Chapter 6

Conclusions

Much work remains to be done, particularly on the modelling of a rotating disk in non-homogeneous media. Ungarish [122] p.56 provides a discussion of the difficulties involved in modelling a dispersion in a rotating flow. The experiments presented here were all performed with lecithin stabilized emulsions because emulsions could not be formed with the other surfactants tried. Lecithin was found to react with potassium hydroxide, though this was not known at the outset. Despite the reaction, satisfactory emulsions were formed and from the results of this work it is possible to draw conclusions with respect to the use of a dispersed medium to transfer oxygen in a fuel cell.

Oxygen and other covalent fluids are only very slightly soluble in aqueous media, and almost completely insoluble in strongly ionic aqueous media. With the aid of a surfactant, a covalent liquid can be stabilized as droplets in a continuous aqueous medium.

Among the surfactants tested lecithin was the only one to produce an emulsion. The engineers at the surfactant division of Dow Chemical suggested in a phone conversation that it would not be possible to formulate an emulsion in a concentrated electrolyte, such as a 20 wt% KOH solution, and could not recommend a surfactant. But a fuel cell requires electrolytes of such concentration, or greater, in order to minimize the Ohmic losses. The electrolyte in an alkaline fuel cell is often 30 wt% KOH, corresponding roughly to the maximum conductivity of a KOH solution. At concen-

trations of KOH above 30% the conductivity is reduced.

Lecithin reacted with the potassium hydroxide (apparently producing ammonia) but produced a satisfactory emulsion. If left for several days the emulsion coagulates, rendering it impractical for long term applications. Brockerhoff [19] discusses the hydrolysis of lecithin in strong alkaline solutions, a fact which was not known at the outset of this work.

The emulsion was used in a rotating disk electrode experiment, and a hydrostatic transient diffusion experiment (so called, Cottrell experiment). Reduction of oxygen from a pure continuous perfluorohexane phase was attempted with an oscillating electrode.

Although the fluid mechanics of a rotating disk in a homogeneous medium are well studied, the behavior of a dispersion can be considerably different from that of a homogeneous phase, particularly near the disk surface. Because the diffusion of species in a liquid is considerably slower than the diffusion of momentum the concentration boundary layer is thin in comparison with the hydrodynamic boundary layer. In order for the dispersed phase to affect the transport properties observed by the rotating disk, the dispersed droplets must enter into the thin concentration boundary layer. Although we have not been able to write the equations for the behavior of the droplets, we can argue based on the calculations presented, the experimental work of others on rotating disks [97], and the theoretical work of others on different flow arrangements [54, 55], that the emulsion droplets are unlikely to remain sufficiently close to the active area of the electrode for sufficiently long, to affect oxygen transfer. As a result, the rotating disk electrode is not suitable for the study of heterogeneous fluids with the assumption that they will behave as homogeneous fluids with constant average properties under all flow conditions. Fluid dynamics affect the apparent properties of heterogeneous fluids, with the result that their parameters cannot simply be measured in one apparatus or flow configuration and extended to others, as is conveniently done with a homogeneous fluid. de Ficquelmont-Loizos et al., [28] and Caprani et al., [21] have reported on the effect of inert particles on mass transfer to a rotating disk electrode. They found that the liquid medium, the particles, and the

disk influenced the results. The author was, regrettably, unaware of their work until the end of this work.

To eliminate the effect of the hydrodynamics of a rotating disk, the emulsion was tested in a transient hydrostatic diffusion experiment (Cottrell experiment). In this experiment, the concentration boundary layer grew in time to a size equal to several droplet diameters. Thus, if the droplets were evenly distributed, several should have been engulfed in the concentration boundary layer and therefore contributed to the oxygen transport, provided that the oxygen can escape from the droplets. No significant enhancement of the oxygen transport rate was observed, which suggests that the lecithin surfactant may present some resistance to the transport of oxygen out of the emulsion droplets, as hypothesized by Kronberger [69] for other emulsions with hydrocarbon based surfactants. The lack of a sound theoretical model to compare with, as noted by Dumont and Delmas [33] in their review, makes it difficult to draw a decisive conclusion. Ju et al. [61], for example, report that fluorocarbon based surfactants present no impediment to mass transfer. This is consistent with the expectation for a thin (of order $1 \mu\text{m}$) surfactant layer. Although the diffusivity of oxygen is higher in perfluorocarbons than in hydrocarbons, it is somewhat surprising that a thin surfactant layer of hydrocarbons would seem to inhibit transfer, while a surfactant layer of perfluorocarbons presents no impediment to transfer.

Given the observation that the emulsion coagulates with time but does not separate, it may be that the lecithin surfactant coagulates around the perfluorocarbon droplets, forming a shell that prevents oxygen transport out of the droplet. Such a shell could be the result of the reaction of lecithin with the potassium hydroxide solution [19]. The time scale for this to occur on the scale of each droplet may be considerably shorter than that required for coagulation of the emulsion.

A reciprocating electrode was used to traverse two continuous phases in an attempt to measure the reduction of oxygen from a perfluorocarbon in the absence of a surfactant. The reciprocating electrode trapped a layer of aqueous solution between the electrode surface and the perfluorohexane. By trapping a layer of aqueous solution at the surface of the electrode the oxygen transport was limited by diffusion across

this layer. No relevant enhancement was measured with the reciprocating electrode.

Although the use of a dispersed phase to transfer oxygen has been mentioned in the literature [56, 69], the author is aware of no discussion of how it can be employed in a practical fuel cell. Fuel cells are typically combined into stacks of cells. As such, to speak of a single cell is misleading. If a cell cannot be built into a stack it is of limited utility. Most fuel cell stacks have a geometric configuration as in Figure 6-1. The reactant gases flow orthogonal to the flow of ions between the electrodes. The gaseous reactants diffuse into the electrodes, while the ionic species diffuse across the membrane. By making the membrane very thin and of large cross section, the resistance to the diffusion of ionic species is reduced.

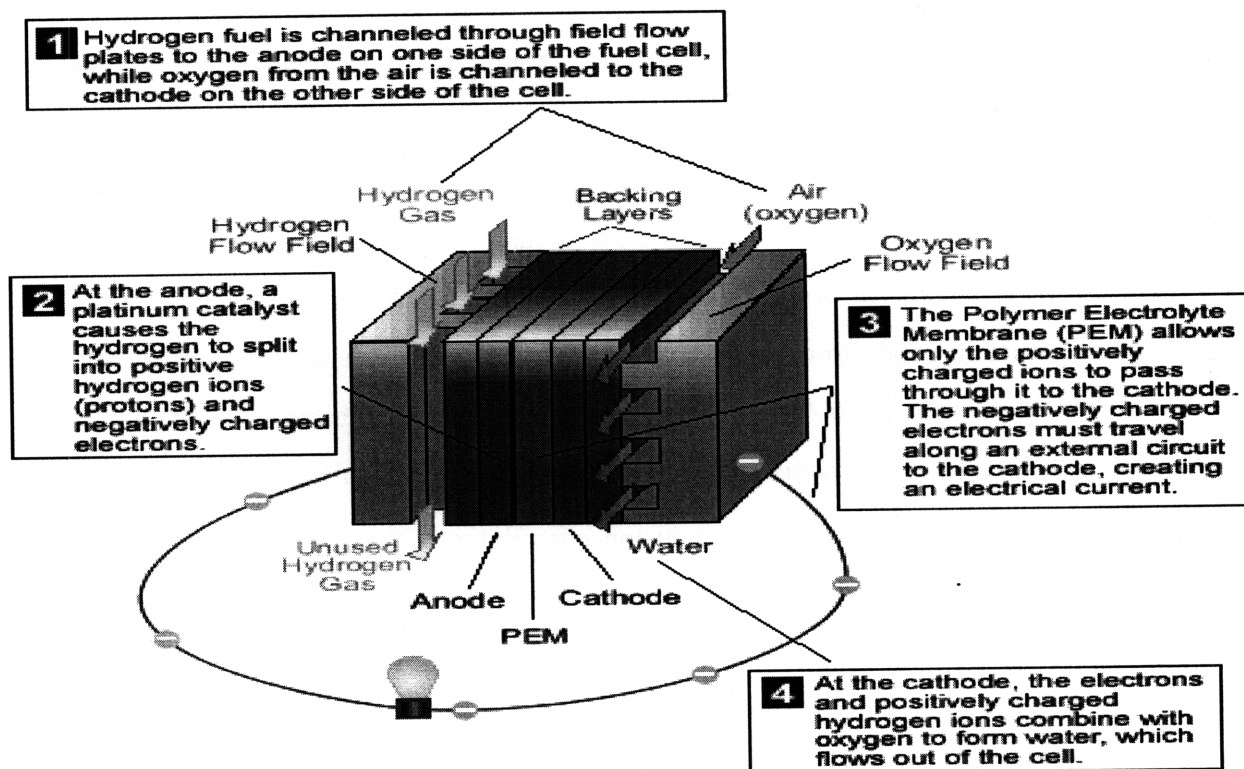


Figure 6-1: Schematic of a fuel cell. The unit shown above would be repeated to form a stack, typically with the cathode of one cell forming the back of the anode of the adjacent cell. Taken without permission from <http://www.fueleconomy.gov/feg/fcvPEM.shtml>.

If a flooded fuel cell is to be constructed, the liquid must be pumped through the

electrodes, which suggests a geometry as shown in Figure 6-2. The difficulty with this geometry is that the cross section for the diffusion of ions is greatly reduced, thereby greatly increasing the ohmic resistance. Other configurations are possible, but because of the basic two dimensional structure of a fuel cell, the problem remains that the flow of ions between the electrodes is orthogonal to the flow of reactive species. As such, either there is a large area for diffusion of ionic species, or a large area for the transport of reactants. It is possible to transport ions by circulating the same electrolyte through both the anode and cathode. In this case, either the electrolyte must be purged of gas to prevent gas crossover, or a fuel cell design such as the membrane-less, mixed reactant, fuel cells discussed by Priestnall and his coworkers [100] must be employed. Without a mixed reactant fuel cell design, producing a configuration that takes full advantage of flooded fuel cell is difficult. In summary, the design of the fuel cell must be made with an eye towards how it may be assembled in a stack. It's of little use to improve the dynamics at the electrodes only to be limited by greatly impeded ion transfer between the electrodes.

The problem of improving fuel cell performance is fundamental in nature. Covalent oxygen and aqueous ionic solutions are only very slightly miscible. The result is that a reaction involving an ionic liquid, a covalent gas, and a solid catalyst will remain confined to the line that is the triple interface. The width of the line will depend on the degree of miscibility and the diffusivity of the gas in the liquid, but will remain small [7].

It is, in principal, possible to formulate an emulsion though it may be difficult and will certainly rely on much trial and error. It is also possible to mix additives with the electrolyte to enhance the transport properties, as has been done by Adams et al. [2], Appleby and Baker [8], and Gang et al. [38], but the problem remains. If the electrode surface is hydrophobic the additive, surfactant, or inner phase of the emulsion may wet the electrode surface, then, as Adams and his coworkers found [2], it may prevent the transport of ionic media. A hydrophobic electrode may also

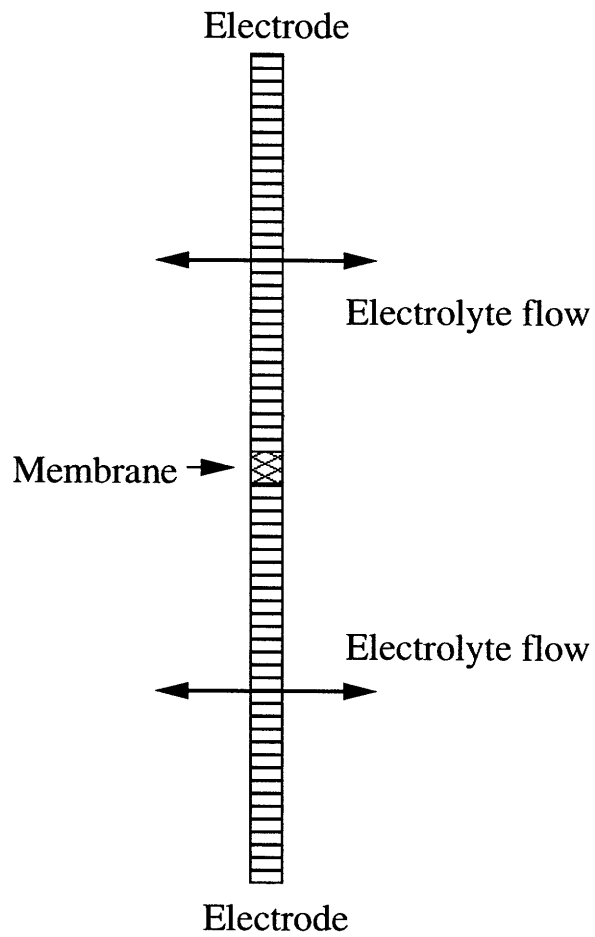


Figure 6-2: A schematic cross section of one possible configuration of a flooded fuel cell showing the electrolyte flow orthogonal to the thin dimension of the electrodes. The membrane area available for transport in this configure is greatly reduced when compared with the typical configuration.

encourage separation of the emulsion by providing a boundary for the inner phase to deposit on. If instead the electrode surface is hydrophilic, the distance of closest approach of the droplets is limited.

The electrolyte of a fuel cell must have a high ionic conductivity so as to minimize the ionic resistance between the electrodes. Therefore, for any study of transport phenomena relevant to fuel cells to be of practical use, it must be conducted in concentrated electrolyte. The injection of a medium to transport oxygen in such an electrolyte is difficult because, to dissolve oxygen, the medium must be covalent and so immiscible with the ionic electrolyte. Much of the research in perfluorocarbon blood substitutes over the past decades has been in the formulation of an emulsion. Once formulated, it is typically proprietary.¹ A suitable emulsion must not only be stable, but must also not foam. The lecithin emulsion foamed, and solidified after some days, both of which make the emulsion unsuitable for practical use.

Even if an emulsion were successfully formulated in a concentrated electrolyte suitable for use in fuel cells, its utility is in question. It is necessary to bring the emulsion droplets very close to the electrode surface in order to transport an increased amount of oxygen. This is possible in large fermentation reactors with vigorous stirring where the reaction occurs in the bulk of the fluid on large, open, dispersed surfaces. It is also possible in blood vessels where the flow is slow and the vessel of the size of an emulsion droplet. It is considerably more difficult to accomplish in a practical fuel cell electrode, at practical oxygen transport rates.

No matter the concentration of oxygen achieved by adding a dispersed phase, the chemical potential in the bulk remains the same as for the pure aqueous phase - both are in equilibrium with each other and with gaseous oxygen at one atmosphere. Therefore, if transport is limited by diffusion at the surface of the electrode the increase of oxygen concentration in the bulk, at a constant chemical potential, does not contribute to the mass transport as an increase in chemical potential (for example, by increasing the pressure) would. Only where there is a depletion of oxygen in the

¹Oxygent, a product of Alliance Pharmaceuticals of San Diego, California is an example. They did not respond to several attempts to contact them.

bulk, or where there is sufficient transport of droplets to the surface, can the addition of an organic phase be useful.

Because of the lack of an exact model to compare the results with, it is difficult to ascertain whether there should be any increase in the reduction current. Given that the chemical potential of oxygen in the emulsion is the same as in the aqueous solution, and given the slow diffusion in liquids, it may well be that oxygen in the bulk is not able to reach the surface of the electrode. The need for a transport model based on chemical potential is evident. Such a model is discussed in various cases [67], but no practical solution for use dispersed media exists [33].

While the length of the reaction line in a typical porous gas diffusion electrode can be increased by making use of increasingly porous electrodes, the increase in reactive area must not be at the expense of mass transport. In this sense, porous gas electrodes compromise between finer features that increase surface area but impede mass transport, and larger features which may have comparatively facile transport, but a comparatively small surface area.

Mass transport remains one of the limiting factors in a fuel cell. The creation of additional surface area through the use of highly porous materials is of little use if there is no transport to the reactive area. Based on the results of this work, the use of an emulsified phase to enhance the transport of gaseous reactions in a fuel cell is not promising.

The focus of this work, and much of the work in the literature, has been on the oxygen electrode. While the hydrogen reaction is more facile than the oxygen reaction and the diffusivity of hydrogen greater than that of oxygen, twice as much hydrogen is required as oxygen. The result is that, in principle, a fuel cell fed hydrogen and oxygen under equal conditions will become transport limited at the anode before the cathode. At currents well below the mass transport limit, the inefficiencies at the oxygen electrode are greater. That is to say, the deviation of the oxygen electrode from its open circuit potential is greater than the deviation of the hydrogen electrode from its open circuit potential for currents that are smaller than the cell's transport limited current. When the transport limited current is approached, it is the hydro-

gen electrode that should become transport limited and consequently, its potential deviates greatly from the open circuit potential.

No mention has been made of the difficulties in generating, transporting, and storing hydrogen, nor, of the cost of platinum. While these are significant obstacles to the adoption of fuel cells, they are beyond the scope of this thesis.

In order to fulfill the promise of efficiencies greater than those obtainable from an internal combustion engine, fuel cells must be capable of developing practical operating currents at voltages close to the open circuit voltage. Even on a platinum catalyst the reactions in a fuel cell, particularly the oxygen reduction, remain impractically slow.

Absent a better catalyst, the only options for producing practical currents from a fuel cell are increasing the reactive area and therefore, necessarily, engineering the mass transport to that area. The difficulties of producing practical currents from a reaction as slow as the reduction of oxygen, whose reactive area is limited to a line that is the triple-interface between the immiscible reactants, make it seem unlikely that fuel cells will see mass adoption as efficient energy conversion devices.

Appendix A

The Relationship Between Potential and Efficiency

The maximum work, W_{ideal} , obtainable from a Voltaic cell is

$$W_{ideal} = \Delta H - T\Delta S \equiv \Delta G \quad (\text{A.1})$$

Where ΔH , ΔS , and ΔG , are the enthalpy, entropy, and Gibbs free energy of reaction, respectively, and T is the absolute temperature.

Electrical work is the product of a charge and the change in potential of that charge. The maximum work obtainable from an electrochemical reaction is

$$W_{ideal} = E_{ideal}nF \quad (\text{A.2})$$

where E_{ideal} is the reversible potential of the cell, n is the number of moles of electrons transferred per mole of reaction, and F is Faraday's constant. The product nF is then the total charge transferred in one mole of reactions. The reversible potential is then

$$E_{ideal} = \frac{W_{ideal}}{nF} = \frac{\Delta G}{nF} \quad (\text{A.3})$$

For the reaction of oxygen and hydrogen



under conditions of standard temperature and pressure (1 atm, 25°C) $\Delta g = 237$ kJ/mole of H_2 reacted, if the product is liquid water. The corresponding ideal potential is $E_{ideal} = 1.229$ V.

The efficiency, η , of a cell defined as the electrical work produced per unit enthalpy of the reaction, is

$$\eta = \frac{W}{\Delta H} \quad (\text{A.5})$$

where W is the work produced, and ΔH is the enthalpy of reaction. For an ideal cell

$$\eta_{ideal} = \frac{W_{ideal}}{\Delta H} = \frac{\Delta G}{\Delta H} \quad (\text{A.6})$$

where Equation A.1 has been used to substitute W_{ideal} with ΔG . Equation A.6 shows that the ideal efficiency of a cell is a function of the enthalpy and Gibbs free energy of reaction, which are functions of state fixed by the temperature and pressure at which the reaction occurs. As a result, the ideal efficiency is fixed by the operating temperature and pressure of a cell. By substituting ΔH in equation A.5 with $\Delta G/\eta_{ideal}$, the efficiency of a non-ideal cell can be written as

$$\eta_{actual} = \frac{W_{actual}}{\Delta H} = \frac{W_{actual}}{\Delta G/\eta_{ideal}} \quad (\text{A.7})$$

The substitution of ΔG in equation A.7 with $E_{ideal}nF$ gives

$$\eta_{actual} = \frac{W_{actual}}{(E_{ideal}nF)/\eta_{ideal}} = \frac{\eta_{ideal}E_{actual}}{E_{ideal}} \quad (\text{A.8})$$

Since the ideal open circuit potential and the ideal efficiency are constants that depend only on the operating temperature and pressure of the cell (for a given cell reaction), the efficiency, at a fixed temperature and pressure, is directly proportional to the operating potential of the cell. Therefore, in order to obtain the highest en-

ergy conversion efficiency, the cell must be operated near its open circuit potential. However, near the equilibrium potential, the chemical reaction is slow, which leads to low current fluxes and consequently low power densities.

Bibliography

- [1] *Private Conversation with D. R. Sadoway.*
- [2] Adams A. A., R. T. Foley, and H. J. Barger. The electroreduction of air in trifluoromethanesulfonic acid monohydrate. *Journal of the Electrochemical Society*, 124(8):1228–1230, August 1977.
- [3] A. A. Adams and H. J. Barger. A new electrolyte for hydrocarbon air fuel cells. *Journal of the Electrochemical Society*, 121(8):987–990, 1974.
- [4] M. A. Al-Saleh, S. Gultekin, A. S. Al-Zakri, and H. Celiker. Effect of carbon dioxide on the performance of Ni/PTFE and Ag/PTFE electrodes in an alkaline fuel cell. *Journal of Applied Electrochemistry*, 24:575–80, 1994.
- [5] W. Albers and J. Th. G. Overbeek. Stability of emulsions in oil ii. charge as a factor of stabilization against flocculation. *Journal of Colloid Science*, 14, 1959.
- [6] A. J. Appleby. Oxygen reduction on oxide-free platinum in 85°C temperature and impurity dependence. *Journal of the Electrochemical Society*, 117, 1970.
- [7] A. J. Appleby, editor. *Fuel Cells: trends in research and applications*. John Wiley & Sons, New York, 1980.
- [8] A. J. Appleby and B. S. Baker. Oxygen reduction on platinum in trifluoromethane sulfonic acid. *Journal of the Electrochemical Society*, 125, 1978.
- [9] P. W. Atkins. *Physical Chemistry 6th edn*. Oxford University Press, Oxford, 1998.

- [10] W. D. Bancroft. The theory of emulsification. *J. Phys. Chem.*, 17:501–520, 1913.
- [11] W. D. Bancroft. The theory of emulsification. *J. Phys. Chem*, 19:275–309, 1915.
- [12] A. J. Bard, editor. *Encyclopedia of electrochemistry of the elements*. Marcel Dekker, New York, 1973.
- [13] A. J. Bard and L. R. Faulkner. *Electrochemical Methods*. John Wiley & Sons, New York, NY, USA, 1980.
- [14] R. B. Bird, W. E. Stewart, and E. N. Lightfoot. *Transport Phenomena*. John Wiley & Sons, New York, NY, USA, 1960.
- [15] K. F. Blurton and A. C. Riddiford. Shapes of practical rotating disc electrodes. *Journal of Electroanalytical Chemistry*, 10, 1965.
- [16] J. O'M. Bockris and A. K. M. Shamsul Huq. The mechanism of electrolytic evolution of oxygen on platinum. *Proceedings of the Royal Society, A*, 237(1209):277–296, 1956.
- [17] D.W.F. Brilman, M.J.V. Goldschmidt, G.F. Versteeg, and W.P.M. van Swaaij. Heterogeneous mass transfer models for gas absorption in multiphase systems. *Chemical Engineering Science*, 55:2793–2812, 2000.
- [18] D.W.F. Brilman, W.P.M. van Swaaij, and G.F. Versteeg. One-dimensional instationary heterogeneous mass transfer model for gas absorption in multiphase systems. *Chemical Engineering and Processing*, 37(6):471–488, 1998.
- [19] H. Brockerhoff. Breakdown of phospholipids in mild alkaline hydrolysis. *Journal of Lipid Research*, 4(1):96, 1963.
- [20] J. Cano and U. Bohm. Mass transfer in packed beds of screens. *Chemical Engineering Science*, 32(2):213–219, 1977.

- [21] A. Caprani, M. M. de Ficquelmont-Loizos, L. Tamisier, and P. Perronneau. Mass transfer in laminar flow at a rotating disk electrode in suspensions of inert particles. *Journal of the Electrochemical Society*, 135(3):635–642, 1988.
- [22] W. Gilber Castellan. Characteristic functions and parameters in the theory of hydrogen overpotential. *Journal of the Electrochemical Society*, 108(7):686–688, July 1961.
- [23] S.-H. Chen and R. Rajagopalan. *Micellar Solutions and Microemulsions*. Springer-Verlag, New York, 1990.
- [24] W. G. Cochran. *Proc. Cambridge Phil. Soc.*, 30, 1934.
- [25] B. E. Conway and J. O'M. Bockris. *Modern Aspects of Electrochemistry*. Plenum Press, New York, 1974. Vol. 9, p.369.
- [26] L. Coppola and Böhm U. Mass transfer to packed beds of screens from non-newtonian fluids. *Chemical Engineering Science*, 40(8):1594, 1985.
- [27] J. Crank. *The Mathematics of Diffusion*. Oxford University Press, Oxford, England, 1957.
- [28] M. M. de Ficquelmont-Loizos, L. Tamisies, and A. Caprani. Mass transfer in laminar flow at a rotating disk electrode in suspensions of inert particles. *Journal of the Electrochemical Society*, 135(3):626–634, 1988.
- [29] S.R. De Groot and P. Mazur. *Non-Equilibrium Thermodynamics*. North-Holland, Amsterdam, 1969.
- [30] W. M. Deen. *Analysis of Transport Phenomena*. Oxford University Press, Oxford, 1998.
- [31] J. J. Delpuech, M. A. Hamza, G. Serratrice, and M. J. Stebe. Fluorocarbons as oxygen carriers. I. An NMR study of oxygen solutions in hexafluorbenzene. *Journal of Chemical Physics*, 70(6):2680–7, March 1978.

- [32] A.M.A. Dias, R.P. Bonifacio, I.M. Marrucho, A.A.H. Padua, and M.F. Costa-Gomes. Solubility of oxygen in n-hexane and in n-perfluorohexane; experimental determination and prediction by molecular simulation. *Physical Chemistry Chemical Physics*, 5(3):543–9, February 2003.
- [33] E. Dumont and H. Delmas. Mass transfer enhancement of gas absorption in oil-in-water systems: a review. *Chemical Engineering and Processing*, 42, 2003.
- [34] D. A. Ellis, S. A. Mabury, J. W. Martin, and D. C. G. Muir. Thermolysis of fluoropolymers as a potential source of halogenated organic acids in the environment. *Nature*, 412, 2001.
- [35] M. J. Francis and R. M. Pashley. the effect of de-gassing on the dispersion of fine oil droplets in water. *Colloids and Surfaces A: Physiochem. Eng. Aspects*, 287, 2006.
- [36] M. G. Freire, A. M.A. Dias, M. A.Z. Coelho, J. A.P. Coutinho, and I. M. Marrucho. Aging mechanisms of perfluorocarbon emulsions using image analysis. *Journal of Colloid Interface Science*, 2005.
- [37] Z. Galus, translated by S. Marcinkiewicz, and translation editor G. F. Reynolds. *Fundamentals of Electrochemical Analysis*. Ellis Horwood Limited, Chichester, England, 1976.
- [38] X. Gang, H. A. Hjuler, C. Olsen, R. W. Berg, and N. J. Bjerrum. Electrolyte additives for phosphoric acid fuel cells. *Journal of the Electrochemical Society*, 140(4):896–902, April 1993.
- [39] G. Geffcken. Solubility [of gases in aqueous solutions]. *Zeitschrift für Physikalische Chemie*, 49:257–302, August 1904.
- [40] S. Goldstein, editor. *Modern Developments in Fluid Dynamics*. Clarendon Press, Oxford, 1938.

- [41] P. Gouérec, L. Poletto, J. Denizot, E. Sanchez-Cotezon, and J. H. Miners. The evolution of the performance of alkaline fuel cells with circulation electrolyte. *The Journal of Power Sources*, 129, 2003.
- [42] K. Grasshoff, M. Ehrhard, and K. Kremling. *Methods of Seawater Analysis*. Verlag Chemie, Weinheim, Germany, 1983.
- [43] D. P. Gregory and A. C. Riddiford. Transport to the surface of a rotating disk. *Journal of the Chemical Society*, 1956.
- [44] D. P. Gregory and A. C. Riddiford. Dissolution of copper in sulfuric acid solutions. *Journal of the Electrochemical Society*, 107(12):950–956, December 1960.
- [45] W.C. Griffin. Classification of surface-active agents by HLB. *Journal of the Society of Cosmetic Chemists*, 1, 1949.
- [46] K. E. Gubbins and R. D. Walker. *Journal of the Electrochemical Society*.
- [47] E. A. Guggenheim. Potential difference between two phases and individual activities of ions. *Journal of Physical Chemistry*, 33:842–849, 1929.
- [48] E. Gulzow. Alkaline fuel cells: a critical view. *Journal of Power Source*, 61:99–104, July 1996.
- [49] F. Haber. *Elektrochem*, 12:415, 1906.
- [50] F. Haber. *Z. Anorg. Allegem. Chem.*, 51:245–289, 1906.
- [51] O. P. Habler and K. F. Messmer. Tissue perfusion and oxygenation with blood substitutes. *Advanced Drug Delivery Reviews*, 40, 2000.
- [52] P. Hiemenz and R. Rajagopalan. *Principles of Colloid and Surface Chemistry*. Marcel Dekker, Inc., New York, 1997.
- [53] R. Hilpert. *Forsch. Geb. Ingenieurwes.*, 4:215, 1933.

- [54] B. P. Ho and L. G. Leal. Inertial migration of rigid spheres in two-dimensional unidirectional flows. *Journal of Fluid Mechanics*, 65(2):365–400, 1974.
- [55] B. P. Ho and L. G. Leal. Migration of rigid spheres in a two-dimensional unidirectional shear flow of a second-order fluid. *Journal of Fluid Mechanics*, 76(4):783–799, 1976.
- [56] U. B. Holeschovsky. *Analysis of Flooded Flow Fuel Cells and Thermogalvanic Generators*. PhD thesis, Massachusetts Institute of Technology, 1994.
- [57] U. B. Holeschovsky, J. W. Tester, and W. M. Deen. Flooded flow fuel cells: a different approach to fuel cell design. *Journal of Power sources*, 63:63–69, 1996.
- [58] F. P. Incropera and D. P. DeWitt. *Fundamentals of Heat and Mass Transfer*. John Wiley & Sons, New York, 1996.
- [59] J. N. Israelachvili. *Intermolecular and Surface Forces*. Academic Press, London, 1985.
- [60] Jang-Ho Jo and Sung-Chul Yi. A computational simulation of an alkaline fuel cell. *Journal of Power Sources*, 84:87–106, 1999.
- [61] L. K. Ju, Lee. J. F., and W. B. Armiger. Enhancing oxygen transfer in bioreactors by perfluorocarbon emulsions. *Biotechnology Progress*, 7(4):323–329, 1991.
- [62] L. K. Ju, J. F. Lee, and W. B. Armiger. Effect of the interfacial surfactant layer on oxygen transfer through the oil/water phase boundary in perfluorocarbon emulsions. *Biotechnology and Bioengineering*, 37, 1991.
- [63] Beth H. Junker, T. Alan Hatton, and Daniel I.C. Wang. Oxygen transfer enhancement in aqueous/perfluorocarbon fermentation systems. I. Experimental observations. *Journal of Bioscience and Bioengineering*, 35(6):578–585, March 1990.

- [64] Beth H. Junker, T. Alan Hatton, and Daniel I.C. Wang. Oxygen transfer enhancement in aqueous/perfluorocarbon fermentation systems. II. Theoretical analysis. *Journal of Bioscience and Bioengineering*, 35(6):586–597, March 1990.
- [65] K. Kinoshita. *Electrochemical Oxygen Technology*. Wiley, New York, 1992.
- [66] J. D. Knudsen and D. L. Katz. *Fluid Dynamics and Heat Transfer*. McGraw-Hill, New York, 1958.
- [67] Dilip Kondepudi and Ilya Prigogine. *Modern Thermodynamics: from heat engines to dissipative structures*. John Wiley, Chichester, New York, 1998.
- [68] K. Kordesch and G. Simader. *Fuel Cells and Their Applications*. VCH, New York, 1996.
- [69] H. Kronberger, K. Bruckner, and Ch. Fabjan. Reduction of oxygen from electrolyte emulsions with high oxygen contents. *Journal of Power Sources*, 86:562–7, March 2000.
- [70] V. G. Levich. *Acta Physicochim*, 17, 1942.
- [71] V. G. Levich. *Acta Physicochem*, 18, 1944.
- [72] V. G. Levich. *Physicochemical Hydrodynamics*. Prentice-Hall Inc., Englewood Cliffs, N.J., 1962.
- [73] J. H. Lienhard and J. H. Lienhard. *A Heat Transfer Textbook*. Phlogiston Press, Cambridge, Massachusetts, 2006.
- [74] E. Longstaff, M. Robinson, C. Bradbrook, J. A. Styles, and I. F. H. Purchase. Genotoxicity and carcinogenicity of fluorocarbons: Assessment by short-term *in-vitro* tests and chronic exposure in rats. *Toxicology and Applied Pharmacology*, 72(1):15–31, 1984.
- [75] K. C. Lowe, M. R. Davey, and B. J. Power. Perfluorochemicals: their applications and benefits to cell culture. *TIBTECH*, 16, 1998.

- [76] N. Maeda, K. J. Rosenberg, J. N. Israelachvili, and R. M. Pashley. Further studies on the effect of degassing on the dispersion and stability of surfactant-free emulsions. *Langmuir*, 20, 2004.
- [77] N. M. Maković, T. J. Schmidt, V Stamenković, and P. N. Ross. Oxygen reduction reaction on Pt and Pt bimetallic surfaces: A selective review. *Fuel Cells*, 1(2):105–116, 2001.
- [78] R. P. Mason. Non-invasive physiology: ^{19}F NMR of perfluorocarbons. *Artificial Cells, Blood Substitutes, and Immobilization Biotechnology*, 22(4):1141–1153, 1994.
- [79] V. I. Matryonin, A. T. Avchinikov, and A. P. Tzedilkin. Investigation of the operating parameters influence on $\text{H}_2 - \text{O}_2$ alkaline fuel cell performance. *International Journal of Hydrogen Energy*, 22(10):1047–1052.
- [80] J. C. Maxwell. *A Treatise on Electricity and Magnetism*. Clarendon, Oxford, 1881. Vol. 1, p. 435.
- [81] Donald McDonald. Johan Wolfgang Döbereiner, the discovery of catalysis and the refining of russian platinum. *Platinum Metals Review*, 9(4):136–139, 1965.
- [82] G. F. McLean, T. Niet, S. Prince-Richard, and N. Djilali. An assessment of alkaline fuel cell technology. *International Journal of Hydrogen Energy*, 27:502–526, 2002.
- [83] J. D. McMillan and D.I.C Wang. Enhanced oxygen transfer using oil-in-water dispersions. *Annals of the New York Academy of Sciences*, 506(1):569–582, 1987.
- [84] A. Mehra. Intensification of multiphase reactions through the use of a microphase - i. theoretical. *Chemical Engineering Science*, 43(4):448–452, 1988.
- [85] A. Mehra. Intensification of multiphase reactions through the use of a microphase - ii. experimental. *Chemical Engineering Science*, 43(4):913–927, 1988.

- [86] Anurag Mehra. Heterogenous modeling of gas absorption in emulsions. *Ind. Eng. Chem. Res.*, 38(6):2460–2468, 1999.
- [87] A. F. Mills. *Heat and Mass Transfer*. Irwin, Chicago, IL, USA, 1995.
- [88] Ian D. Morrison and Ross Sydney. *Colloidal, Dispersions, Suspensions, Emulsions, and Foams*. John Wiley, New York, 2002.
- [89] E. Nagy and A. Moser. Three-phase mass transfer: Improved pseudo-homogenous model. *AICHE J.*, 41(23), 1995.
- [90] John S. Newman. Schmidt number correction for the rotating disk. *The Journal of Physical Chemistry*, 70(4):1326–1327, 1966.
- [91] John S. Newman. *Electrochemical Systems*. Prentice Hall, Englewood Cliffs, N.J., 1991.
- [92] J. D. Newson and A. C. Riddiford. The kinetics of the iodine redox process at platinum electrodes. *Journal of the Electrochemical Society*, 108(7):699–706, July 1961.
- [93] J. D. Newson and A. C. Riddiford. Limiting currents for the reduction of triiodide ion at a rotatin platinum disk cathode. *Journal of the Electrochemical Society*, 108(7):695–698, July 1961.
- [94] Su-Moon Park, Stanley Ho, Saravana Aurliah, Michael F. Weber, Charles A. Ward, and Ronald D. Venter. Electrochemical reduction of oxygen at platinum electrodes in koh solutions - temperature and concentration effects. *The Journal of the Electrochemical Society*, 133(8):1641–1649, August 1986.
- [95] R. Pashley. Effect of degassing on the formation and stability of surfactant-free emulsions and fine teflon dispersions. *Journal of Physical Chemistry B*, 107, 2003.

- [96] P. Pint and S. N. Flengas. The behavior of an oscillating solid microelectrode for voltammetric studies in aqueous and molten salt solutions. *Journal of the Electrochemical Society*, 123(7):1042–1047, July 1976.
- [97] O. A. Povarov, O. I. Nazarov, L.A. Ignatevskaya, and A. I. Nikolskii. Interaction of drops with boundary layer on rotating surface. *Inzhenerno-Fizicheskii Zhurnal*, 31(6):1068–1073, 1976.
- [98] K. W. Pratt and J. C. Johnson. Vibrating wire electrodes - i. literature review, design and evaluation. *Electrochimica Acta*, 27(8):1013–1021, 1982.
- [99] R. G. Pratt, S. R. Thomas, R. W. Millard, R. C. Samarantunga, and M. H. Naseem. Quantitation of perfluorocarbon blood substitutes in tissues using f-19 magnetic resonance spectroscopy. *Biomaterials, Artificial Cells, and Immobilization Biotechnology*, 20(2), 1992.
- [100] M. A. Priestnall, V. P. Kotzeva, D. J. Fish, and E. M. Nilsson. Compact mixed-reactant fuel cells. *Journal of Power Sources*, 106, 2002.
- [101] S. R. Radel and N. H. Navidi. *Chemistry*. West Publishing Company, New York, NY, USA, 1994.
- [102] A. R. Reti. *Rate Limiting Steps on Fuel Cell Electrodes*. PhD thesis, Massachusetts Institute of Technology, 1963.
- [103] A. C. Riddiford. The rotating disk system. *Adv. Electrochem. Eng.*, 1964.
- [104] Jean G. Riess. Understanding the fundamentals of perfluorocarbons and perfluorocarbon emulsion relevant to in vivo oxygen delivery. *Artificial Cells, Blood Substitutes, and Biotechnology*, 33, 2005.
- [105] J. L. Rols, J. S. Condoret, C. Fonade, and G. Goma. Mechanism of enhanced oxygen transfer in fermentation using emulsified oxygen-vectors. *Biotechnology and Bioengineering*, 35, 1990.

- [106] P. N. Ross. Evaluation of tetrafluoroethan-1,2-disulfonic acid as a fuel cell electrolyte. *Journal of the Electrochemical Society*, 130(4):882–885, 1983.
- [107] Z. M. Salameh, M. A. Casacca, and W. A. Lynch. A mathematical model for lead-acid batteries. *IEEE Transactions on Energy Conversion*, 7(1):93–98, March 1992.
- [108] H. Schlichting. *Boundary Layer Theory*. McGraw Hill, New York, 1968.
- [109] W. Schottky and H. Rothe. *Handbook Experimental Physik (Handbook of Experimental Physics, reference on page 4 of Vetter's book)*. 1928.
- [110] EG&G Service. *Fuel Cell Handbook, Fifth Edition*. B/T Books, Orinda, CA, US, 2000.
- [111] R.K. Spence, E.D. Norcross, Joseph Costabile, Sue McCoy, Aurel C. Cernaianu, James B. Alexander, Mark J. Pello, Umur Atabek, and Rudolph C. Camishion. Perfluorocarbons as blood substitutes: The early years. experience with fluosol da-20 *Artificial Cells, Blood Substitutes, and Immobilization Biotechnology*, 22(4):955–963, 1994.
- [112] M. J. Stebe, G. Serratrice, and J. J. Delpuech. Fluorocarbons as oxygen carriers. An NMR study of nonionic fluorinated microemulsions and of their oxygen solutions. *Journal of Physical Chemistry*, 89(13):2837–43, June 1985.
- [113] V. Stiles and G. Cady. Physical properties of perfluoro-n-hexane and perfluoro-2-methylpentane. *Journal of the American Chemical Society*, 74(15):3771–3773, 1952.
- [114] K. A. Striebel, F. R. McLarnon, and E. J. Cairns. Fuel cell cathode studies in aqueous k_2CO_3 and koh. *Journal of the Electrochemical Society*, 137(11):3360–3367, November 1990.
- [115] K. A. Striebel, F. R. McLarnon, and E. J. Cairns. Oxygen reduction on pt in aqueous k_2CO_3 and koh. *Journal of the Electrochemical Society*, 137(11):3351–3359, November 1990.

- [116] T Tadros. Principles of emulsion stabilization with special reference to polymeric surfactants. *Journal of Cosmetic Science*, 57(2):153–69, March 2006.
- [117] Th. Tadros. *Applied Surfactants*. Wiley-VCH, New York, NY, 2006.
- [118] K. Tammeveski, T Tenno, J. Claret, and C. Ferrater. Electrochemical reduction of oxygen on thin-film pt electrodes in 0.1 m koh. *Electrochimica Acta*, 42(5):893–897, 1997.
- [119] M. K. Tham, R. D. Walker, and K. E Gubbins. Diffusion of oxygen and hydrogen in aqueous potassium hydroxide solution. *The Journal of Physical Chemistry*, 74(8):1747–51, April 1970.
- [120] R. E Treybal. *Mass-Transfer Operations*. McGraw Hill, New York, NY, US, 1980.
- [121] T. Ukita, N. Bates, and H. Carter. Studies on the alkaline hydrolysis of lecithin: synthesis of cyclic1,2-glycerophosphate. *Journal of Biological Chemistry*, 216(2):867, 1955.
- [122] M. Ungarish. *Hydrodynamics of Suspensions: Fundamentals of Centrifugal and Gravity Separation*. Springer, New York, 1993.
- [123] Klaus J. Vetter. *Electrochemical Kinetics; Theoretical and Experimental Aspects*. Academic Press, New York, London, 1967.
- [124] Th. von Kármán. Über laminare und turbulente reibung. *Zeitschrift für angewandte Mathematick und Mechanik*, 1, 1921.
- [125] L. W. Winkler. *Ber. dtsh. chem. Ges.*, 21, 1888.